From the Research Center Borstel
Leibniz-Center for Medicine and Biosciences
Department of Molecular Infection Biology
Director: Prof. Dr. rer. nat. Ulrich Schaible

Division of Microbial Interface Biology
PD Dr. rer. nat. Norbert Reiling

Characterization of macrophage Frizzled1 expression and the role of Wnt3a-induced signaling in experimental *M. tuberculosis* infection

Inaugural Dissertation
for
Obtaining the Doctorate Degree
of the University of Lübeck
- From the Faculty of Science and Technology -

Submitted by
Jan Neumann
of Kiel

Lübeck, 2010

Doctoral dissertation approved by the Faculty of Technology and Sciences of the University of Lübeck

Date of doctoral examination: 31.05.2010

Chairman of the examination committee: Prof. Dr. rer. nat. N. Tautz

First reviewer: PD Dr. rer. nat. N. Reiling

Second reviewer: Prof. Dr. rer. nat. U. Schaible

Für meine Frau Katrin, meinen Sohn Justus und
in Gedenken an meine Freundin Antje Hübner

Table of contents

1. Introduction

1.1 Wnt/Frizzled signaling

Wnt/Frizzled (Fzd) signaling pathways are evolutionarily highly conserved, ranging from most simple metazoan life forms (such as the placozoan *Trichoplax*) to humans[1;2]. Wnt signaling is essential during and after embryogenesis for regulating numerous processes of animal development, including cell fate decisions, axis formation, limb and organ formation as well as tissue homeostasis and self-renewal. Due to its fundamental functions during development and homeostasis, hypo- or hyperactive Wnt/Fzd signaling is often linked to pathophysiological processes, such as developmental defects or cancer[3]. In addition, these pathways were recently shown to regulate inflammatory processes and immunological function. Specifically, the Wnt/β-catenin pathway, which is involved in the expansion and regulation of stem cells, was associated with the resolution of inflammation and reconstitution of tissue homeostasis.

The prototypical example of a bacteria-induced chronic inflammatory lung disease is tuberculosis, which is caused by acid fast bacteria of the *Mycobacterium tuberculosis* complex. Experimental infections with microorganisms have been successfully used to uncover the intricacies governing the interplay between innate and adaptive immunity[4;5]. The major focus of the current work was to characterize the role of Wnt/Fzd signaling in mycobacterial infections.

1.1.1 Wnt ligands and Frizzled receptors

The name “Wnt” is an acronym composed of the gene names *wingless* and *Int-1*. Both genes were described at about the same time and were found to encode identical proteins. Nüsslein-Volhard and colleagues found that deletion of the gene *wingless* (*wg*) resulted in a *Drosophila melanogaster* mutant unable to develop wings[6]. In parallel Nusse and Varmus identified murine *Int-1* (integration site 1) to be an integration locus of the mouse mammary tumor virus (MMTV)[7;8].

To date, 19 Wnt homologs have been identified in mice and humans, showing distinct expression patterns and functions[9]. Mammalian Wnt proteins range in molecular weight from 39 kDa to 46 kDa, featuring 23 to 24 cysteine residues of which the spacing is highly conserved. These residues may be involved in the formation of multiple disulfide bonds required for the correct folding of Wnt homologs. Yet, little is

known about the structure of Wnt proteins. Although secreted, Wnts have been difficult to purify. One reason may be their low solubility due to acylation of the polypeptide chain. To date, only active Wnt3a and Wnt5a have been purified from conditioned medium. Both homologs were shown to be palmitoylated at cysteine residues Cys77 (Wnt3a) and Cys104 (Wnt5a)[10;11]. In addition to Cys77, Wnt3a was shown to be modified with palmitoleic acid (C16:1) at Ser209. It is very likely that this unusual fatty acid modification is shared by other Wnt homologs, since amino acid residues adjacent to serine 209 are highly conserved among Wnts[12]. Lipid modifications of Wnt proteins have been suggested to require the acyltransferase Porcupine (Porc), which is located within the endoplasmatic reticulum (ER)[13].

Another characteristic of Wnt proteins is that they become N-glycosylated within the endoplasmatic reticulum at multiple glycosylation sites[14]. These post-translational modifications are a prerequisite for the release and function of Wnt molecules. It was shown that glycosidase-treatment of Wnt3a and 5a had no influence on their function as a ligand, but glycosylation was rather required for acylation and secretion. Acylation in contrast was shown to be a prerequisite for secretion and binding of Wnt ligands to their corresponding receptors[15;16]. In addition to glycosylation and acylation, secretion of Wnt proteins requires the presence of the protein Wntless (Wls; also known as Evenness interrupted (Evi) and Sprinter)[17]. Wls is a multispan transmembrane protein predominantly localized within the Golgi apparatus promoting the release of Wnts into the extracellular milieu[18].

On the one hand short-range biologic effects are likely to be achieved by accumulation of Wnts in close proximity of the secreting cell. On the other hand its “stickiness” due to lipid modifications has prompted different models of how Wnts may perform long-range effects and activation of target genes more than 20 cell diameters in distance from the secreting cell[19]. One model for long-range effects could be, that Wnt molecules cluster to form a Wnt-micelle with the lipid chains facing the interior. This aggregation was implicated for morphogenic hedgehog (Hh) proteins, which are very similar to Wnts in structure and function[20;21]. Another model suggests that Wnt proteins are integrated into lipoprotein particles or bound to mobile components of the extracellular matrix and are transported or diffuse to their target cells[22;23].

Wnt ligands bind to Frizzled receptors (Fzd), which are seven-pass transmembrane proteins[24]. To date 10 Fzd homologs have been reported in mice and humans with a primary sequence of 540 to 700 amino acids. Fzd receptors possess three major regions: an extracellular region, a central core composed of seven hydrophobic membrane-spanning alpha-helices linked by 3 extra- and 3 intracellular loops, and a cytoplasmatic region. In the extracellular region, an N-terminal cysteine rich domain (CRD) containing 10 highly conserved cysteine residues serves as a ligand-binding site[24;25]. It is proposed that for the tight binding of Fzd receptors, ligands bound to the cysteine rich domain additionally interact with the core region of the receptor to initiate signaling[26;27]. Another feature of the extracellular region is the presence of two N-linked glycosylation sites[25]. Even though its biological relevance is still unknown, it has been discussed to be involved in the control of receptor maturation within the ER or ligand binding[28].

Fzds are known to bind multiple Wnt ligands and vice versa. Biochemical analyses of *Drosophila* Fzd orthologs (Dfz1 and Dfz2) showed that both Dfz1 and Dfz2 bind Wg, but with different dissociation constants. Whereas the affinity between Wg and Dfz2 was relatively high (K_d approx. 1 nM), the affinity of the ligand-receptor complex between Dfz1 and Wg was 10-fold lower[29]. Thus, different Wnt ligands may have variable affinities for a certain Fzd receptor. In the cytoplasmatic region the C-terminal tail was shown to include a PDZ-binding domain. This Fzd receptor region serves as a common motif for intracellular binding proteins such as Dishevelled (see below), providing a protein-interacting interface[30,31]. In addition, single amino acid exchanges in the first or third intracellular loop (iLoop1, 3) of the core region disabled Fzd signaling, indicating a pivotal role of the intracellular loops.

Fzd receptors have recently been classified as a novel class of G protein-coupled receptors (GPCR)[32]. However, this classification was controversially discussed, due to the fact that Fzd receptors lack characteristic motifs of GPCRs. Yet, each of the three known Wnt signaling pathways (see below) depends on the activation of heterotrimeric G proteins (composed of $G\alpha$, -β, -γ subunits)[33-36]. Several reasons indicate that Fzds function as GPCRs: (i) like all members of the GPCR superfamily Fzds are heptihelical receptors; (ii) Fzd function is sensitive to pertussis toxin; (iii) Fzd function is sensitive to depletion of $G\alpha_{o/q}$ or $G\beta$ subunits[37;38]. In addition, (iv) subunit $G\alpha_o$ was shown to coimmunoprecipitate with Fzd receptors, which dissociates after

Wnt3a treatment, indicating a conformational change of the G protein after agonist stimulation[35].

1.1.2 The Wnt/Frizzled signaling pathways

To date, at least three different signaling cascades are known, which can be activated through binding of a Wnt ligand to its corresponding Fzd receptor: the Wnt/β-catenin pathway, the Wnt/Ca^{2+} pathway and the planar cell polarity (PCP) pathway (Fig. 1).

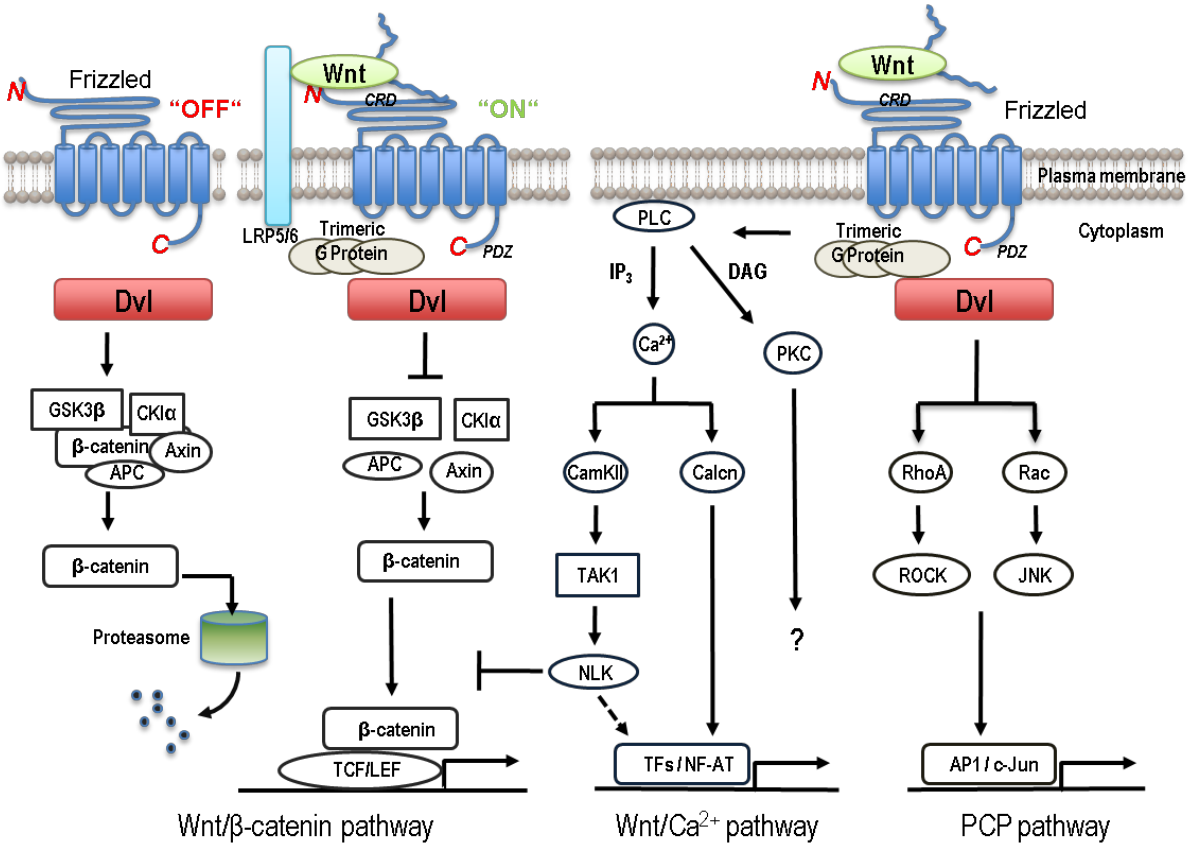

Figure 1: Signaling cascades induced by Wnt/Frizzled interactions.
Wnt ligands activate at least three intracellular signaling cascades through Frizzled (Fzd) receptors, in which trimeric G proteins and the phosphoprotein Dishevelled (Dvl) are involved: the Wnt/β-catenin pathway, the Wnt/Ca^{2+}pathway and the planar cell polarity (PCP) pathway[39]. A detailed description of the figure is given in the text (modified after Kikuchi et al., 2006).

In all three signaling pathways G proteins and the cytoplasmic phosphoproteins Dishevelled1-3 (Dvl1-3) are critically involved. However, the exact mechanism leading to the phosphorylation of Dvl and the molecular interaction between G proteins and Dvl are still unclear[33;40].

The best studied Wnt-induced signaling cascade is the Wnt/β-catenin pathway, which is often referred to as the canonical Wnt pathway. In the absence of a Wnt ligand

("OFF", see Fig. 1), cytoplasmatic β-catenin is constantly degraded due to the activity of a degradation complex. This complex is composed of the scaffold protein Axin, the tumor suppressor adenomatous polyposis coli (APC) as well as the two kinases glycogen synthase kinase 3β (GSK3β) and casein kinase 1α. β-catenin bound to Axin and APC becomes subsequently phosphorylated by GSK3β and CK1α. Phosphorylated β-catenin is recognized by the E3 ubiquitin ligase β-TrCP and ubiquitinated for proteasomal degradation. In the presence of a Wnt ligand ("ON", see Fig. 1), Fzd and co-receptor LRP5/6 (low-density-lipoprotein receptor-related protein 5/6) activate G proteins and Dvl, which promote the recruitment of GSK3β and scaffold protein Axin to the LRP5/6 co-receptor. In consequence the degradation complex is disrupted resulting in the stabilization of intracellular β-catenin levels. Cytoplasmatic β-catenin is then transportated into the nucleus, where it binds and activates transcription factors T cell factor (Tcf) and lymphoid enhancer factor (Lef). Tcf/Lef induces the expression of several target genes such as *C-myc*, *Cyclin D1* or the negative feedback regulator *Axin2*. The β-catenin pathway is primarily associated with multiple developmental processes and maintenance of stem cells (see section 1.1.4 for detailed functions).

The Wnt/Ca^{2+} pathway is characterized by an increase in intracellular Ca^{2+} concentration. It involves activation of phospholipase C (PLC) through Dvl and heterotrimeric G proteins. PLC hydrolyzes phosphatidylinositol 4,5-bisphosphate (PIP_2) to inositol 1,4,5,-trisphosphate (IP_3) and diacylglycerol (DAG). Whereas IP_3 increases intracellular Ca^{2+} concentrations leading to the activation of calcium/calmodulin-dependent kinase II (CamKII) and calcineurin (Calcn), DAG directly activates protein kinase C (PKC). PKC is a pleiotropic protein kinase involved in numerous cellular processes, and discussed to inhibit the Wnt/β-catenin pathway[41]. Calcn further influences the activity of transcription factors such as NF-AT to regulate the induction of gene expression[42]. CamKII was shown to activate MAP kinases transforming growth factor beta (TGF-β) activated kinase-1 (TAK1) and nemo-like kinase (NLK)[43]. Especially TAK1 is associated with the activation of the NF-κB pathway[44], whereas NLK was shown to inhibit the Wnt/β-catenin pathway. The Wnt/Ca^{2+} signaling cascade has been associated with the regulation of cell proliferation and migration[45]. In addition, novel findings indicate a role of the Wnt/Ca^{2+} pathway in the regulation of pro-inflammatory responses[46;47].

Most tissues require positional information for their three-dimensional orientation and cellular alignment. The Wnt/planar cell polarity pathway (PCP) mediates the regulation of tissue polarity through cytoskeleton rearrangements but also regulates cell migration. The best studied example of active PCP signaling is the alignment of hair and fur. Many different factors participate in the regulation of the PCP pathway. However, the coordination and interaction of different signaling molecules involved in this pathway remain uncompletely understood[48]. It is most commonly accepted that after ligand binding Fzd receptors engage G proteins and/or Dvl proteins, which lead to the sequential activation of small GTPase Rho and Rho-associated kinase (ROCK) or the activation of the small GTPase Rac and c-jun N-terminal kinase (JNK)[48-50]. The PCP pathway leads to the activation of transcription factors AP-1 or c-Jun.

Besides the “classical” Wnt signaling cascades, which critically depend on Fzd receptor interaction, additional non-Frizzled receptors for Wnts have recently been described. These receptors include the receptor tyrosine kinases ROR2 and Ryk. ROR2 is characterized by an extracellular CRD and a kringle domain as well as an intracellular kinase and proline-rich domain. ROR2 was shown to induce a signaling cascade similar to the PCP pathway. Wnt5a was identified to bind ROR2 and activate c-Jun N-terminal kinase (JNK), thereby inhibiting β-catenin signaling[50]. In this study Wnt5a/ROR2 interactions were shown to target the expression of the paraxial protocadherin gene (*Papc*) which coordinates the polarity of cells during morphogenic movements. Thus, ROR2-deficient mice show skeletal, genital, lung and cardiovascular abnormalties[51]. Ryk features an extracellular domain similar to that of the Wnt inhibitory factor WIF (see above) and an intracellular PDZ-binding domain that is also present in the C-terminal moiety of Fzd receptors. In consequence, Ryk may either cooperate with Fzd receptors to induce β-catenin signaling or act autonomously as a guidance receptor during development of the central nervous system[52;53].

The Wnt/Fzd signaling network is controlled by multiple modes of regulation: The finding that Wnt and Fzd genes are differentially expressed in various tissues during all stages of the life cycle indicates a highly complex transcriptional control due to Wnt- and Fzd-inducing molecules. Post-translational modifications, such as acylation or glycosylation (e.g. through Porc or Wls), followed by intracellular trafficking

represent additional sites of regulation. It was shown that Fzd receptors were actively retained by the protein Shisa within the endoplasmatic reticulum, which was demonstrated to inhibit post-translational maturation and trafficking to the cell surface[28]. In addition, the protein GOPC (Golgi-associated PDZ and coiled-coil motif containing protein) has been observed to directly regulate the vesicle transport of Fzd receptors from the Golgi apparatus to the plasma membrane [54]. Secreted inhibitors may block the binding of Wnt proteins to their targeting cells. These inhibitors include soluble Frizzled-related proteins (sFRP), Wnt inhibitory factor (WIF), Sclerostin (SOST) or Dickkopf (DKK)[39]. Finally, Wnt ligands were shown to bind multiple Fzd receptors with varying affinities and initiating different signaling cascades, whose mediators are also subject to various modes of regulation. The multitude of positive or negative ways of regulation may explain the plethora of functions during and after development in which Wnt pathways are involved.

1.1.3 Frizzled1

Major parts of the current study were dedicated to the regulation and function of murine Fzd1. In mice Fzd1 is located on chromosome 5 (chromosome 7 in humans). The primary sequence of the receptor is comprised of 642 amino acids (647 aa in human Fzd1) resulting in an approx. mass of 70 kDa. Based on nucleotide sequence homology, its most closely related paralogs are Fzd2 (78% identity) and Fzd7 (77% identity). Fzd1 contains two putative N-linked glycosylation sites within the N-terminal cysteine rich domain (Asn125, Asn226). The C-terminal tail of Fzd1 includes the KTXXXW-motif (PZD-binding site) and is composed of 25 amino acids. Thus, Fzd1 possesses the shortest C-terminal moiety of the known Fzd homologs.

The Wnt homologs Wnt3a and Wnt7b were demonstrated to bind to Fzd1[55;56]. In addition, Fzd1 may also bind *Xenopus* ortholog XWnt8 or the *Drosophila* ortholog Wg[57;58], indicating its evolutionarily conserved origin. Many reports have shown that the Wnt/β-catenin pathway is activated upon stimulation of Fzd1. However, Bikkavilli and colleagues indicated that besides the β-catenin pathway Wnt3a may also stimulate the PCP pathway in murine ES cells transfected with Fzd1[27].

Fzd1 was shown to require G protein subunits $G\alpha_o$ and $G\alpha_q$ for signal transduction[59]. Yet, reports on physiological functions of Fzd1 in primary cells are scarce. According to phenotypic analyses of LacZ reporter mice, the Fzd1 promoter is active in various tissues and organ systems including the central nerve system, urinary bladder and

blood vessels[60]. Highest mRNA levels were detected in various organ systems including the lung, the kidneys, the skin and the female reproductive tract[60]. As reported in a recent review, Fzd1 knockout mice seem to be viable. However, the authors refer only to personal communications, since no phenotype of Fzd1-deficient mice has been published[61].

Induction of Fzd1 mRNA was first reported in rat osteoblastic osteosarcoma cells (UMR 106), where it was induced by parathyroid hormone (PTH) or epidermal growth factor (EGF). The authors suggested an involvement of Fzd1 in bone morphogenesis and differentiation[62;63]. To date, additional reports have demonstrated that growth factors play an important role in the regulation and induction of Fzd1 during development. Especially TGF-β superfamily member bone morphogenic protein (BMP2) was shown to directly modulate Fzd1 expression and is generally known to be interconnected with Wnt/Fzd signaling pathways[64;65]. Regulation of Fzd1 expression by growth factors was best characterized during bone and cartilage formation as well as development of vasculature[56;66]. Fzd1 was also shown to be induced by luteinizing hormone (LH) during ovogenesis, where it was implicated in the modulation of the ovulatory phase[67]. Different growth factors and hormones were demonstrated to activate homeobox genes (*Hox*), which encode transcription factors highly involved in developmental processes such as self-renewal and expansion of hematopoietic stem cells (HSC)[68]. It was demonstrated that overexpression of homeobox genes *Hoxa9* and *Hoxa10* induced Fzd1 transcription in human umbilical cord $CD34^+$ cells, implicating a function of Fzd1 in the self-renewal and differentiation of HSC.

Fzd1 expression was mostly demonstrated by mRNA analyses. On protein level, an increased expression of Fzd1 was repeatedly detected in pathophysiological settings. Based on immunohistochemical analyses, the receptor was identified in malignant human breast tissue[69] and at the invasion front of different types of poorly differentiated colon cancers[70;71]. Apart from the context of tumor progression, which is highly linked with aberrant Wnt/Fzd signaling, Chacón and colleagues localized Fzd1 in various regions of the hippocampus of Alzheimer's disease patients[72].

1.1.4 The Wnt/β-catenin signaling pathway

Deletion of β-catenin in mice causes a lethal phenotype prior to gastrulation of the blastula, indicating the very fundamental function of this pathway and its essential

role in developmental processes[73]. During early embryogenesis, β-catenin determines the formation of the body axis and is a prerequisite for mesoderm formation[74;75]. Different loss- and gain-of-function mutations in mice have shown the involvement of β-catenin signaling in limb and organ formation[75;76-79]. In *Drosophila*, Wg/β-catenin signaling was demonstrated to govern developmental processes through the establishment of a Wg gradient by altering gene expression in a concentration-dependent manner. Thereby Wg/β-catenin signaling elicits different responses at various distances from the Wg-secreting cell[19;80;81].

It is well known that β-catenin signaling is highly active in various stem cell populations involved in the maintenance of tissue homeostasis. Active regions of stem cell niches include paneth cells in crypts of gut mucosa, plaques of the skin, osteoblasts/osteoclasts in bone, or hematopoietic stem cells[3;82]. Thus, aberrant β-catenin signaling is often associated with different types of tumors, such as colon cancer, hair follicle tumors, diseases of altered bone mass or leukemia[83;84]. Wnt/β-catenin signaling controls the expression of target genes such as *Oct4, Sox2, Nanog* or *C-myc*, which regulate cell cycle decisions[85]. These genes encode transcription factors that are utilized in a novel *in vitro* system to generate pluripotent stem cells (IPSCs, inducible pluripotent stem cells) from epidermal fibroblasts[86;87]. Its very essential function on self-renewal cells has made the Wnt/β-catenin pathway an attractive target for cancer research and regenerative medicine.

In regenerative medicine hematopoietic stem cells (HSCs) and mesenchymal stem cells (MSCs) are of special interest, because both represent multipotent stem cell populations in the adult. Stimulated by Wnt/β-catenin signals, MSCs possess a high potential of tissue remodeling and wound healing, which is due to its capability to differentiate into several mesenchymal cell types (e.g. fibroblasts, osteoblasts, adipocytes, or muscle cells) and tissues[88;89]. MSCs were shown to interact with HSCs and to mediate immunosuppressive functions on antigen-specific T cells[90]. Thus, β-catenin pathways may be linked to immunoregulatory functions. With regard to HSC and hematopietic cells, Wnt/β-catenin pathways were recently shown to regulate the differentiation of T and B cells, activation of regulatory T cells as well as dendritic cell maturation [82;91]. Moreover, the role of β-catenin signaling in immune cells and inflammation has become a new field of interest that may provide novel treatment approaches, such as the use of MSCs as immunosuppressants in chronic autoimmune diseases[89;92;93]. Many cancers and chronic autoimmune diseases, in

which mediators of the β-catenin pathway were shown to be enhanced or reduced, are suggested to result from repetitive tissue inflammation leading to (stem) cell injury. Thus, misguided β-catenin signaling in pathophysiology may reflect aberrant functions of the Wnt/β-catenin pathway to maintain tissue homeostasis.

Of note, it has been reported that stimulation of human monocytes with lipopolysaccharide (LPS) led to β-catenin stabilization and target gene expression by members of the Tcf/Lef family[94]. LPS was also demonstrated to inhibit GSK-3β and to induce β-catenin signaling in human alveolar macrophages[95]. Since the inflammatory effects of conserved bacterial structures on human macrophages are well characterized, the authors suggested a role of β-catenin signaling in the regulation of innate immunity and inflammation.

1.2 The role of pattern recognition receptors in bacterial infection

The innate immune system is the first line of defense in microbial infections, of which macrophages, dendritic cells, mast cells, natural killer cells and granulocytes are its most prominent cell populations[96]. The innate immune system is equipped with pattern recognition receptors (PRR) which specifically recognize pathogen-associated molecular patterns (PAMPs) of invading microbes[97]. PRRs are allocated in three different compartments: the extracellular compartment, the intracellular compartment and the plasma membrane of innate immune cells. Soluble receptors of the extracellular compartment belong to the family of pentraxins or represent components of the complement system. Recognition of conserved microbial structures such as lipopolysaccharide (LPS), lipoteichoic acids (LTA) or zymosan may lead to the activation of complement pathways. Depending on the activation of the complement system, intruding microbes may be lysed or opsonized for phagocytic clearance[98;99]. Important cytoplasmatic PRRs are members of the NLR-(nucleotide-binding oligomerization domain-like receptors) and RLR-family (retinoic acid-inducible gene-like receptors). The latter are involved in the recognition of viral nucleic acids and anti-viral defense[100]. Members of the NLR-family are NOD1 and NOD2 (nucleotide-binding oligodimerization domain) that detect peptidoglycan of Gram-positive and Gram-negative bacteria. Further members of the NLR-family include NALP-proteins (NACHT-LRR-PYD-containing proteins), which sense conserved structures of bacteria, viral RNA and also endogenous signals of necrotic

cells[101]. Among the antimicrobial functions of the innate immune system, phagocytosis is one of the most important mechanisms in the elimination of pathogens. Phagosomal uptake is mediated by neutrophil granulocytes, macrophages and dendritic cells. Certain PRRs within the plasma membrane of phagocytes enable the cells to internalize pathogens but also apoptotic cells. These receptors include members of the C-type lectins, such as the mannose receptor (MR) or DC-SIGN, as well as scavenger receptors (e.g. SRA, CD36, or MARCO), which possess a broad ligand specificity[99]. A major function of macrophages and dendritic cells is to process microbial antigens in the phagolysosome for presentation by MHC (major histocompatibility complex) class II molecules to antigen-specific $CD4^+$ T cells. In addition, antigens primarily processed within the cytoplasm are presented to antigen-specific cytotoxic T cells via MHC class I molecules.

Besides membrane associated PRRs that directly stimulate phagosomal uptake, others exclusively induce signaling cascades upon recognition of PAMPs. The family of Toll-like receptors (TLRs) senses a broad spectrum of ligands, that covers conserved structures of viruses, bacteria, fungi and parasites[102]. Toll-like receptors are highly conserved among vertebrates and invertebrates. Upon activation, TLRs initiate a network of numerous signaling cascades that critically support an efficient immune response. The number of TLR homologs within a single species may vary from 1 (*Coenorhabditis elegans*) to 222 in the sea urchin *Strongylocentrotus purpuratus*[103]. 10 TLR homologs are known in humans (TLR1 – 10) and 12 homologs in mice (TLR1 - 9, TLR11 - 13)[104], of which TLR1, TLR2, TLR4, TLR5, TLR6 and TLR9 are most critical for the recognition of conserved bacterial structures.

TLR2 was reported to mediate signaling cascades following activation by conserved structures of Gram-positive bacteria[105]. After recognition of ligands, TLR2 heterodimerizes with co-receptors TLR1 or TLR6, which in the absence of TLR2 are not capable of inducing a signaling cascade[106]. Different PAMPs were described to bind and activate TLR2: lipoteichoic acids (LTA), peptidoglycan (PG), phosphatidyl myo-inositol mannosides (PIM) and lipoarabinomannan (LAM) from mycobacteria[107;108]. In addition, eukaryotic structures were also reported to be recognized by TLR2: glycolipids such as lipophosphoglycans of parasites (*Leishmania major*) or polysaccharides from yeasts, e.g. zymosan (*Saccharomyces cervisiae*)[109;110]. The lipopeptide Pam_3CSK_4 can be produced synthetically, avoiding contamination with additional bacterial structures. It resembles the aminoterminal

moiety of lipoproteins, which are located in high amounts within the bacterial cell wall. Synthetic lipopeptides represent the smallest units shown to activate TLR2[111;112]. Recent publications demonstrateds that lipoprotein or lipopeptide derivates may be the only conserved structures likely to directly bind and activate TLR2 and associated co-reptors TLR1 or TLR6[113-115]. Based on crystal structure analyses, Jin et al. provided evidence that the three lipid chains of Pam_3CSK_4 were prerequisite to mediate heterodimerization of TLR2-TLR1[116]. Thus, published TLR2 ligands such as PG are currently controversially discussed.

Another well-characterized Toll-like receptor is TLR4, which, together with its essential co-receptor MD-2 (myeloid differentiation protein-2), mediates signal transduction in response to lipopolysaccharide (LPS) of Gram-negative bacteria[111;117]. The only ligand that has been shown to stimulate TLR5 is flagellin, which is the major component of the bacterial flagellum. Different from TLR2, -4 and -5, which are located within the plasma membrane, TLR9 is present in the endosomal compartment, where it is activated upon binding to unmethylated (CpG motif) double stranded bacterial or viral DNA.

The central signaling pathway of TLR induced cell activation leads to the translocation of transcription factor NF-κB into the nucleus[118] (Fig. 2). Agonist-induced dimerization of TLRs leads to conformational changes of the intracellular Toll/Interleukin-1-receptor (TIR-) domain, thereby recruiting different adapter proteins[119]. To date 5 adapter proteins are known to mediate signaling cascades, of which myeloid differentiation primary response gene 88 (MyD88) is shared by all TLR homologs except TLR3[120]. Binding adaptor proteins via TIR-TIR interactions leads to sequential recruitment and activation of MyD88 adapter-like protein (MAL, also known as TIRAP), MyD88, IL-1-receptor associated kinases (IRAK1, 4) and TNF receptor-associated factor 6 (TRAF6)[104]. This signaling cascade further activates TGF-β-activated kinase 1 (TAK1, in association with TAK binding proteins1-3 (TAB)), which then phosphorylates subunit IKKβ of the IKK complex (IκB kinase complex composed of IKKα, -β, -γ). In the absence of a signal, subunits p50 and p65 of the NF-κB family are associated with inhibitory IκB proteins (e.g. IκBα). Following activation, IKK phosphorylates IκB and targets these inhibitory proteins for degradation by the proteasome, thereby allowing p50/p65 dimerization and translocation into the nucleus. The MyD88-dependent signaling pathway may also stimulate further mitogen-activated protein kinases (MAPKs) through TAK1

phosphorylation, resulting in the activation of the transcription factor AP1[104]. In addition to MyD88-dependent signaling cascades, TLR4 activation also includes activation of adapter protein TRIF (TIR domain containing adapter inducing interferon-β; Fig. 2). The TRIF-dependent pathway sequentially recruits adapter proteins TRAM (TRIF-related adapter molecule) and TRIF, which activate IKKε and TBK1 (TRAF family member-associated NF-κB activator-binding kinase 1), leading to the phosphorylation and dimerization of transcription factor interferon regulatory factor 3 (IRF3). Translocation of IRF3 induces gene expression of type I interferons[104]. TRIF also intersects with the MyD88-dependent pathway through TRAF6 and RIP1 (receptor-interacting protein 1), which mediate NF-κB activation[120] (Fig. 2). NF-κB induces the expression of a large array of pro-inflammatory target genes[121], such as *Tnf* or *Interleukin* 12 (IL-12). These genes encode cytokines that are strong inducers of an appropriate immune response in the defense against most pathogens. Its multiple functions include the recruitment and activation of additional immune cells and the stimulation of the adaptive immune system. The successful interplay between the innate and adaptive immune system is essential to mount an efficient immune response.

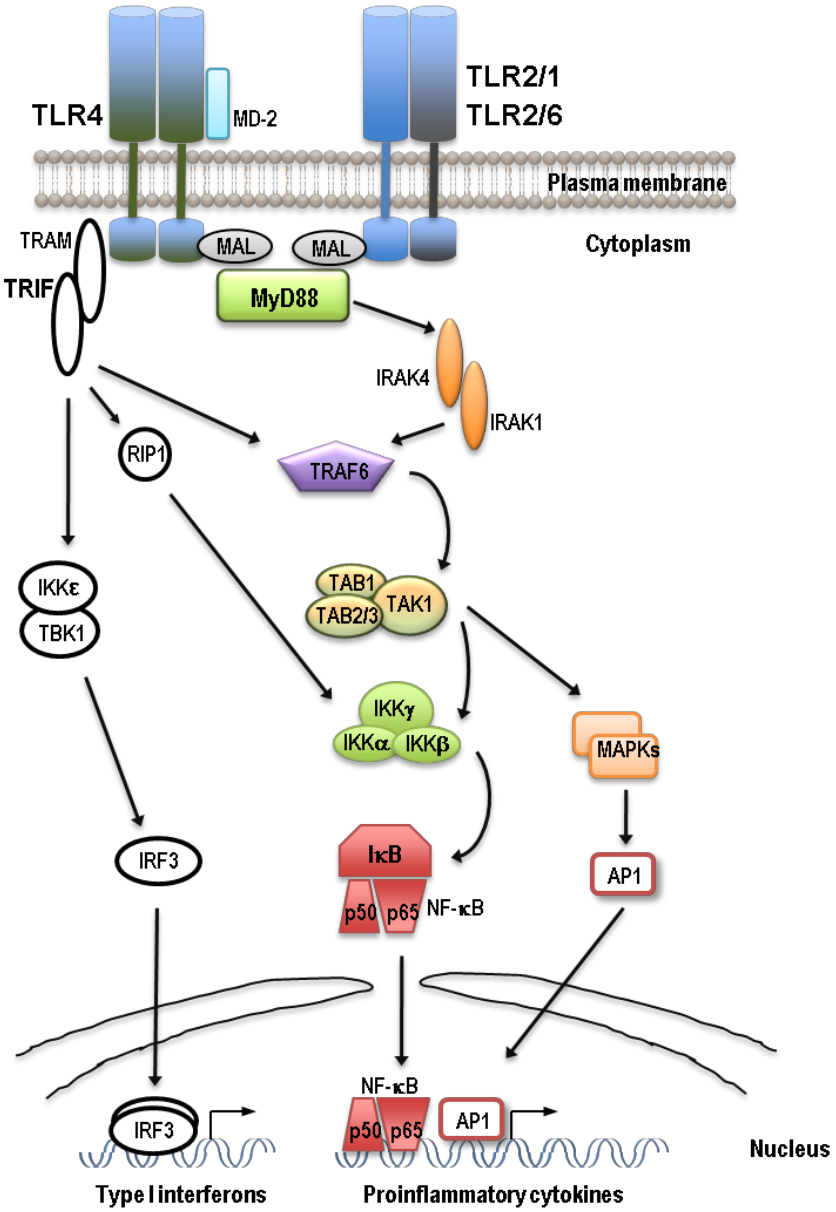

Figure 2: Signaling cascades of TLR2- and TLR4-induced cell activation.
The MyD88-dependent pathway activates transcription factors NF-κB and AP1, which promote gene expression of pro-inflammatory cytokines. Stimulation of TLR4 also induces TRIF-dependent pathways (open circles). Activation of TRIF leads to the phosphorylation and dimerization of transcription factor IRF3, which implements gene expression of type I interferons. In parallel the TRIF-dependent pathway induces NF-κB activation through the proteins RIP1 and TRAF6. The detailed figure is described in more detail in the text (modified after Akira et al., 2006)[104].

1.3 The role of macrophages in mycobacterial infection

According to the World Health Organization (WHO), it is estimated that one third of the world's population (approx. 2 billion people) is infected with tubercle bacilli. The actual WHO report on global tuberculosis control indicates 9.27 million new cases of TB in 2007 and 1.58 million deaths, which ranks tuberculosis as the bacterial-induced infectious disease with the highest prevalence and mortality. Tuberculosis is caused

by closely related bacterial species that are represented within the *Mycobacterium tuberculosis* complex (MTBC). Besides its best studied member *M. tuberculosis*, the MTBC is comprised of *M. africanum*, *M. microti*, *M. caprae* and *M. bovis*[122]. Acid fast bacilli of the genus *Mycobacterium* are classified to the phylum of *Actinobacteria* (Gram-positive high in G+C ratio). Infection with *M. tuberculosis* is primarily due to droplet transmission. Whereas 90% of the infected individuals remain latently infected during their lifetime, 10% will develop active TB. Latent infection may be conceived as a lifelong persistence of mycobacteria that are contained within granulomatous lesions by an effective immune response of the host.

Other mycobacteria such as *M. avium* are opportunistic pathogens, which especially affect immuno-compromised individuals. It is mostly isolated from AIDS patients, but may also affect infants, elderly people or patients with chronic lung diseases[123-125]. *M. avium*-infection or infection with additional members of the *Mycobacterium avium* complex (MAC) is associated with non-tuberculous mycobacteria (NTM) disease. Despite different modes of transmission, the symptoms of NTM disease are reminiscent of tuberculosis that include coughing, chest pain, fever, weight loss and night sweats[126].

A characteristic feature of tuberculosis is the formation of granulomatous lesions (tubercle = little node, nodule, granuloma), which represent a focal accumulation of mononuclear cells for the local containment of mycobacteria at the site of infection[127]. The center of a granuloma consists of infected macrophages and other mononuclear cells that may fuse to form multinuclear giant cells. It is surrounded by T cells, B cells, often assembled in aggregates, as well as fibroblasts which may produce a fibrous cuff. At later stages of the disease the center contains characteristic caseous detritus composed of necrotic tissue, cell debris and both, viable and dead mycobacteria. Granulomas are rather dynamic structures, as immune cells constantly move in and out of the lesion[128]. The maintenance of a granuloma is tightly regulated by the local production of cytokines and chemokines, such as TNF, IFN-γ and RANTES or MCP-1. Experiments using TNF as well as TNF receptor deficient mice demonstrated a pivotal role of TNF in the initiation, and also in the maintenance of the granuloma structure[129;130].

Even though tuberculosis is a systemic disease and can manifest in various tissues and organs, it is primarily associated with the respiratory system[131]. The number, size and location of necrotizing lesions in the lung determine the extent of disease that

may result in the destruction of large parts of lung tissue and may eventually cause the loss of pulmonary function[132]. In addition, the caseous center of a granuloma may liquefy and rupture, spreading the contained bacterial load into the bronchi. The release of mycobacteria into an oxygen-enriched environment further accelerates the mycobacterial growth and intrapulmonary dissemination[132]. A tuberculosis patient becomes contagious, when mycobacteria-containing droplets are actively transmitted by exhalated aerosols, e.g. by coughing of softened caseum.

Following inhalation, mycobacteria are primarily taken up by alveolar macrophages. Macrophages are the preferred habitat of *M. tuberculosis*, in which the bacteria persist and replicate. Thus, the pathogens have evolved mechanisms to prevent antimicrobial functions of these professional phagocytes. Commonly, phagocytosis of bacteria leads to the maturation and fusion of the phagosome with the lysosome, resulting in a microenvironment that is detrimental to most microbes. The lysosomal compartment contains several hydrolases capable of degrading microorganisms at acidic conditions (pH 4.5). *M. tuberculosis* actively arrests phagosomal maturation and thereby generates conditions for its intracellular survival[133]. Successful containment of mycobacterial growth and killing of mycobacteria requires the recruitment of additional effector cells, such as activated monocytes, neutrophils and T-lymphocytes to the center of inflammation. The release of TNF plays an essential role in the cell-mediated immunity against *M. tuberculosis*. Early after the initial contact to mycobacteria and its conserved structures, macrophages produce large quantities of TNF[134;135]. In a paracrine manner, the cytokine affects the surrounding tissue and vasculature and increases the extravasation of inflammatory cells to the infectious foci[136;137]. This is achieved by reducing the blood flow of neighboring blood vessels and enhancing the permeabilitiy of the vascular wall, as well as the expression of adhesion molecules on endothelial cells. In addition, TNF further stimulates the secretion of chemokines and chemokine receptors, thus regulating the recruitment of immune cells from the blood stream to the site inflammation along a chemokine gradient. Chemokines prominently up-regulated by TNF are MCP-1 (monocyte chemoattractant protein), MIP-1α and MIP-1β (macrophage inflammatory protein), or RANTES that bind to receptors CCR2 and CCR5[131;138;139].

Another major cytokine of the early innate immune response is interleukin-12 (IL-12), which supports the differentiation of naïve $CD4^+$ T cells into type 1 T-helper (T_h1) cells and stimulates secretion of interferon-γ (IFN-γ) by lymphocytes[140]. T_h1 cells are

the backbone of the adaptive immune response against *M. tuberculosis* infection, orchestrating multiple antimicrobial functions[141;142]. Among these functions, secretion of IFN-γ seems to be most essential[143;144]. IFN-γ released by lymphocytes (including CD4, CD8 T cells and natural killer (NK) cells) acts synergistically with TNF leading to the activation of inducible nitric oxide synthase (NOS2 or iNOS) in macrophages[145]. NOS2 uses L-arginine as a substrate to catalyze the formation of nitric oxide (NO) and reactive nitric oxide intermediates (RNI), thus enabling the macrophage to kill mycobacteria[146;147]. Yet, experiments comparing NOS2-deficient mice with IFN-γ knockout mice indicated that prolonged survival of knockout mice was affected by additional IFN-γ-dependent functions independent of the induction of NOS2[131]. In this context it was shown that IFN-γ induces autophagy in mycobacteria-containing macrophages to eradicate *M. tuberculosis*[148]. Belonging to the 47-kDa guanosine triphosphatase family, LRG-47 was suggested to be involved in these processes[149]. IFN-γ was demonstrated to activate LRG-47, which was shown to function as a critical vacuolar trafficking protein involved in the disposal of intracellular pathogens[150]. Taken together, these data demonstrate that a tight regulation of innate and adaptive immune defenses is a prerequisite for an effective control of mycobacterial growth.

1.4 Wnt/Fzd signaling in *M. tuberculosis* infection

In 2000, it was first discovered that Wnt/Fzd signaling contributed to chronic inflammation in rheumatoid arthritis patients[151]. It took another five years until it was first demonstrated that Wnt/Fzd signaling was directly linked to microbe-induced immune responses[152]. Analyzing the immune response after *M. tuberculosis* infection of macrophages *in vitro*, Blumenthal et al. showed that the human innate and adaptive immunity were regulated by Wnt and Fzd homologs, in this particular case, by Wnt5a and Fzd5[153]. Subsequent reports corroborated these initial findings, additionally demonstrating the role of Wnt/Fzd signaling in pro-inflammatory cytokine secretion, the recruitment of immune cells and cell migration[91;154]. In the current study, the established mouse model of experimental *M. tuberculosis* infection was used to analyze the regulation of Wnt/Fzd signaling and its involvement in the cell-mediated immune response *in vitro* and *in vivo*.

1.5 Objectives

Wnt/Frizzled signaling pathways are largely unexplored in infectious or inflammatory settings. In the current work first experiments indicated an up-regulation of transcripts of the murine heptihelical transmembrane receptor Frizzled1 in response to experimental *Mycobacterium tuberculosis* infection *in vivo*. For that reason *in vitro* studies were carried out to investigate the mechanisms leading to the induction of the receptor.
The first aim of the current study was to answer the question:

- Do mycobacteria and conserved bacterial structures stimulate Frizzled1 expression in macrophages, and which signaling cascades are involved?

Stimulation of Frizzled1 with Wnt ligands is closely associated with the induction of Wnt/β-catenin signaling. Despite intensive studies on this signaling pathway, its function in the regulation of innate immune responses has scarcely been characterized.
Therefore the second part of this study focused on the questions:

- Does activation of the Wnt/β-catenin pathway influence murine macrophage effector functions?
- How does *M. tuberculosis* infection affect Wnt/β-catenin signaling in the mouse model?

2. Material and Methods

2.1 Material

2.1.1 Laboratory equipment

Autotechnicon	(PathCentre; SHANDON, Pittsburgh, PA, USA)
Cell counter	(CASY2 TT; SCHÄRFE SYSTEM, Reutlingen)
Centrifuge	(Rotanta460R; HETTICH, Hanau)
Centrifuge	(MIKRO22R; HETTICH)
Centrifuge	(MIKRO200R; HETTICH)
Digital camera	(Digital Sight DS-Ri1 & DS-L1; NIKON, Düsseldorf)
ELISA-reader	(Synergy 2; BIOTEK, Winooski, VT, USA)
Elutriation rotor	(JE-6B-rotor; BECKMAN, München)
Flow cytometer	(FACS Calibur; BD BIOSCIENCES, Heidelberg)
Incubation chamber	(THERMO SCIENTIFIC, Rockford, IL, USA)
Infection cages	(MARINE- & INDUSTRIETECHNIK - MIT, Hamburg)
Inhalation system	(Modell 099C A4224; GLAS-COL, Terre Haute, IN, USA)
Laminar airflow cabinet	(THERMO SCIENTIFIC)
Luminometer	(Biolumat LB 9505, BERTHOLD, Wildbad)
Microscope	(Leica DM LB; LEICA, Nussloch)
Microscope	(ZEISS, Oberkochen)
Mini-Trans Blot cell	(BIO-RAD, München)
Odyssey detection system	(LI-COR, Lincoln, NE, USA)
Orbital shaker	(KS 260; IKA, Staufen)
PAGE-system	(Mini-Protean Tetra cell; BIO-RAD)
Peristaltic pump	(Thomafluid E25; RTC, Heidelberg)
Pipettes	(EPPENDORF, Hamburg)
Pipette aid	(Pipetboy; INTEGRA BIOSCIENCES, Fernwald)
Potter	(GLAS-COL)
Rotary microtome	(Leica RM2155; LEICA)
Rotary cryo-microtome	(Leica CM1850; LEICA)
Spectrophotometer	(NanoDrop ND-1000; PEQLAB, Erlangen)
Thermocycler	(C1000 thermal cycler; BIO-RAD)
Thermocycler	(LightCycler; ROCHE, Mannheim)

Thermocycler	(LightCycler 480; ROCHE)
Thermomixer	(Thermomixer compact; EPPENDORF, Hamburg)
Tissue embedding center	(Leica EG1140C; LEICA)
3D Tumbling shaker	(Polymax 1040; HEIDOLPH, Schwabach)
Ultrasonic bath	(35 kHz; BANDELIN, Berlin)
Waterbath	(GFL1052; GFL, Burgwedel)
Waterbath	(SW 20; JULABO, Seelbach)

2.1.2 Laboratory supplies

Centrifuge tubes	(15 ml, 50 ml; SARSTEDT, Nümbrecht)
Culture dish	(10 cm ∅, SARSTEDT)
FACS tube	(Falcon 5 ml; BD BIOSCIENCES, Heidelberg)
Filter unit	(pore size ∅ 0.45 µm; SARSTEDT)
Flat-bottom micro plate	(6-well, 24-well; NUNC, Roskilde, Denmark)
Glass capillaries	(ROCHE, Mannheim)
Glass slides/ Coverslips	(LANGENBRINCK, Emmendingen)
Histogrid	(SIMPORT, Bernard-Pilon, Canada)
LightCycler multiwell plate	(96-well; ROCHE, Mannheim)
Lumi vials	(3 ml; BERTHOLD, Wildbad)
Maxi Sorp micro plate	(96-well; NUNC, Roskilde, Denmark)
Micro tubes	(1,5 & 2,0 ml; SARSTEDT)
Needles/ Syringes	(BD BIOSCIENCES)
Neubauer chamber	(BRAND, Wertheim)
Nunclon surface dish	(Nunclon™D-Surface; NUNC)
PCR reaction tubes	(0.2 ml lid chain; SARSTEDT)
Pipettes	(Steripette 5 to 25 ml; SIGMA-ALDRICH)
Pipette tips	(10 to 1000 µl; SARSTEDT)
Pestle/ Potter tubes	(RETTBERG, Göttingen)
Round-bottom micro plate	(96-well; NUNC)
Teflon coated Cell culture bag	(VueLife™ 72; CELLGENIX, Freiburg)
Tissue culture flask	(75 cm^2; SARSTEDT)
V-bottom micro plate	(96-well; NUNC)

2.1.3 Reagents, buffer solutions and media

2.1.3.1 Reagents

Acetone	(MERCK, Darmstadt)
Acrylamide/Bisacrylamide	(40% solution; SERVA, Heidelberg)
Alfazyme solution	(PAA, Pasching, Austria)
Ammonium acetate	(MERCK)
Ammonium persulfate	(APS; SERVA)
Aqua ad injectabilia	(sterile, pyrogen- and RNase-free; B. BRAUN MELSUNGEN AG, Melsungen)
Aqua bidest	(double deionized water; Research Center Borstel)
Bovine serum albumin	(BSA; SIGMA-ALDRICH, Deisenhofen)
Brain heart infusion agar	(DIFCO, Heidelberg)
Bromophenol blue	(SERVA)
Bromochloropropane	(BCP; SIGMA-ALDRICH)
Citric acid	(MERCK)
3,3'-Diaminobenzidine tablet set	(DAB Sigma FAST; SIGMA-ALDRICH)
N,N-dimethylformamide	(PERSPECTIVE BIOSYSTEMS, Hamburg)
Dimethylsulfoxid	(DMSO, SIGMA-ALDRICH)
Dithiothreitol	(DTT; SIGMA-ALDRICH)
Dulbecco´s Modified Eagle's Media	(DMEM high glucose; PAA)
Ethylene glycol tetraacetic acid	(EGTA; SIGMA-ALDRICH)
Fetal calf serum	(FCS, heat inactivated (30 min, 56°C); BIOCHROM, Berlin)
Formalin	(37%; MERCK)
Kaiser's glycerol gelatine	(MERCK)
L-glutamine	(BIOCHROM)
Lithium chloride	(SIGMA-ALDRICH)
Low fat dried milk	(GABLER-SALITER GMBH, Obergünzburg)
Lucigenin	(9,9`-bis-(N-methylacridinium nitrate); ROCHE)
G418	(BIOCHROM)
Glycine	(SERVA)
Glycogen	(ROCHE)

Glycerol	(MERCK)
HBSS	(Hanks' balanced salt solution; PAA)
HEPES	(4-(2-hydroxyethyl)-1-piperazineethanesulfonic acid; PAA)
Hematoxylin staining solution	(modified after Gill; MERCK)
Hydrochloric acid	(MERCK)
Hydrogen peroxide	(MERCK)
Igepal CA-630	(SIGMA-ALDRICH)
2-mercaptoethanol	(SIGMA-ALDRICH)
Methanol	(MERCK)
Middlebrook 7H9	(DIFCO)
Middlebrook 7H10 Agar	(DIFCO)
Nutrient Broth	(DIFCO)
Nitrocellulose membrane	(SARTORIUS, Göttingen)
Oleic acid, Albumine, Dextrose, Catalase	(OADC; BECTON DICKINSON, Heidelberg)
Paraformaldehyde	(PFA; MERCK)
Penicilline/Streptomycine	(BIOCHROM)
Phenol/guanidine isothiocyanate solution	(TriFast; PEQLAB, Erlangen)
Ponceau solution	(THERMO SCIENTIFIC)
Potassium chloride	(SIGMA-ALDRICH)
Potassium ferrocyanide	(SIGMA-ALDRICH)
2-propanol	(MERCK)
Protease inhibitor	(Complete; ROCHE)
Protein molecular weight standard	(broad range 6.5-175.0 kDa, NEW ENGLAND BIOLABS, Schwalbach)
Roti Block	(10 x concentrated; ROTH)
Sodium azide	(MERCK)
Sodium chloride	(MERCK)
Sodium deoxycholate	(SIGM-ALDRICH)
Sodium dodecyl sulfate	(SDS; AMERSHAM BIOSCIENCES)
Sodium glutamate	(MERCK)
Sodium hydrogen carbonate	(MERCK)
Sodium pyruvate	(PAA)
Spermidine HCL	(SERVA)

Stripping solution	(THERMO SCIENTIFIC)
Sucrose	(SIGMA-ALDRICH)
Sulfuric acid, 95-97%	(MERCK)
SYBR green	(INVITROGEN, Carlsbad, CA, USA))
3,3`,5,5`-Tetramethylbenzidine	(TMB; SIGMA-ALDRICH)
N,N,N`,N`-Tetramethylethylendiamine	(TEMED; SERVA)
Thimerosal	(ROTH, Karlsruhe)
Tissue freezing medium	(JUNG, Nussloch)
Tris(hydroxymethyl)-aminomethan	(SERVA)
Trypan blue	(SIGMA-ALDRICH)
Trypsin-EDTA solution	(0,05% Trypsin, 0,02% EDTA (w/v) in PBS; BIOCHROM)
Tween 20	(SIGMA-ALDRICH)
Tween 80	(SIGMA-ALDRICH)
Water PCR-grade	(ROCHE)
Western blot filter paper	(SCHLEICHER & SCHUELL, Dassel)
X-gal (5-bromo-4-chloro-3-indoly β-D-galactoside)	(INVITROGEN)
Xylene	(MERCK)

2.1.3.2 Stimuli

Mycobacteria: Mycobacterial strains *M. avium* (strain SE01)[155] and *M. tuberculosis* (strain H37Rv, ATCC 9679/00) were grown in Middlebrook 7H9 medium (DIFCO) containing 10% OADC (oleic acid, albumine, dextrose, catalase; BD BIOSCIENCES), 0.5% glycerol and 0.05% Tween 80 (SIGMA-ALDRICH). The optical density was measured at a wavelength of 600 nm (OD_{600}) and midlog phase cultures were harvested at an OD_{600} = 0.4. Cells were then frozen at -80°C until use. To determine the number of CFU per ml, aliquots of frozen culture were thawed and homogenized using a sterile 1 ml syringe with 26 gauge needle (BD BIOSCIENCES). Serial dilutions were prepared and 100 µl of diluted culture were plated onto Middlebrook 7H10 agar plates containing 10% heat inactivated bovine serum (BIOWEST) for colony enumeration after 19 to 21 days of incubation at 37°C. To rule out the presence of lipopolysaccharide (LPS), all strains were tested with a *Limulus*

amebocyte lysate assay (BIOWHITTAKER, Walkersville, MD). The effective LPS concentration in the experiments at inoculum ratios of 10:1 was below 2 pg/ml.
For *in vitro* experiments, bacterial aliquots were thawed, homogenized using a sterile 1 ml syringe with 26 gauge needle (BD BIOSCIENCES), centrifuged for 10 min at 835 x g and resuspended in PBS.

LPS: *Salmonella enterica* derived lipopolysaccharide (LPS; serotype Friedenau H909) was kindly provided by Prof. Dr. H. Brade, Research Center Borstel.

Pam_3CSK_4: Synthetic lipohexapeptide (Pam_3CSK_4; [(S)-[2,3-Bis(palmitoyloxy)-(2-RS)-propyl]-N-palmitoyl-(R)-Cys-(S)-Ser-(S)-Lys_4-OH]) is an analog to triacylated lipopeptides of Gram-positive bacteria[111;156] and was kindly provided by Prof. Dr. K.-H. Wiesmüller (EMC Microcollections, Tübingen, Germany).

Zymosan: *Saccharomyces cervesiae* derived zymosan was acquired from SIGMA-ALDRICH, Deisenhofen.

2.1.3.3 Recombinant proteins and antibodies

Cytokines

- Human macrophage colony-stimulating factor (rh M-CSF; R&D SYSTEMS)
- Murine interferon gamma (rm IFN-γ; PEPROTECH, Rocky Hill, NY)
- Murine interleukin 10 (rm IL-10; PEPROTECH)
- Murine tumor necrosis factor alpha (rm TNF-α; PEPROTECH)
- Murine TNF-α (standard used in ELISA; R&D SYSTEMS)

Recombinant Wnt/Frizzled proteins:

- Murine Frizzled1/Fc fusion protein (R&D SYSTEMS)
- Murine Wnt3a (rm Wnt3a; R&D SYSTEMS)

Enzymes

Taq-DNA-polymerase (INVITROGEN)

Detection reagents used in Western Blot analysis

For Western Blot analysis, the following primary mono- and polyclonal antibodies were used in combination with fluorochrome-labeled (AlexaFluor680 or IRDye800) secondary reagents for near infrared detection using an Odyssey detection system (LICOR) (Tab.1):

Tab.1: Detection reagents used in Western blot analysis

Description	Host / Isotype	Target Size	Conjugation	Supplier	Dilution [Stock]
			Primary Antibodies		
mouse β-catenin MAb	Mouse IgG1	~ 92 kDa	-	BD BIOSCIENCE	1:1000 [250µg/ml]
human / mouse Frizzled1 MAb	Rat IgG2a	~71 kDa	Biotin	R&D SYSTEMS	1:500 [200µg/ml]
human / mouse GAPDH MAb	Mouse IgG1	~ 35 kDa	-	HYTEST	1:20.000 [2mg/ml]
mouse iNOS polyclonal	Rabbit IgG	~ 125 kDa	-	MILLIPORE	1:1000 [410µg/ml]
mouse Wnt3a MAb	Rat IgG2a	~ 39 kDa	-	R&D SYSTEMS	1:500 [200µg/ml]
			Secondary Antibodies		
Anti-mouse	Goat IgG	-	AlexaFluor680	MOL. PROBES	1:10.000 [1mg/ml]
Anti-rabbit	Goat IgG	-	IRDye800	ROCKLAND	1:10.000 [1mg/ml]
Anti-rat	Sheep IgG	-	IRDye800	ROCKLAND	1:10.000 [1mg/ml]
			Streptavidin Conjugate		
Biotin	-	-	AlexaFluor680	MOL. PROBES	1:10.000 [1mg/ml]

Detection reagents used in FACS analysis

Prior to flow cytometric analysis, cells were incubated with Mouse BD Fc Block (FCγIII/II Block; BD BIOSCIENCES) to avoid non-specific binding of the antibodies that were used for staining of specific epitopes. Isotype controls were utilized to reassess the specificity of obtained antibodies (Tab.2).

Tab.2: Detection reagents used in FACS analysis

Description	Host / Isotype	Conjugation	Supplier	Dilution [Stock]
		Fc-Blocker		
mouse FcγIII/II Block	Rat IgG2b	-	BD BIOSCIENCES	1:40 [500 µg/ml]
		Primary Immunoglobulins		
human /mouse Frizzled1 MAb	Rat IgG2a	Biotin	R&D SYSTEMS	1:20 [200 µg/ml]
mouse F4/80 Mab	Rat IgG2b	FITC	ABD SEROTEC	1:100 [100 µg/ml]
mouse CD86	Rat IgG2a	PE	BD BIOSCIENCES	1:320 [200 µg/ml]
human CD14	Mouse IgG2b	FITC	BECKMAN COULTER	1:20 [125 µg/ml]
Isotype Ctrl.	Rat IgG2a	Biotin	BIOLEGEND	1:50 [500 µg/ml]
Isotype Ctrl.	Rat IgG2b	FITC	BIOLEGEND	1:500 [500 µg/ml]
Isotype Ctrl.	Rat IgG2a	PE	CALTAG	1:160 [100 µg/ml]
Isotype Ctrl.	Mouse IgG2b	FITC	DAKO	1:20 [200 µg/ml]
		Streptavidin Conjugate		
Streptavidin	-	Cy5	DIANOVA	1:60 [1 mg/ml]

Detection reagents used in immunohistochemistry

For immunohistochemical detection of Wnt3a protein in lung sections of *M. tuberculosis*-infected and uninfected mice, the following antibodies and streptavidin conjugate were used (Tab.3):

Tab.3: Detection reagents used in immunohistochemistry

Description	Host / Isotype	Conjugation	Supplier	Dilution [Stock]
		Primary Antibody		
mouse Wnt3a MAb	Rat IgG2a	-	R&D SYSTEMS	1:30 [100 µg/ml]
		Secondary Antibody		
Anti-rat	Goat IgG	Biotin	DIANOVA	1:500 [1 mg/ml]
		Streptavidin Conjugate		
Streptavidin	-	HRP	DIANOVA	1:500 [1 mg/ml]

Detection reagents used in mouse TNF-ELISA

The release of TNF was quantified by ELISA using DuoSet reagents (R&D SYSTEMS) (Tab.4):

Tab.4: Detection reagents used in mouse TNF-α-ELISA

Description	Isotype	Conjugation	Dilution
Capture Antibody anti-mouse-TNF polyclonal	Goat IgG	-	1:180 [800 ng/ml]
Detection Antibody anti-mouse-TNF polyclonal	Goat IgG	Biotin	1:180 [200 ng/ml]
Streptavidin	-	HRP	1:200

2.1.3.4 Kits

Transcriptor High Fidelity cDNA Synthesis Kit (ROCHE)

- Transcriptor High Fidelity Reverse Transcriptase (blend of a recombinant reverse transcriptase and a proofreading mediating enzyme)
- Transcriptor High Fidelity Reaction Buffer, 5x concentrated
- Protector RNase Inhibitor
- dNTP mix, PCR-grade
- Random Hexamer Primer
- DTT
- Water, PCR-grade

LightCycler Probes Master Kit

- LightCycler® 480 Probes Master, 2x concentrated
- Water, PCR-grade

2.1.3.5 Inhibitor

BAY 11-7082

BAY 11-7082 ((2E)-3-[(4-Methylphenyl)sulfonyl]-2-propenenitrile, CALBIOCHEM) was described as an inhibitor of IκBα phosphorylation, leading to decreased NF-κB release and subsequent decreased expression of adhesion molecules.[157]

2.1.3.6 Oligonucleotides

Tab.5: Primers used in SYBR-green quantitative real-time PCR

Gen (mouse)	sense	antisense	Annealing [*T*]	Elong. [*t*]	Aq. [*T*]
Fzd1	ttcctgctggccggtttcgtgtca	ctgggctcatgggcgggtgtgg	63°C-55°C	15 s	86°C
Hprt	gcagtacagccccaaaatgg	aacaaagtctggcctgtatccaa	60°C	5 s	79°C
Ifn-γ	gctctgagacaatgaacgct	aaagagataatctggctctgc	60°C	15 s	80°C
Tnf	ctgtagcccacgtcgtagc	ttgagatccatgccgttg	60°C	15 s	80°C

Tab.6: Primers and hydrolysis probes used for probe-based quantitative real-time PCR

Gene (mouse)	sense	antisense	Amplicon	UPL No.
Arg1	cctgaaggaactgaaaggaaag	ttggcagatatgcagggagt	72 bp	2
Axin2	gcaggagcctcacccttc	tgccagtttctttggctctt	69 bp	50
Cxcl1	ataatgggcttttacattctttaacc	agtcctttgaacgtctctgtcc	75 bp	2
Fzd1	gaggagggagccgaaaaa	ttcggcacaaagttccaa	89 bp	102
Fzd2	gctcttcgtatacctgttcatcg	gatgcggaagagtgacacg	67 bp	4
Fzd3	tccatgggcgtaggaaaa	tccctcaggagtgactgagc	85 bp	1
Fzd4	actttcacgccgctcatc	tggcacataaaccgaacaaa	72 bp	19
Fzd5	tgtcactgggattcttggtg	gggccggtagtctcatagtg	94 bp	76
Fzd6	ttaagcgaaaccgcaagc	ttggaaatgaccttcagccta	148 bp	81
Fzd7	gggtatctctgtgtagccctga	agaggcaggtggatgtctgt	85 bp	21
Fzd8	ctagaggtgcaccagttttgg	tgctacacagaaagaacttgaggt	73 bp	22
Fzd9	cacagagggtcccaggataa	catcattaaataactctgcactggac	67 bp	29
Fzd10	atggaaaccaagccagtgtg	ctccccccttcctctccac	60 bp	95
Hprt	tcctcctcagaccgctttt	cctggttcatcatcgctaatc	90 bp	95
Il-10	cagagccacatgctcctaga	tgtccagctggtcctttgtt	79 bp	41
Il-12	atccagcgcaagaaagaaaa	ctacgaggaacgcacctttc	70 bp	94
Lck	cgtgtgtgaaaactgccact	gggagagatccctcataggtg	114 bp	21
LysM	ggaatggctggctactatgg	tgctctcgtgctgcgctaaa	64 bp	64

Sftpc	ggtcctgatggagagtccac	gatgagaaggcgtttgaggt	94 bp	56
Scgb	gatcgccatcacaatcactg	gggcagatgtccgaagaag	69 bp	56
Tnf	ctgtagcccacgtcgtag	ttgagatccatgccgttg	97 bp	102
V-cam1	tggtgaaatggaatctgaacc	cccagatggtggtttcctt	86 bp	34
Wnt3a	cttagtgctctgcagcctga	gagtgctcagagaggagtactgg	92 bp	76
Wnt7b	gcgtcctctacgtgaagctc	tcttgttgcagatgatgttgg	72 bp	81
Universal Probe Library (UPL; ROCHE): www.universalprobelibrary.com				

2.1.3.7 Buffers and cell culture media

Unless indicated otherwise, buffers and solutions were prepared using *aqua bidest* (Research Center Borstel).

General Buffers

Phosphate buffered saline (PBS):

140 mM NaCl
2.7 mM KCl
8.1 mM NaH_2PO_4
1.5 mM KH_2PO_4
pH 7.2

Tris-buffered saline (TBS):

10 mM Tris/HCl
150 mM NaCl
pH 8.0

Buffers and soutions used for:

- **Generation of lung homogenates and colony enumeration assays**

Homogenization buffer:

1 Tablet protease inhibitor (Complete; ROCHE)
10 ml PBS

***Solution used for serial dilution*:**

0.05% (v/v) Tween-80
ad *aqua ad injectabilia*

- **SDS-PAGE and Western Blot**

5 x lysis buffer:

312.5 mM Tris/HCl
140 mM 2-Mercaptoethanol
10% (w/v) SDS
50% (v/v) glycerol
pH 7.8, bromophenolblue

2 x sample buffer:

125 mM Tris/HCl
100 mM DTT
4% (w/v) SDS
20% (v/v) glycerol
pH 7.8, bromophenolblue

Resolving gel buffer:

1.5 M Tris/HCl
pH 8.8

Stacking gel buffer:

0.5 M Tris/HCl
pH 6.8

Ammoniumperoxidsulfate- (APS-) solution:

10% (w/v) APS

SDS-solution:

10% (w/v) SDS

Electrophoresis running buffer:

25 mM Tris
192 mM Glycine
0.5% (w/v) SDS
pH 8.3

Western Blot buffer:

25 mM Tris
192 mM Glycine
20% (v/v) Methanol
pH 8.3

Blocking buffers:

5% (w/v) bovine serum albumin (BSA) in T-TBS
5% (w/v) low fat dry milk in T-TBS

Roti block:

10% (v/v) 10 x Roti ImmunoBlock®
ad T-TBS

Tris-buffered saline with Tween (T-TBS):

0.1% (v/v) Tween 20
ad TBS

Others:

- Ponceau S solution
- Stripping solution
  (both THERMO SCIENTIFIC)

- **Flow cytometry (FACS)**

Azide-PBS:

121 mM NaCl
2.7 mM KCl
10 mM Na_2HPO_4 x 2 H_2O
1.5 mM KH_2PO_4
15 mM NaN_3
pH 7.2

FACS buffer:

3% (v/v) FCS
0,1% (w/v) NaN_3
ad PBS

- **X-gal staining**

Tissue freezing buffer:

33% (v/v) Tissue freezing buffer (JUNG)
ad *aqua ad injectabilia*

2x X-gal fix buffer:

162 mM Na_2HPO_4
38 mM NaH_2PO_4
10 mM EGTA
4 mM $MgCl_2$
pH 7.4

Fixative:

4% (w/v) PFA
(from 8% stock solution)
1x X-gal fix buffer
(mix 8% PFA and 2x X-gal fix buffer 1:1)

X-gal buffer:

81 mM	Na_2HPO_4
19 mM	NaH_2PO_4
2 mM	$MgCl_2$
0.01% (w/v)	Sodium Deoxycholate
0.02% (v/v)	Igepal CA-630

X-gal substrate solution:

1 mg/ml	X-gal
1 mM	Spermidine HCl
5 mM	$K_3Fe(CN)_6$
5 mM	$K_4Fe(CN)_6$ x 6 H_2O

ad X-gal buffer

- **Immunohistochemistry**

Formalin:

4% (v/v)	Formalin

ad PBS

Citrate buffer:

10 mM	Citrate

H_2O_2 solution:

1% (v/v)	H_2O_2

ad PBS

Blocking solution / Reagent diluent:

5% (v/v)	FCS

ad PBS

3,3'-Diaminobenzidine tablet set (SIGMA-ALDRICH):

1 Tablet	DAB
1 Tablet	Urea

ad 5 ml *aqua bidest*

Other:

Gill's haematoxylin solution (MERCK)
Kaiser's glycerol gelatine (MERCK)

- **TNF ELISA**

Washing buffer:

0.05% (v/v)	Tween 20

ad PBS

Reagent diluent:

1% (w/v)	BSA

ad PBS (sterile filtrated)

Blocking buffer:

1% (w/v)	BSA
5% (w/v)	Sucrose
0.05% (w/v)	NaN_3

ad PBS

Tetramethylbenzidine- (TMB-) solution:

20 mM	3,3',5,5'-Tetramethylbenzidine
10% (v/v)	Acetone
90% (v/v)	Ethanol
50 mM	H_2O_2

Substrate buffer:

33 mM	Citric acid

pH 4.1

Washing buffer:

0.05% (v/v)	Tween 20

ad PBS

Substrate solution:

5% (v/v)	TMB solution

ad substrate buffer

Stopping solution:

1 M	H_2SO_4

Media

Murine Macrophage Medium (MMM):

	DMEM (PAA)
10% (v/v)	FCS (i.a.)
4 mM	L-Glutamine
10 mM	HEPES
1 mM	Sodium pyruvate

Macrophage differentiating medium:

	MMM
100 U/ml	Penicilline
100 µg/ml	Streptomycine
50 ng/ml	Recombinant human M-CSF

L Cell culture medium:

	DMEM (PAA)
4 mM	L-Glutamine
10 mM	HEPES
1 mM	Sodium pyruvate
100 U/ml	Penicilline
100 µg/ml	Streptomycine

Selective L Cell culture medium:

	DMEM (PAA)
4 mM	L-Glutamine
10 mM	HEPES
1 mM	Sodium pyruvate
0.4 mg/ml	G418

Hanks' balanced salt solution (HBSS)/ 0.1% BSA:

	HBSS (PAA)
0.1% (w/v)	BSA
pH 7.2	

Human monocyte differentiating medium:

	RPMI 1640 (PAA)
10% (v/v)	FCS (i.a.)
4 mM	L-Glutamine
2 ng/ml	Recombinant human M-CSF
2% (v/v)	Human serum
100 U/ml	Penicilline
100 µg/ml	Streptomycine

Human macrophage culture medium:

	RPMI 1640 (PAA)
10% (v/v)	FCS
4 mM	L-Glutamine

Chemiluminescence medium (CL-medium):

	RPMI 1640 without phenol red (PAA)
20 mM	HEPES

2.1.4 Cell lines

L Cells

Murine fibroblast derived L-929 cells (or L Cells) were purchased from the American Type Culture Collection (ATCC; Manassas, VA, USA) and served as negative control for transgenic L Cells.

L Wnt-3a

Wnt3a transgenic murine L Wnt-3a fibroblasts were purchased from the American Type Culture Collection (ATCC). L Wnt-3a cells secrete biologically active Wnt-3a for the production of Wnt3a conditioned media[158;159].

L Wnt-5a

Wnt5a transgenic murine L Wnt-5a fibroblasts were purchased from the American Type Culture Collection (ATCC). L Wnt-5a cells secrete biologically active Wnt-5a for the production of Wnt5a conditioned media[160].

2.1.5 Mouse strains

All wild type mice (WT) and gene deficient knockout mice (deficient, $^{-/-}$) used were kept under specific pathogen-free conditions. For each experiment knockout and wild type mice were matched for age (10 to 12 weeks) and sex (male or female). In all experiments healthy animals were used, as attested by the corresponding animal facility (CHARLES RIVER, Sulzfeld; Research Center Borstel, Borstel). All animal experiments were approved by the Ministry of Environment, Kiel, Germany.

C57BL/6 (WT)

Wild type mice, strain C57BL/6 (CHARLES RIVER, Sulzfeld), served as immune competent control mice, matching the genetic background of gene deficient mice.

TLR2$^{-/-}$- Knockout Mice

Mice deficient for Toll-like recptor 2 (TLR2$^{-/-}$) were obtained from the Technnical University of Munich (Germany) and maintained at the animal facility at the Research Center Borstel. Mice were backcrossed 10 generations to a C57BL/6 genetic background.

MyD88$^{-/-}$- Knockout Mice

Mice deficient for myeloid differentiation primary response gene 88 (MyD88$^{-/-}$) were originally obtained from Shizuo Akira (Department of Biochemistry, Hyogo College of Medicine, Japan) and maintained at the animal facility at Research Center Borstel. Mice were backcrossed 10 generations to a C57BL/6 genetic background.

TNF- Knockout Mice

Mice deficient for tumor necrosis factor (TNF$^{-/-}$) were originally acquired from Manolis Pasparakis (Department of Molecular Genetics, Hellenic Pasteur Institute, Athens, Greece) and maintained at the animal facility at Research Center Borstel. TNF knockout mice were generated to a C57BL/6 genetic background.

Fzd1$^{+/LacZ}$ Reporter Mice

Fzd1$^{+/LacZ}$ reporter mice (B6.129P2-Fzd1$^{tm1-Dgen}$/J) were developed by Deltagen Inc. (San Mateo, CA, USA) and acquired from Jackson Laboratory (Bar Harbor, ME, USA). The mice were maintained at the animal facility at the Research Center Borstel. Congenic Fzd1$^{+/LacZ}$ reporter mice were backcrossed at least 6 generations to C57BL/6J mice.

2.2 Methods

2.2.1 Cultivation of cell lines

Unless indicated otherwise, all cells were incubated at 37°C in a humidified and 5% CO_2 enriched atmosphere.

2.2.1.1 Cultivation of L Cell lines

Stably transfected clones of transgenic mouse fibroblast cell line, L Wnt-5a and L Wnt-3a (ATCC), were cultivated using 10 ml of L Cell culture medium containing 0.4 mg/ml of G418, whereas non-transfected parental L-929 cells (L Cells) were grown in L Cell culture medium in the presence of penicilline and streptomycine (see 2.1.3.7). Cells were grown to confluency in a 75 cm^2 tissue culture flask (SARSTEDT, Newton, NC, USA). After 3 to 4 days the culture medium was discarded and cells were detached by 5 minute incubation in 3 ml Trypsin-EDTA solution (0,05% Trypsin, 0,02% EDTA (w/v) in PBS; BIOCHROM) at 37°C. The cells were then carefully rinsed off the bottom of the culture flask with 20 ml PBS, transferred to a 50 ml tube and centrifuged at 300 x g for 10 minutes at 4°C. Afterwards the supernatant was removed and cells were resuspended in 2.5 ml of fresh L cell culture medium. 1/10 volume of the cell suspension was used for subcultivation.

2.2.1.2 Generation of Wnt conditioned media

For Wnt3a stimulation assays conditioned medium derived from L Wnt-3a cells (ATCC) was generated. Conditioned medium derived from non-transgenic parental L Cells severed as control. To obtain conditioned media, 1/10 volume of L Cell suspensions (see 2.2.1.1) derived from passage 3 to 13 was applied to 10 ml L Cell culture medium devoid of antibiotics and seeded on the bottom a 75 cm^2 tissue culture flask (SARSTEDT). After 2 days in culture, the medium was collected and filtrated (0.45 µm, SARSTEDT). HEPES solution was added to a final concentration of 10 mM. At all times conditioned media were used on the same day.

2.2.2 Isolation and cultivation of primary cells

2.2.2.1 Isolation and cultivation of peritoneal exudates cells

To isolate *in vivo* differentiated peritoneal exudate cells (PEC), mice were euthanized with CO_2 and superficially disinfected using 70% ethanol. Mice were fixed to a preparation plate and the fur was ventrally removed. Cells were washed out off the peritoneum with 6 to 8 ml of pre-warmed MMM that was injected intra-peritoneally through a 24-gauge needle and a 10 ml syringe. After short perturbation of the peritoneum, exudate cells were collected through a 24-gauge needle and 10 ml syringe and transferred to a 50 ml tube. Following a 10 min centrifugation step at 4°C, 300 x g, the supernatant was discarded and the cells were resuspended in 5 ml fresh MMM (see 2.1.3.7). Viable PEC were determined by diluting 10 µl cell suspension in 90 µl trypan blue solution. 10 µl of cell containing trypan blue solution were counted in a Neubauer chamber to calculate the number of non-stained (viable) cells. For further experiments 0.5 x 10^6 viable cells were seeded into a 24-well flat-bottom microtiter plates (NUNC) in a volume of 0.5 ml per well and allowed to adhere by overnight cutlivation. To remove non-adhering cells, each well was rinsed twice with 1 ml PBS the day after seeding and fresh medium was added (0.5 ml MMM/well).

2.2.2.2 Generation of murine bone marrow-derived macrophages

Isolation of murine bone marrow cells

For the generation of bone marrow-derived macrophages (BMDM) mice were euthanized with CO_2 and superficially disinfected using 70 % ethanol. The animals were fixed on preparation plates, opened and hind leg's bones were removed using sterile tweezers and scissors. After femora and tibia were thoroughly cleared from soft tissue, the bones were aseptically opened on both sides and bone marrow cells were rinsed out off the marrow cavity into a 50 ml tube using a 26 gauge needle and a syringe filled with 20 ml ice-cooled MMM. Following centrifugation of the cells for 10 min (at 4°C, 300 x g), the cell pellet was resuspended in 10 ml macrophage differentiating medium containing 50 ng/ml M-CSF (see 2.1.3.7).

Generation of murine macrophages from bone marrow cells

Freshly isolated bone marrow cells resuspended in macrophage differentiating medium, were seeded into a 10 cm Nunclon surface dish (NUNC). Following 24 h of cultivation, non-adherent cells were harvested and transferred to a 50 ml tube. After a 10 min centrifugation step at 4°C, 300 x g, the supernatant was removed and cells were resuspended in fresh macrophage differentiating medium. The number of viable cells was determined by trypan blue staining and counting in a Neubauer chamber (see also 2.2.2.1). Subsequently the cells were seeded into culture dishes (SARSTEDT), each containing approx. 1 x 10^7 viable cells in a volume of 10 ml macrophage differentiating medium. The cells were then cultivated for 6 days and additional 10 ml of fresh differentiating medium were added on day four of cultivation. On day seven, medium was discarded and cells were detached by adding 3 ml pre-warmed Alfazyme solution to each plate. After incubation at 37°C, 5% CO_2 for 10 min, the culture dishes were rinsed twice with 10 ml PBS and the cells were transferred to a 50 ml centrifugation tube. The cells were separated from the PBS by centrifugation at 300 x g (4°C, 10 min) and resuspended in 10 ml MMM. For further experiments the number of viable macrophages was determined by trypan blue staining as decribed above.

2.2.2.3 Generation of human monocyte derived macrophages

Isolation of peripheral blood mononuclear cells

Venous blood was collected from healthy volunteering donors. To avoid coagulation, 5 parts of whole blood were mixed with 1 part 3.8% trisodium citrate solution and diluted 1:1 with PBS. The blood cells were separated by discontinous density centrifugation after Bøyum[161]. For this purpose 40 ml of diluted blood were slowly stacked onto 10 ml of pancoll (density of 1.077g/ml) within a sterile 50 ml centrifugation tube and centrifuged at room temperature at 300 x g for 42 min using a swing out rotor (slow acceleration, centrifuge brake switched off). After centrifugation the supernating plasma was discarded and the PBMC containing interphase carefully transferred to a sterile 50 ml centrifugation tube using a sterile pasteur pipette. The cells were resuspended in PBS to a final volume of 50 ml and centrifuged for 10 min at 300 x g, 4°C. Following an additional repeat of this washing step, the PBMCs were resuspended in HBSS/0.1% BSA. To obtain most efficient separation of PBMCs by subsequent elutriation the cell concentration was not to exceed 5x10^6 cells per ml. For this reason the cell

concentration was determined using an electronic cell counter (Casy2; SCHÄRFE SYSTEM, Reutlingen).

Isolation of human monocytes from peripheral blood mononuclear cells

Isolation of human mononuclear cells by elutriation is based on the principle of counterflow centrifugation. This method allows the separation of heterogeneous PBMCs into distinct subpopulations according to their sedimentation characteristics. Elutriation was performed applying a modified protocol after Contreras et al.[162].

Prior to elutriation the rotor (JE-6-B-rotor; BECKMAN, München) and the tubing system were sequentially rinsed with 70% ethanol and 500 ml sterile deionized water avoiding air inclusions. Subsequently the system was equilibrated using 250 ml HBSS/0.1% BSA. At 3200 rotations per minute and a rotor temperature of 12°C the PBMCs were loaded into the system using a flow rate (regulated by a calibrated peristaltic pump (RTC, Heidelberg)) of 31 ml/min. Following a given elutriation protocol (Tab. 7) distinct cell populations of PBMCs were separated by continuously increasing the flow rate of medium, and the desired cell fractions were collected in a sterile centrifugation tube. After elutriation 50 ml of the monocyte fraction were centrifuged for 10 min at 300 x g, 4°C and resuspended in 10 ml PBS. The size and purity of the cell fraction was determined using a CASY2 cell counter (SCHÄRFE SYSTEM).

Tab. 7 Elutriation protocol

Flow rate [ml/min]	Volume [ml]	Fraction
33	200	Loading of PBMC
36	50	Rinse
38	50	Rinse
40	300	Small lymphocytes
41	50	Lymphocytes
42	50	Lymphocytes
43	50	Lymphocytes
44	50	Lymphocytes
45	200	Big lymphocytes
46	150	Rinse
47	150	Rinse
48	150	Rinse
49	50	Monocytes
50 + stop	50	Monocytes (pure)

Generation of macrophages from human monocytes

The differentiation of human monocytes to macrophages was performed in a teflon coated cell culture bag (VueLife™ 72; CELLGENIX, Freiburg) in the presence of 2 ng/ml human M-CSF and 2% human serum (modified after Andreesen et al. and Becker et al.[163;164]). Freshly elutriated human monocytes (purity > 95%) were resuspended in pre-cooled monocyte differentiating medium to a final concentration of 2 - 3x10^7 viable cells per 50 ml and stored on ice. Using a sterile 50 ml syringe, 50 ml of monocyte suspension were transferred into a teflon coated cell culture bag and incubated for 7 days. After one week, the differentiated human macrophages were harvested by placing the culture bag in ice water (0°C) for 1 h, thus allowing the cells to detach from the teflon surface. In addition, the cells were mechanically detached by carefully tugging the bags over the edge of the laminar airflow cabinet. Subsequently the contents of the teflon bags were transferred to a sterile 50 ml centrifugation tube and centrifuged for 10 min at 300 x g and 4°C. The supernating medium was removed and the macrophages resuspended in fresh cell culture medium. The number of viable cells was determined by trypan blue staining and counting in a Neubauer chamber.

2.2.3 Stimulation of macrophages

2.2.3.1 Stimulation

Unless mentioned otherwise, cells were incubated and cultivated at 37°C in a humidified atmosphere containing 5% CO_2. Stimuli were added to the cells under sterile conditions at room temperature at concentrations indicated.

5x10^5 bone marrow-derived macrophages or peritoneal exudate cells were seeded in a volume of 0.5 ml MMM onto the bottom of each well of a 24-well flat-bottom microtiter plate (NUNC) and were allowed to adhere overnight. For FACS experiments 4 x 10^6 cells were seeded in a volume of 4 ml MMM onto the bottom of a 6-well flat-bottom microtiter plate (NUNC) and were incubated overnight. For experimentation human macrophages were treated likewise, with the exception that 0.8 x 10^6 cells were used per ml culture medium. Macrophages were infected with *M. tuberculosis* (strain H37Rv) and *M. avium* (strain SE01) at the indicated multiplicities of infection (MOI) for the times indicated. LPS, synthetic lipopeptide (Pam_3CSK_4) or

recombinant murine tumor necrosis factor alpha (TNF-α, PEPROTECH) were used as control stimuli.

In co-stimulation experiments, IFN-γ or IL-10, (both PEPROTECH) were added 24 h prior to infection and remained during infection as indicated. To analyze nuclear factor kappa B (NF-κB) dependent signaling, the compound BAY 11-7082 (SIGMA-ALDRICH) was added to the cells 45 min prior to infection and remained during the experiments. DMSO served as solvent control and was used at a concentration of 0.03% (v/v). To examine the influence of Wnt conditioned media on primary cells, murine macrophage medium (MMM) was completely removed and replaced by 0.5 ml of fresh conditioned medium. If the cells were stimulated prior to the exchange of MMM against conditioned medium, the stimuli were again added to the conditioned medium to maintain the stimulatory conditions. Subsequently macrophages were incubated as indicated. To inhibit Wnt3a-mediated β-catenin signaling, recombinant Fzd1/Fc fusion protein (R&D SYSTEMS) was pre-incubated with conditioned media for 45 min at 4°C. After pre-incubation, the conditioned medium was applied to the cells as described above.

2.2.3.2 Sample preparation

For detection of TNF secretion by cytokine-ELISA, cells were placed on ice, supernatants were collected and frozen at -20°C until use. For isolation of RNA and total protein, supernatant of each well was removed and cells were lysed in 0.5 ml phenol/guanidine isothiocyanate solution (TriFast, PEQLAB). After addition of 150 µl PBS the cell lysates were transferred into a sterile RNase-free 1.5 ml reaction tube. Following 10 min of incubation at room temperature the lysates were frozen at -80°C until use. For isolation of total protein, macrophages were placed on ice and medium was discarded. Cells were washed twice with 1 ml PBS (4°C) and lysed in 2 x sample buffer. The lysates were stored at -20°C for later analysis by Western blot. Prior to flow cytometric measurements supernatant medium was removed and cells were detached during 10 min of incubation in 1 ml Alfazyme solution (PAA). Thereafter, cells were placed on ice and transferred to a 5 ml falcon tube (BD BIOSCIENCES), remaining cells were detached by rinsing the bottom of the well twice with 2 ml of 4°C cooled FACS buffer. The cells were centrifuged at 300 x g (10 min, 4°C) and resuspended in an appropriate volume of FACS buffer.

2.2.4 *In vivo* experiments

2.2.4.1 Aerosol infection of mice

For experimental *M. tuberculosis* aerosol infection, mice were placed in individual aerosol cages (Marine und Industrie Technik, Hamburg) that were designed to fit into the inhalation exposure system (GLAS-COL, Terre-Haute, IN). Aliquots of *M. tuberculosis* (strain H37Rv) were thawed and aggregates of mycobacteria were resolved by homogenization through a 26-gauge needle and a 1 ml syringe (BD BIOSCIENCES). Based on former titrations, an inoculum size of 2 x 10^6 colony forming units (CFU) was used to obtain a dose of infection of 100 CFU per lung. The inoculum was diluted in a final volume of 6 ml *aqua ad injectabilia* (BRAUN). 500 µl of the bacteria suspension were taken to determine the exact inoculum size by plating of serial dilutions onto Middlebrook 7H10 agar plates containing 10% heat inactivated bovine serum (BIOWEST, Paris, France). The remaining 5.5 ml of suspension were cautiously transferred into the nebulizer of the exposure system by a 20-gauge needle and a 10 ml syringe. The system was closed and the infection of mice was started in a program of 900 s preheating, 2400 s nebulizing, 2400 s cloud decay and 900 s of decontamination by UV light. During infection the flow of air was kept at 60 CFH (cubic feet per hour = 1,68 m^3/h) and at the beginning of nebulization the air pressure was set to 10 CFH (= 0.28 m^3/h). Following infection within the exposure system, the animals were carefully placed into individually ventilated cages (IVCs) and the inhalation exposure system was again started as described using 6 ml 2% Buraton for decontamination. One day after aerosol infection, three indicator mice (C57Bl/6) were sacrificed to determine the actual pulmonary dose of infection through colony enumeration assay (see 2.2.4.4).

2.2.4.2 Lung extraction from *M. tuberculosis*-infected mice

At different time points post-infection *M.tuberculosis* infected mice were euthanized with CO_2 to determine the bacterial burden, pathology and immunologic parameters in the lung. The mice were superficially disinfected, immobilized and opened aseptically. The lungs of the infected mice were removed, weighed and split as follows: the superior lobe and post-caval lobe of the lung were weighed and used for colony enumeration assay as well as total protein extraction; the inferior lobe was removed for cryo-sectioning; the middle lobe was weighed, placed into a reaction

tube and was shock frozen in liquid nitrogen for later use in RT-PCR analysis. Finally the left lung was weighed and collected for immunohistochemistry. The lobes were subsequently treated as described below.

2.2.4.3 Generation of lung homogenates and sampling of total protein

The superior and post-caval lobe of a mouse lung were admitted into a potter tube (RETTBERG) containing 3 ml homogenization buffer. The lobes were homogenized using a potter (GLAS-COL) and -20°C pre-cooled pestle (RETTBERG). 1 ml of the lung homogenate was subsequently used in colony enumeration assay to determine the bacterial burden. To sample total protein, 500 µl of lung homogenate were centrifuged for 10 min at 10.000 x g and 4°C. 400 µl of the supernatant homogenate were transferred to a new reaction tube and supplemented with 100 µl of 5 x lysis buffer for sampling of total protein. The protein was denaturated for 5 min at 95°C, cooled on ice and stored at -20°C until use. The remaining homogenate was equally split into two sterile micro tubes and stored at -80°C.

2.2.4.4 Colony enumeration assay

For colony enumeration assays lung homogenates derived from mice sacrificed at indicated time points were used. To determine the mycobacterial burden within the infected lung, tenfold serial dilutions of 500 µl lung homogenate (see 2.2.4.3) were prepared in 4.5 ml sterile water containing 0.05% Tween 80. 100 µl of diluted lung suspension were plated onto Middlebrook 7H10 agar plates containing 10% heat inactivated bovine serum (BIOWEST) and were incubated at 37°C for 19 – 21 days. Colonies on plates were enumerated and bacterial burden was expressed as log10 CFU per lung.

2.2.4.5 Lung preparation for histological analyses

For later sectioning of frozen lung tissue using a cryo-microtome, the inferior lobe was filled with 1 ml tissue freezing buffer through a 26-gauge needle, carefully wrapped in aluminum foil and was shock frozen in liquid nitrogen. The left lung was used for paraffin embedded sectioning. For preparation the lung tissue was fixed for 24 h in 4% formalin and thereafter dehydrated (45 min 50% ethanol, 45 min 70% ethanol, 45 min 95% ethanol, 3 x 45 min 100% ethanol, 3 x 45 min xylol, 2 x 60 min

65°C paraffin) using an autotechnicon (SHANDON). Following dehydration the lung and a histology grid were placed into a cast mold of a tissue embedding center (LEICA) and embedded in 65°C paraffin. After cooling the paraffin blocks were stored at 4°C until use.

2.2.4.6 X-gal staining of frozen cryostat sections

Using a -18°C pre-cooled rotary cryo-microtome (Leica CM1850; LEICA) 5 µm sections were cut from frozen lung tissue (inferior lobe) and carefully mounted on glass slides (LANGNBRINCK). Immediately after sectioning, the tissue was air dried for 1 h and the glass slides placed into a 15 ml staining jar. The slides were then fixed for 7 min in 4% paraformaldehyde/1x fix buffer and sequentially washed three times for 30 min in X-gal buffer. After removal of X-gal buffer 15 ml of 37°C pre-warmed X-gal substrate solution were added to the staining jar and the glass slides were incubated overnight at 37°C avoiding light exposure. The following day, the slides were sequentially washed two times for 5 min in 37°C pre-warmed X-gal buffer, one time for 2 min in PBS, and quickly rinsed with *aqua ad injectabilia* (BRAUN). Afterwards the glass slides were removed from the staining jar, air dried for 5 min and subsequently covered with 70 µl Kaiser's glycerol gelatine (MERCK) and a cover slip. Photo documentation was performed using a digital camera (Digital Sight DS-L11; NIKON) connected to a bright field microscope (Leica DM LB; LEICA).

2.2.4.7 Immunohistolochemical analysis of paraffin sections

Preparation of paraffin sections

Using a rotary microtome (Leica RM2155; LEICA) 2 µm sections of paraffin embedded lung tissue were cut from ice cooled paraffin blocks and carefully transferred to a cooled waterbath for smoothening. Thereafter the sections were cautiously placed into a 37°C pre-warmed waterbath (GFL1052; GFL) and allowed to stretch out for 5 min. In a final step the sections were mounted on a glass slide (LANGENBRINCK) and dried for 4 h at 37°C.

Immunohistochemical staining for Wnt3a detection

Prior to immunohistochemical staining, the paraffin was removed from the embedded lung sections. Prepared glass slides were immersed for 10 min in 100% xylene and

sequentially placed into decreasing dilutions of acetone (10 min 100%, 10 min 70% and 10 min 40%). Subsequently the slides were washed in *aqua bidest* and three times in PBS buffer. For epitope reconstitution the lung sections were boiled for two min in citrate buffer using a pressure cooker (FISSLER). The cooker was cooled down and the sections were washed three times in PBS buffer. Afterwards the tissue was incubated in 1% (v/v) H_2O_2/PBS (10 min room temperature) to quench endogenous peroxidase activity and for bleaching of erythrocytes. Following a washing step in PBS the sections were blocked for 45 min at room temperature in PBS supplemented with 5% (v/v) FCS to prevent non-specific binding of the antibody. The sections were washed again and subsequently incubated with 200 µl anti-Wnt3a monclonal antibody (R&D SYSTEMS) diluted in 5% (v/v) FCS/PBS. After a washing step the lung tissue was stained with goat anti-rat biotinylated secondary antibody (DIANOVA) and after washing, incubated with streptavidin-horseradish peroxidase (streptavidin-HRP; DIANOVA) for detection of antigen. Secondary antibody and tertiary reagent were diluted in 5% (v/v) FCS/PBS and were used in a volume of 200 µl per glass slide. The tissue preparations were incubated for 45 min at room temperature in a lightproof wet chamber. Following addition of substrate solution (3,3'-diaminobenzidine, DAB; SIGMA-ALDRICH) the preparations were incubated for 10 to 15 min in the dark at room temperature. The enzymatic reaction was stopped through washing in PBS. Immunohistochemical detection of Wnt3a was followed by haematoxylin counterstaining of nuclei after Gill[165] (see below).

Haematoxylin counterstaining

Following immunohistochemical staining for Wnt3a detection (see above), the chromatin of lung sections was dyed with hematoxylin to distinguish different cells within the lung tissue by histological analysis[166;167]. The sections were immersed in hematoxylin for 3 min at room temperature and rinsed with running tap water (room temperature) for 10 min. Subsequently each glass slide was covered with 70 µl Kaiser's glycerol gelatine (MERCK) and a cover slip. Photo documentation was performed using a digital camera (Digital Sight DS-Ri1; Nikon) connected to a microscope (Leica DM LB; LEICA).

2.2.5 Molecular biology methods

2.2.5.1 RNA isolation from tissue and cell lysates

Generation of tissue-lysates for RNA isolation

For the generation of tissue lysates the middle left lobe of a murine lung (see 2.2.4.2) were thawed in a potter tube containing 1 ml phenol/guanidine isothiocyanate solution (TriFast, PEQLAB). The tissue was homogenized and lysed using a potter device (B. Braun) and -20°C precooled pestle (Rettberg). 300 µl of PBS were added to the lysate and incubated for 10 min at room temperature. Afterwards, the tissue-lysate was equally dispensed into two sterile and RNase free micro tubes and frozen at -80°C

RNA isolation

Frozen tissue- (see above) or cell lysates (see 2.2.3.2) were thawed at room temperature and subsequently placed on ice. The lysates were supplemented with 100 µl bromochloropropane (BCP, SIGMA-ALDRICH), shaken for 15 s and placed on ice for 10 min. To separate the RNA containing aqueous phase from the DNA, lipid and protein containing interphase and organic phase, the samples were centrifuged for 10 min at 12,000 x g, 4°C. The reaction tubes were carefully placed on ice again and 300 µl of the aqueous phase were transferred to a new sterile and RNase-free reaction tube containing 1.5 µl glycogen (ROCHE) to facilitate precipitation of the RNA. The remaining interphase and organic phase were stored at 4°C. The RNA was precipitated by adding an equal volume of ice-cold 2-propanol to the RNA solution. After 10 min of incubation on ice the RNA was pelleted by centrifugation at 12,000 x g and 4°C. Following the removal of the supernatant, the RNA pellet was washed twice with 1 ml ice-cold 75% ethanol and centrifuged at 12,000 x g, 4°C. Subsequent to the last washing step, the RNA was solved in 25 µl PCR-grade H_2O (ROCHE) at 60°C. After 10 min the RNA was quickly cooled on ice and frozen at -80°C.

2.2.5.2 Reverse transcription

Prior to reverse transcription the RNA (see 2.2.5.1) was thawed on ice and the concentration was determined by using a spectrophotometer (NanoDrop ND-1000, PEQLAB). The RNA samples were appropriately diluted in PCR-grade Water

(ROCHE) to receive equal concentrations of RNA. The RNA amounts of different sample preparations used for reverse transcription ranged from 100 ng to 500 ng. For first strand cDNA synthesis a reverse transcription kit (Transcriptor High Fidelity cDNA Synthesis, ROCHE) was used. Synthesis was performed in two steps using a sterile PCR-reaction tube. The first step was to prevent secondary structures of the RNA and to allow annealing of random hexamer primers to the RNA strand. In a second step master mix containing the reverse transcriptase was added to the samples for cDNA synthesis. Incubation of both steps was accomplished in a thermocycler (BIO-RAD). Each reaction was composed of the following reagents and the thermocycler programmed as follows:

Step 1:

X µl	RNA (100 – 500 ng)
2 µl	random hexamer primer
11.4 µl	ad PCR-grade H_2O

Program (RTHEX):

1 s	94°C
10 min	65°C
∞	4°C

Step 2:

4 µl	5 x reaction buffer
2 µl	dNTPs
1 µl	DTT
0.5 µl	RNase inhibitor
1.1 µl	reverse transcriptase

Program (RTMASTER):

15 min	55°C
5 min	85°C
∞	4°C

After first strand synthesis 10 µl PCR-grade water were added to the cDNA. The samples were transferred to a sterile 1.5 ml reaction tube and stored at -20°C.

2.2.5.3 Quantitative real-time polymerase chain reaction (qRT PCR)

Quantitative real-time PCR amplification was performed using a LightCycler® carousel-based system and LightCycler® 480 system (ROCHE). For cDNA amplification gene specific oligonucleotide primer pairs were used in a SYBR green assay (see 2.1.3.6, Tab. 3) and hydrolysis probe-based assay (see 2.1.3.6, Tab. 4).

SYBR green assay

The carousel-based LightCycler® system was applied in the SYBR green based method of relative RNA quantification. 1 µl cDNA and 9 µl master mix of reagents were pipetted into glass capillaries that were kept at 4°C and mixed by short centrifugation of the contents to the bottom of the capillaries at 400 x g. In each reaction the following reagents and LightCycler® settings were used:

1 µl	cDNA Template
	Master Mix (per sample):
4.60 µl	PCR-grade H_2O
1.40 µl	10 x PCR-buffer
0.70 µl	50 mM $MgCl_2$
0.50 µl	100 µM dNTP
0.60 µl	100 mM BSA
0.40 µl	6.25 µM sense primer
0.40 µl	6.25 µM antisense primer
0.20 µl	1 mM SYBR green
0.20 µl	5 U *Taq*-DNA-polymerase

Program:

[*t*]	[*T*]		
15 s	95°C	*Initial Denaturation*	
5 s	95°C	*Annealing*	*45 Cycles*
10 s	$\mathbf{x_1}$°C		
$\mathbf{x_2}$ s	72°C	*Elongation*	
1 s	$\mathbf{x_3}$°C	*Analysis*	
0 s	95°C	*Denaturation*	
15 s	72°C	*Final Elongation*	
65°C to 95°C at 0.1°C/s		*Melting Curve (constant analysis)*	

To prevent secondary structures of cDNA and oligonucleotides the samples were initially denaturated at 95°C. In the following 45 cycles of the polymerase chain reaction the cDNA was amplified and in each amplification cycle fluorescence of SYBR green was measured. For each gene specific primer pair that was used the annealing temperature, elongation time and analysis temperature were to be optimized in advance (see Tab. 3). To ensure the specificity of each real-time PCR reaction a melting curve of the PCR products was examined, resulting in a specific peak for each gene specific amplicon.

Hydrolysis probe-based assay

Instead of a fluorescent dye, the hydrolysis probe-based quantitative real-time PCR assay (*Taq*Man® assay*) uses chemically modified probes composed of 8 to 9 nucleotides (locked nucleic acids, LNA) to guarantee the specificity of the PCR

* The term "*Taq*Man® assay" is a registered trade mark shared by ROCHE AG and Applied Biosystems Inc., who developed this method of "hydrolysis probe-based quantitative real-time polymerase chain reaction". For simplicity reasons the registered name is commonly used. *Taq*Man® is an acronyme composed of *Taq* DNA polymerase and the video game PacMan, emblematically describing 5'-3' polymerase activity on the one and 5' nuclease-mediated cleavage of hydrolysis probes on the other hand.

reaction. These LNA probes contained two labels, a fluorescence reporter and a fluorescence quencher, in close proximity to each other and were used with gene-specific primers. The assay was based on the principle that a LNA probe specifically bound to template DNA was cleaved through 5' nuclease activity of the *Taq*Man® DNA polymerase during PCR amplification. When excited, cleaved fluorescence reporter labeled nucleotides of the LNA probe emitted a fluorescent signal that was then analyzed.

For relative quantification of RNA expression a *Taq*Man® assay kit (LightCycler® 480 Probes Master, ROCHE) was applied in a 96-multiwell plate LightCycler® 480 system. To minimize the standard error a master mix was produced and 8 µl were added to each well containing 2 µl of cDNA. The 96-multiwell plate (ROCHE) was sealed with a clear foil (ROCHE) and centrifuged for 2 min at 400 x g, prior to PCR reaction. In each reaction the following reagents and LightCycler® 480 settings were used:

Reagents:		Program:			
2 µl	cDNA Template	[*t*]	[*T*]		
	Master Mix (n = 1):	900 s	95°C	*Hot Start Induction*	
1.9 µl	PCR-grade H2O	1 s	95°C	*Denaturation*	
5 µl	2 x reaction mix	5 s	60°C	*Annealing*	*55*
1 µl	sense primer 6.25 µM	1 s	72°C	*Elongation*	*Cycles*
1 µl	antisense primer 6.25 µM	0 s	72°C	*Analysis*	
0.1 µl	LNA probe				

To start the PCR reaction the *Taq*Man® DNA polymerase (ROCHE) contained within the 2 x reaction mix had to be activated through incubation at 95°C for 15 min. The amplification progress in each of the 55 cycles was analyzed at 72°C.

Relative Quantification of mRNA Expression

The relative concentration of mRNA of a single gene of interest (target gene) was expressed as the normalized ratio of the target gene and the low-copy reference gene *Hprt* (*hypoxanthine phosphoribosyltransferase*). For quantification purposes, lung homogenate derived cDNA served as internal standard (pure, 1:2, 1:8, 1:32, 1:128, 0) during PCR reaction. Relative concentrations of diluted standard cDNA

(pure = 100, 1:2 = 50, […], 1:128 = 0.781, H_2O = 0) were defined to calculate the error and efficiency of the PCR run by the LightCycler® software. Derived from these data and the second derivative maximum of the analyzed increase in fluorescence of each sample, the ratio between the expression of the reference gene *Hprt* and the target gene was calculated by the software. Additionally, this ratio was normalized to the HPRT ratio of an independent internal calibrator, giving the normalized ratio of a target gene.

2.2.6 Biochemical methods

2.2.6.1 Protein extraction from phenolic cell lysates

Different from the described methods for protein extraction (see 2.2.3.2 and 2.2.4.3), protein contained in the organic phase and interphase of cell lysates derived from phenol/guanidine isothiocyanate solutions had to be further purified. First the DNA was removed from the lysates by adding 150 µl of 100% ethanol and precipitation (12,000 x g, 15 min, 4°C). The supernatant was transferred to a new sterile 2 ml reaction tube and 750 µl 2-propanol were added. After 10 min incubation at room temperature the total protein was precipitated (12,000 x g, 10 min, 4°C). The supernatant was discarded and the protein pellet was washed three times through incubation in 2 ml guanidine hydrochloride/ 95% ethanol for 20 min at room temperature and centrifugation at 7,500 x g (5 min, 4°C). By incubating the protein pellet in 2 ml 100% ethanol for 20 min at room temperature residual guanidine hydrochloride was removed. Following a further centrifugation step the supernatant was removed and the protein solved in 150 µl 2 x sample buffer. The samples were stored at -20°C until use.

2.2.6.2 Preparation of whole cell and tissue lysates for western blotting

Samples were sequentially thawed at room temperature, denaturated for 5 min at 95°C, cooled on ice and centrifuged for 5 min at 10,000 x g. The supernatant was used in SDS-polyacrylamide-gelelectrophoresis (SDS-PAGE).

2.2.6.3 SDS-polyacrylamide-gelelectrophoresis (SDS-PAGE)

The Mini-Protean Tetra Electrophoresis System (BIO-RAD) was used for SDS-PAGE. One-dimensional gelelectrophoresis was carried out using a discontinuous

gel system as described by Laemmli[168]. After focusing in a large-pore non-restrictive 4% polyacrylamide gel (pH 6.8) the samples were separated according to their molecular mass in a 12% resolving gel (approx. 4 cm in length x 10 x 1.5 mm). Gels were prepared as follows:

Reagents (stock solutions)	**12% Resolving Gel (pH 8.8)**	**4% Stacking Gel (pH 6.8)**
Aqua bidest	3.75 ml	3.08 ml
Resolving / Stacking gel buffer	2.13 ml	1.25 ml
40 % (w/v) Acrylamide/Bis solution, 37.5:1	2.55 ml	0.63 ml
10% (w/v) SDS solution	85 µl	50 µl
1 M TEMED	5 µl	5 µl
10% (w/v) APS	25 µl	25 µl

7.5 ml of unpolymerized resolving gel mixture were filled into the 1.5 mm space between two glass plates that were fixed in a casting stand (BIO-RAD). The upper edge of the gel was flattened by filling of the residual space with 2-propanol and left for polymerization. After 45 min the 2-propanol was completely removed and replaced by the prepared unpolymerized mixture of stacking gel. A 10- or 15-well comb was carefully inserted to form the sample slots followed by another 45 min of polymerization. The gel was removed from the casting stand and clamped to an electrode stand. Two gels were attached to each side of one electrode stand and run at the same time. The electrophoresis chamber between the glass plates as well as the chamber tank were carefully filled with 1 l running buffer before the samples were applied onto the gel. Equal amounts of protein in a volume of 15 to 50 µl and 5 µl of prestained molecular weight marker (6.5 – 175 kDa, NEW ENGLAND BIOLABS) were loaded into each slot of the stacking gel. Electrophoresis was started at 70 V for the first 15 min to focus the protein into the resolving gel and was continued at 200 V until the visible bands formed by bromophenol blue in the sample buffer had moved to the end of the gel.

2.2.6.4 Western blot

The stacking gel was removed and the resolving gel was used for protein transfer in a wet blot system (Mini Trans-Blot Electrophoretic Transfer Cell, BIO-RAD). For preparation of the protein transfer onto a nitrocellulose membrane, two fiber pads, four sheets of filter paper and one nitrocellulose membrane (4 cm x 10 cm) for each prepared gel were equilibrated in blotting buffer. On one side of an opened gel holder

cassette one fiber pad, two sheets of filter paper and the nitrocellulose membrane were placed. On top of the nitrocellulose membrane the gel was cautiously spread, avoiding inclusion of air. The remaining sheets of paper and foam pad were placed on top and the cassette was closed. Facing the membrane towards the anode the cassette was placed into an electrode module within an ice cooled buffer tank filled with 750 ml blotting buffer (4°C). Keeping the blotting chamber at 4°C the wet blot was performed transferring negatively charged protein from the gel onto the nitrocellulose membrane at 75 V, 0.16 A/cm^2 for 90 min. To verify the protein transfer and to fix the protein to the membrane, the blot was reversibly stained in Ponceau S solution (THERMO SCIENTIFIC). By washing two times for 5 min in T-TBS, the Ponceau staining was removed.

2.2.6.5 Immunodetection of protein

For the specific detection of protein the blots were blocked at room temperature in T-TBS containing 5% low fat dried milk for 60 min. For the detection of Wnt3a 5% (w/v) BSA/T-TBS were used. After the membrane was washed three times in T-TBS (15 min, 25°C) using an orbital shaker at 100 rpm (IKA), the primary antibody diluted in Roti block (see 2.1.3.3) was added for incubation overnight at 4°C on a 3D tumbling shaker at 25 rpm (HEIDOLPH). The next day the blot was washed three times as described above and incubated at room temperature with the fluorochrome-labeled (AlexaFluor680 or IRDye800) secondary antibody (see 2.1.3.3) diluted in Roti block for 60 min and shaking at 100 rpm (sheep anti rat IgG used for detection of Wnt3a was diluted in 10% (w/v) low fat dried milk/T-TBS). After removal of the secondary antibody the blot was washed again three times, maintained in T-TBS and was scanned using an Odyssey detection system (Ver. 2.1, LI-COR) at the following settings: resolution 84 µm, intensity 2-3, grey scale image, automatic sensitivity detection, brightness and contrast were adjusted equally from the automated image.
As a loading control anti-GAPDH antibody was used for detection of constitutively expressed glyceraldehyde 3-phosphate dehydrogenase. The blot was cleared off immunoglobulins by incubating the membrane for 45 min in stripping solution (THERMO SCIENTIFIC) at room temperature. Subsequently the blot was processed as described above.

2.2.6.6 Flow cytometry

Extracellular FACS staining

For FACS staining 8.0 x 105 macrophages stimulated as described above (see 2.2.4) were transferred to one well of a 96-well V-bottom-plate and centrifuged (300 x g, 5 min, 4°C). The supernatant was discarded and murine macrophages were resuspended in 50 µl FACS buffer containing FcγIII/II Block to prevent non-specific binding of immunoglobulines to Fc receptors (see 2.1.3.3, Tab. 2). After 25 min at 4°C the incubation was stopped by washing of the cells in 200 µl FACS buffer and centrifugation at 300 x g (5 min, 4°C). The supernatant was removed and cells were incubated for 25 min in the dark at 4°C with 50 µl biotinylated anti-Fzd1 (R&D SYSTEMS) diluted in FACS buffer, followed by Cy5-conjugated streptavidin (DIANOVA). After the first staining steps rat anti-mouse F4/80 (FITC; ABD SEROTEC), anti-mouse CD86 (PE; BD BIOSCIENCES) or anti-human CD14 (FITC; BECKMAN COULTER) were added for double staining of the cells, respectively. Rat IgG2aκ (Biotin) and rat IgG2bκ conjugated with FITC (both BIOLEGEND) as well as IgG2a (PE; CALTAG) or mouse IgG2b (FITC; DAKO) were used as isotype controls. After each incubation cells were washed as described above. In a final step macrophages were washed, fixed in FACS buffer containing 1% (v/v) paraformaldehyde (PFA) and transferred into a 5 ml falcon tube (BD BIOSCIENCES) for use in a flow cytometer (FACS Calibur; BD BIOSCIENCES). The macrophage population was determined by gating on forward, side scatter profile. In each measurement 10.000 to 50.000 cells were counted. The cut off for positive stained cells was set with regard to the isotype controls (± 3%). The cells were monitored by density plot analysis and positive gated populations were determined by quadrant statistics. When FACS staining was performed in the absence of cell permeabilization, direct binding of mAbs to cell membranes or molecules exposed on the surface of cells was visualized. This is termed “extracellular staining” in the text to reflect the fact that exposure of the analyzed molecule to the surrounding medium was necessary to record a fluorescent signal.

Intracellular FACS staining

For intracellular FACS staining 8.0 x 105 macrophages stimulated as described above (see 2.2.3) were transferred to one well of a 96-well V-bottom-plate and centrifuged (300 x g, 5 min, 4°C). The supernatant was discarded and the

macrophages were fixed for 10 min at 37°C by resuspending the cells in FACS buffer containing 3% (v/v) PFA. After fixation the cells were washed and permeabilized for 30 min at 4°C in FACS buffer containing 90% (v/v) methanol (modified after Krutzik and Nolan, 2003 (PMID 14505311)). Subsequently the cells were washed and treated as described above.

2.2.6.7 ELISA

Murine TNF was quantified using the DuoSet ELISA system (R&D SYSTEMS) as recommended by the manufacturer (see 2.1.3.3). The capture antibody was diluted 1:180 in PBS to a working concentration of 800 ng/ml. Flat-bottom 96-well maxi sorp micro plates were coated with 50 µl per well and sealed with an adhesive strip during an overnight incubation at room temperature. Plates were washed four times with washing buffer and saturated by filling the wells with 300 µl of blocking buffer. After at least 1 h of incubation at room temperature followed by four washing steps, 50 µl of sample and 2-fold serial dilutions of standard (2 ng/ml to 7.81 pg/ml in reagent diluent) were applied to the wells and incubated for 2 h at room temperature. Washing was repeated four times before 50 µl of the detection antibody (200 ng/ml) were added to the wells for a 2 h incubation at room temperature. Following four washing steps, 50 µl streptavidin-conjugated horseradish peroxidase (using a working dilution of 1:200 in reagent diluent) were applied to each well and removed after 20 min of incubation. Subsequently the microtiter plates were washed again as described above. Avoiding exposure to light, 50 µl substrate solution were pipetted into each well starting the peroxidase-mediated coloring reaction, which was stopped after 10 to 20 min by adding 50 µl of H_2SO_4. The extinction was measured for each well using a multi-channel photometer. The ELISA micro plate reader (Synergy2; BIOTEK) was set to 450 nm and an additional wavelength was set on 540 nm for wavelength correction ($A_{450nm\text{-}540nm}$). From the absorption of standard serial dilutions, a standard curve was created and used for calculation of cytokine concentrations in the samples.

2.2.6.8 Chemiluminescence measurements

Generation of reactive oxygen intermediates (ROI) by BMDM was determined in a 6-chanel-luminometer (Biolumat LB 9505, BERTHOLD) by measurement of

chemiluminescence (CL) in the presence of 130 µg/ml lucigenin (9,9'-bis(*N*-methylacridinium nitrate); Roche). The quantum yield of samples was detected by photomultipliers connected to lightproof and 37°C temperated vial chambers. The sensitivity of the luminometer was set to 375 nm to 620 nm. Prior to CL-measurements 2 x 10^5 BMDM in a volume of 200 µl CL-medium were seeded onto the bottom of a lumi vial (BERTHOLD). The chemiluminescent reagent lucigenine (ROCHE) was added to a final concentration of 250 µM. The cells were incubated for 45 min in an incubation chamber at 37°C and 5% CO_2. Afterwards the vials were placed in preheated (37°C) vial chambers of the luminometer. The lid of each chamber was closed avoiding external light disturbances and the chemiluminescence was recorded. Following 5 min of blank measurements, the vial chamber was opened and Fzd1/Fc fusion protein (3 µg/ml), zymosan (130 µg/ml) and human serum (10 µl) were added to the cells. The vials were gently agitated and placed again into the measuring chamber. The lids were closed and the measurement was continued for an additional 25 min to analyze the CL resulting from the reaction between reactive oxygen intermediates (ROI) and lucigenin. To visualize the results as counts per minute (CPM), the blank values were used to adjust the graphs of individual measurements to a common origin. This calculation was performed using correction software programmed by Dr. Martin Ernst (Research Center Borstel).

2.2.7 Statistical analyses

For statistical analyses the mean values of technical replicates of at least three independent *in vitro* experiments were log transformed after Willems et al.[169]. The differences between untreated and treated cells or wild type and knockout mice derived cells were defined to be significant using the Student's two-tailed *t*-test (confidence interval 95%) of paired observations. At least four biological replicates were used for statistical analyses of *in vivo* experiments assuming nonparametric distribution. The differences between untreated and treated mice were defined to be significant using the the Mann-Whitney-u-test. All values shown represent the mean ± standard error of the mean (SEM).

3. Results

3.1 Analyses of the Wnt/β-catenin pathway in *M. tuberculosis*-infected mice

The Wnt/β-catenin pathway has been well characterized in developmental processes during and after embryogenesis[78;170]. The epithelial surface in barrier organs (gut, skin, lung) is constantly exposed to environmental and microbial assaults. This dynamic process can be viewed as one regulating the equilibrium between pro- and anti-inflammatory, destructive, regenerative and remodeling activities in order to maintain "homeostasis" or advantageously balanced functional condition of the tissue. In this study, the term "tissue homeostasis" is used several times to denote exactly this tightly regulated functional optimization of stressed tissue. Regarding the lung, it was shown that maintenance of the homeostasis and architecture are highly connected with functions modulated by the Wnt/β-catenin pathway[76]. The homeostasis and function of the respiratory system are severely altered during inflammation and infection. In a recent report, strong induction of the Wnt/β-catenin pathway after acute lung injury was shown[171]. Yet, little is known about the role of Wnt/β-catenin signaling in chronic inflammations. Therefore, essential mediators of the Wnt/β-catenin pathway were analyzed in the experimental mouse model of *M. tuberculosis* aerosol infection.

3.1.1 The experimental model: aerosol infection of mice with *M. tuberculosis*

C57BL/6 mice were infected with 100 colony forming units (CFU) *M. tuberculosis* (strain H37Rv) via the aerosol route. One day after infection the lungs of three control mice were homogenized and plated for colony enumeration, quantifying the effective mycobacterial dose used in the experiment. To document the progression of the infection, the mycobacterial growth in the lungs of mice challenged with *M. tuberculosis* was monitored by colony enumeration assay on day 21 and day 42 post-infection (Fig. 3A). In parallel total RNA was isolated from lung homogenates of *M. tuberculosis*-infected mice and untreated mice.

Following the first three weeks post-infection a significant increase in bacterial burden by 5 log units was detected, reaching a stationary phase that remained until day 42. To examine the transcriptional activation of marker genes associated with inflammation, the expression of TNF mRNA and IFN-γ mRNA was analyzed (Fig. 3B,

C). Compared to uninfected wild type mice (day 0) a significant up-regulation of TNF transcripts on day 21 and day 42 post-infection was detected.

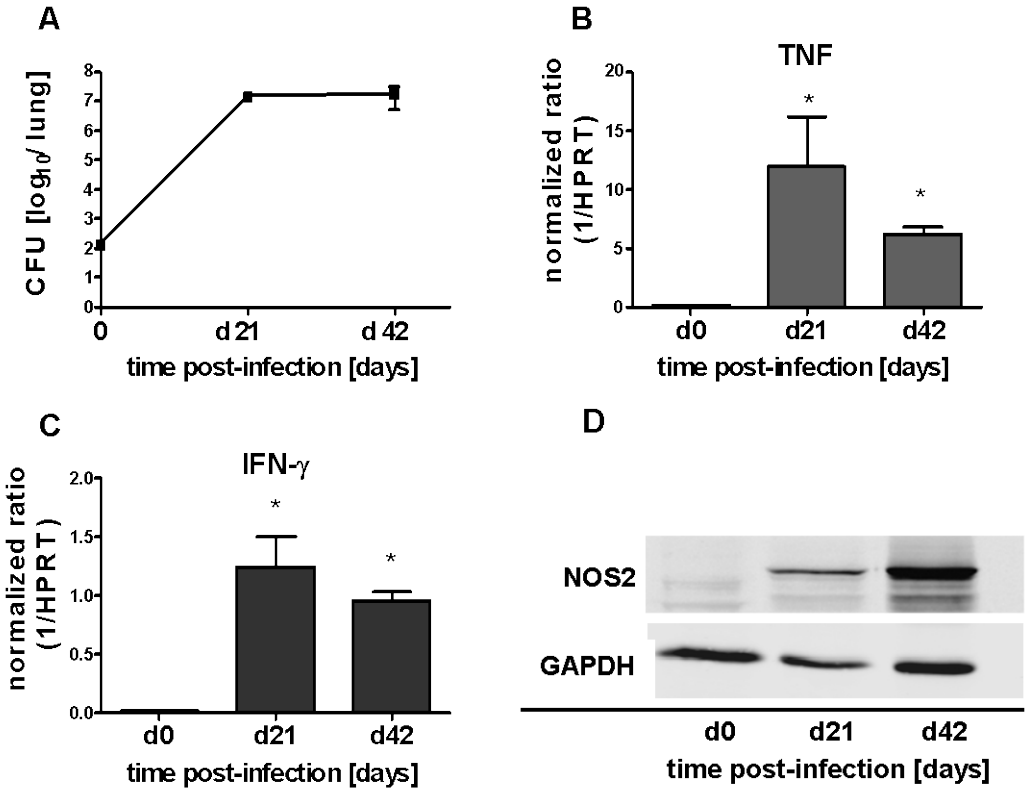

Figure 3. Bacterial growth, TNF, IFN-γ transcription and NOS2 protein expression in lung homogenates of *M. tuberculosis*-infected mice.
C57BL/6 mice were infected with *M. tuberculosis* (strain H37Rv) via the aerosol route with 100 CFU per lung. For each experiment five mice matching in sex and age were sacrificed at indicated time points. **(A)** The lungs were aseptically removed and bacterial growth was determined by colony enumeration assay, indicating colony forming units (CFU) per lung. The results represent the mean ± SEM of five mice. Total RNA was isolated from lung homogenates and reverse transcribed. Cytokine mRNA expression of **(B)** TNF and **(C)** IFN-γ was determined by quantitative real-time PCR analysis, showing the normalized ratio of target gene and reference gene (hypoxanthine phosphoribosyl-transferase, *Hprt*). The results represent the mean ± SEM of four mice. Statistical analysis was performed by the Mann-Whitney-u-test defining differences between uninfected (d0) and infected mice as significant (*$p < 0.05$).
(D Equal protein amounts of five lung homogenates per indicated time point after infection were pooled and separated by SDS-PAGE. After protein transfer to a nitrocellulose membrane the blot was incubated with anti-NOS2 antibody. Following incubation with secondary reagents, the blot was analyzed using an Odyssey near-infrared detection system. Additional Western blot analysis of GAPDH was performed to ensure equal loading of protein.

Similar results were obtained for the expression of IFN-γ mRNA. TNF and the lymphokine IFN-γ are important activators of macrophage effector functions. IFN-γ significantly enhances the expression of nitric oxide synthase 2 in macrophages, which catalyzes the production of nitric oxide and reactive nitrogen intermediates

(RNI). Upon infection with *M. tuberculosis*, mice deficient for IFN-γ fail to release RNI and are unable to control mycobacterial growth[144]. According to the published molecular mass of NOS2 protein, a band of approx. 125 kDa was identified in lung homogenates of *M. tuberculosis*-infected mice by Western blot analysis (Fig. 3D). Induction of NOS2 was not detected in lung homogenates of uninfected mice (d0), whereas a drastic increase of NOS2 protein was observed on day 21 and day 42 post-infection.

3.1.2 Expression of cell type specific genes.

It is known that *M. tuberculosis* infection causes a strong infiltration of immune cells into the lung to the site of inflammation. Thereby, the pathogen severely affects the homeostasis of the respiratory system. To measure the cell influx of immune cells and to examine the relation between immune cells and epithelial cells during the course of infection, cell type specific marker genes were analyzed.

Lung homogenates of *M. tuberculosis*-infected and uninfected mice were generated, and total RNA was extracted. Reverse transcription was performed prior to the analysis by quantitative real-time PCR. The following cell type specific marker genes were monitored, which are usually used for the generation of cell type specific knockout mice[172-174]: leukocyte-specific protein tyrosine kinase (*Lck*) expressed by $CD4^+$ or $CD8^+$ T cells, lysozyme M (*LysM*) being a marker gene for myeloid cells and surfactant associated protein C (*Sftpc*) as well as secretoglobin1A1 (*Scgb*) as markers for alveolar (type 2) and bronchiolar epithelial cells (clara cells)[175;176]. Figure 4A shows that on day 21 and day 42 post-infection a strong increase in Lck transcription was detected (25- to 40-fold). Similarly but to a lesser extend, expression of the *LysM* gene in myeloid cells was increased by 2- to 2.5-fold (Fig. 4B). In contrast, the expression of epithelial marker genes *Sftpc* and *Scgb* was decreased by 85% to 90% during the course of *M. tuberculosis* infection, suggesting a relative numeral decrease of epithelial cells in the inflamed lung (Fig. 4C). Whereas in uninfected mice (day 0) the mRNA expression level of epithelial cell derived Sftpc and Scgb was above that of Lck and LysM, the relation had switched on day 21 and day 42 post-infection (Fig. 4).

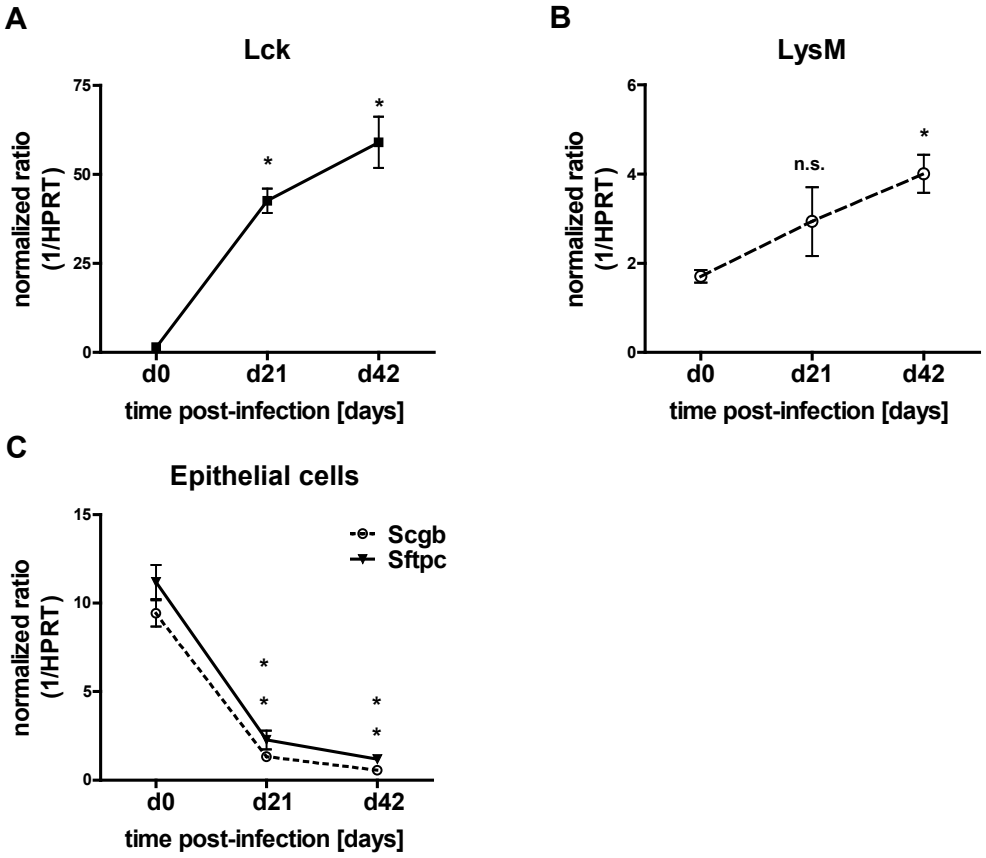

Figure 4. Cell specific marker gene expression in lung homogenates of *M. tuberculosis*-infected mice.
C57BL/6 mice were infected via the aerosol route with 100 CFU *M. tuberculosis*. For each experiment four mice matching in sex and age were sacrificed at indicated time points. Lung homogenates were generated for isolation of total RNA. After reverse transcription the mRNA expression of cell type specific target genes was determined by quantitative real-time PCR analysis (*Taq*Man® assay). The following target genes were analyzed as markers specific for: **(A)** bronchiolar epithelial cells (*Scgb*) and alveolar epithelial cells (*Sftpc*), **(B)** lymphoid cells, *Lck* and **(C)** myeloid cells, *LysM*. Delineated is the normalized ratio of target gene and reference gene (HPRT). The results represent the mean ± SEM of four mice. Statistical analysis was performed by the Mann-Whitney-u-test defining differences between uninfected (d0) and infected mice as significant (*$p < 0.05$).

3.1.3 Expression of Fzd homologs

Having observed an inflammatory phenotype of C57BL/6 mice challenged with *M. tuberculosis*, the expression of Wnt/Fzd signaling intermediates of the β-catenin pathway during the course of infection was of special interest. Lung homogenates generated from mice on day 21 and day 42 post-infection were examined by quantitative real-time PCR. In a systematic screen of 10 Frizzled homologs, the transcripts of most homologs (Fzd3, -4, -7, -8, -9 and -10) were significantly decreased. However, the mRNA expression of Fzd1 and Fzd5 was found to be significantly up-regulated (Fig. 5). Compared to control mice, transcripts of Fzd1 were increased by 2- to 3-fold on day 21 and 42 post-infection.

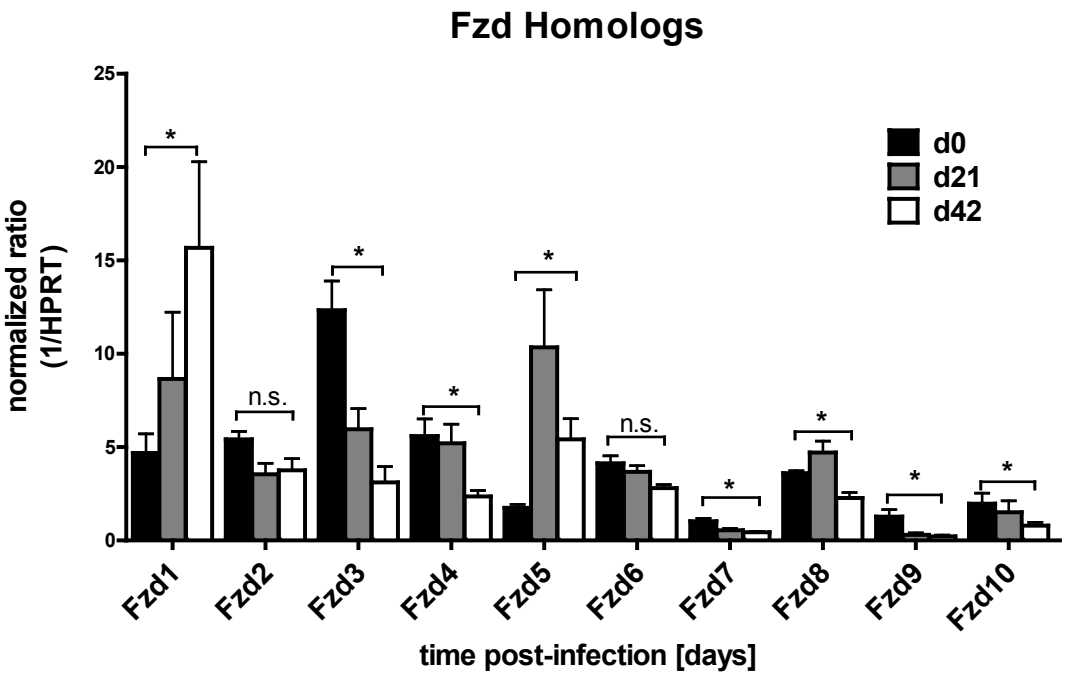

Figure 5. Analysis of Fzd1 - 10 mRNA expression in lung homogenates of *M. tuberculosis*-infected mice.
C57BL/6 mice were infected with *M. tuberculosis* via the aerosol route at an effective dose of approx. 100 CFU per lung. For each experiment four mice matching in sex and age were sacrificed at indicated time points. Total RNA was isolated from lung homogenates and reverse transcribed. mRNA expression of Fzd homologs 1 to 10 was determined by quantitative real-time PCR analysis (*Taq*Man® assay), showing the normalized ratio of target gene and reference gene (HPRT). The results represent the mean ± SEM of four mice. Statistical analysis was performed by the Mann-Whitney-u-test defining differences between uninfected (d0) and infected mice as significant (*$p < 0.05$).

In addition, immunoblot analysis of lung homogenates revealed a decreased expression of total Fzd1 protein on day 21 and day 42 post-infection (Fig. 6). Fzd1 was detected indicating a double band of approx. 70 kDa, which corresponded to the theoretical mass of Fzd1 (71 kDa).

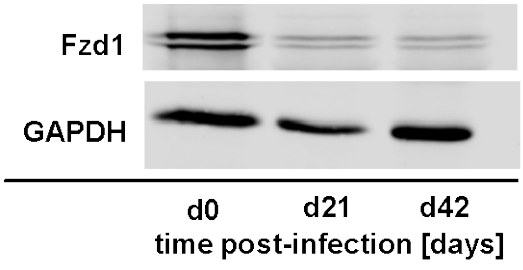

Figure 6. Fzd1 protein expression in lung homogenates of *M. tuberculosis*-infected mice.
The lungs of C57BL/6 mice were aseptically removed and homogenized. Equal concentrations of total protein of five mice per indicated time point were pooled and separated by SDS-PAGE. After protein transfer to a nitrocellulose membrane the blot was incubated with anti-Fzd1 antibody. Following incubation with secondary reagents, the blot was analyzed using an Odyssey near-infrared detection system. Detection of recombinant Fzd1/Fc fusion protein indicated the specificity of the anti-Fzd1 antibody (see Fig. 21). Additional immunoblot analysis of GAPDH was performed to ensure equal loading of protein.

3.1.4 Localization of Fzd1 promoter activity

To localize Fzd1 expressing cells *in vivo*, the lungs of untreated heterozygous Fzd1$^{+/LacZ}$ reporter mice were aseptically removed and frozen in tissue freezing buffer for cryo-sectioning. Cuts were mounted on glass slides and incubated with X-gal (bromo-chloro-indolyl-galactopyranoside) substrate solution. Enzymatic cleavage of X-gal by β-galactosidase, which is encoded by the *LacZ* reporter gene down-stream of the Fzd1 promoter, resulted in an insoluble blue reaction product (5,5'-dibromo-4,4'-dichloro-indigo). Enzymatic cleavage of X-gal by β-galactosidase, which is encoded by the *LacZ* reporter gene down-stream of the Fzd1 promoter, resulted in an insoluble blue reaction product (5,5'-dibromo-4,4'-dichloro-indigo). Blue stained cells indicating Fzd1 promoter activity were visualized by bright field microscopy. Fzd1 promoter activity was detected in lung vessels of Fzd1$^{+/LacZ}$ reporter mice (Fig. 7A, B). In addition, activation of the Fzd1 promoter was found in cells of the outer rim of bronchioles and in single cells of the alveolar tissue (Fig. 7C – E). Murine lung sections from wild type mice (negative control) remained negative after incubation with X-gal solution (Fig.7F).

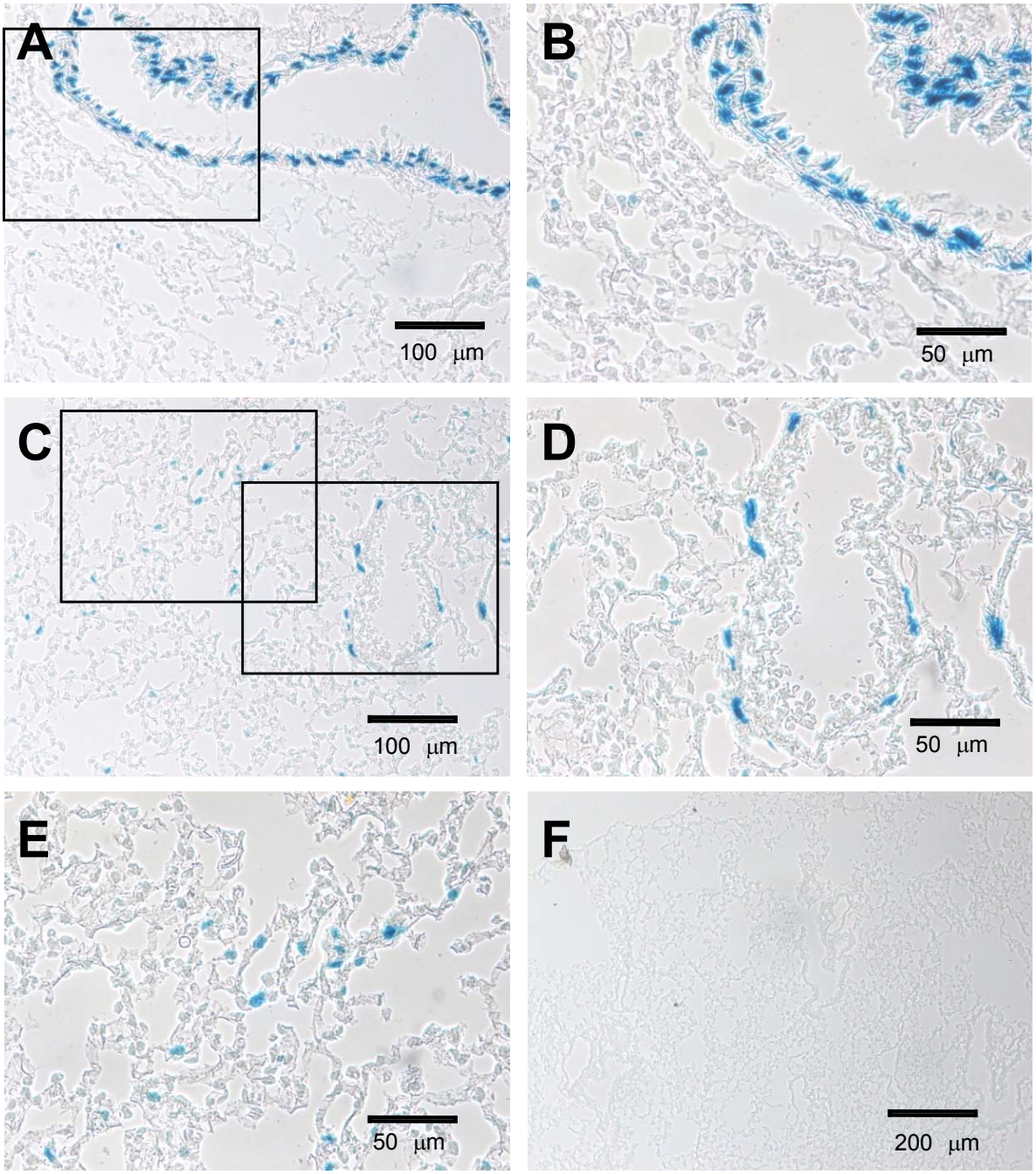

Figure 7. Localization of Fzd1 promoter activity in lung tissue of Fzd1$^{+/LacZ}$ reporter mice.
For microscopical analysis cryo-sections (5 µm thick) were cut from frozen lungs of heterozygous Fzd1$^{+/lacZ}$ reporter mice **(A-E)** and C57BL6 mice, which were used as negative control **(F)**. The cryo-sections were mounted on glass slides and incubated overnight in X-gal substrate solution. β-galactosidase expression (*LacZ* gene) due to Fzd1 promoter activity resulted in a blue staining of cells. Representative sections from one out of four mice are shown (magnification 100 x, 200 x, 400 x)

3.1.5 Expression of Fzd1 ligands Wnt3a and Wnt7b

The most prominent ligands reported to bind to receptor Fzd1 are the Wnt homologs 3a and 7b. Wnt3a is one of the best characterized Wnt homologs associated with the induction of β-catenin signaling, whereas Wnt7b is known to activate the β-catenin pathway especially during lung development[56;177]. To address whether Wnt3a and Wnt7b expression are regulated in response to *M. tuberculosis* infection *in vivo*, lung homogenates generated on day 21 and day 42 post-infection were examined. By quantitative real-time PCR analysis, Wnt3a was found constitutively expressed in the lungs of infected and uninfected mice (Fig. 8A). In contrast, transcripts of Wnt7b were significantly increased 2.5- and 3.5-fold on day 21 and day 42 post-infection (Fig. 8B). Due to the limited availability of suitable antibodies, further analyses focused on the localization of Wnt3a protein.

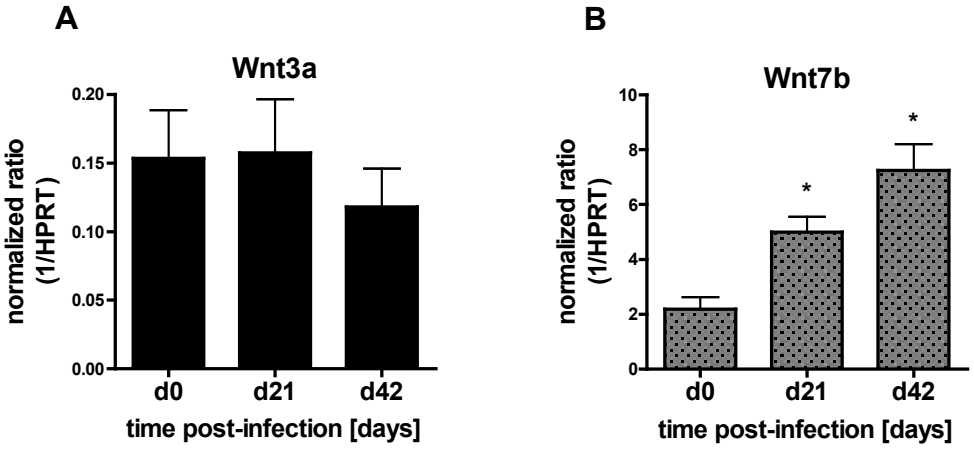

Figure 8. Analysis of Wnt3a and Wnt7b transcription in lung homogenates of *M. tuberculosis*-infected mice.
(A, B) Lungs of C57BL/6 mice infected via the aerosol route with 100 CFU *M. tuberculosis* per lung were prepared at indicated time points. For each experiment four mice were matched in sex and age. Lung homogenates were prepared and total RNA was isolated. After reverse transcription the mRNA expression of Wnt3a and Wnt7b was determined by quantitative real-time PCR analysis (*Taq*Man® assay), showing the normalized ratio of target gene and reference gene (HPRT). The results represent the mean ± SEM of four mice. Statistical analysis was performed by the Mann-Whitney-u-test defining differences between uninfected (d0) and infected mice as significant (*$p < 0.05$).

3.1.6 Localization of Wnt3a protein

Constitutive mRNA expression of Fzd1 ligand Wnt3a was observed in lung homogenates of *M. tuberculosis*-treated mice from day 0 to day 42 post-infection. To localize Wnt3a expression in lungs of uninfected or *M. tuberculosis*-infected mice, immunohistochemical analyses were performed.

Paraffin sections were incubated with monoclonal anti-Wnt3a antibody, followed by a biotin labeled secondary antibody and horseradish peroxidase (HRP-) conjugated streptavidin. Additional haematoxylin counterstaining was performed (Fig. 9). Wnt3a was detected in lung sections of both, uninfected (Fig. 9A, B) and infected mice (Fig. 9C, D). In the lung tissue of mice treated with *M. tuberculosis*, infiltrating mononuclear cells were observed in close proximity to the bronchioles. However, cells expressing Wnt3a were localized in the bronchiolar epithelium of uninfected and infected mice (Fig. 9A - D). Paraffin sections that were stained in the absence of the anti-Wnt3a antibody were used as negative control (Fig. 9E).

Additional immunohistochemical analyses were performed to examine whether Wnt3a was present in granulomatous lesions of mice infected with 100 CFU *M. tuberculosis*. Paraffin embedded lung tissue that was prepared on day 42 post-infection, was stained as described above for the localization of Wn3a protein. Figure 10 shows a granulomatous lesion representing strong infiltration of mononuclear cells. Wnt3a was not detected in granulomatous or inflamed lung tissue (Fig. 10A - C). Paraffin sections that were stained in the absence of the anti-Wnt3a antibody were used as negative control (Fig. 10D - F).

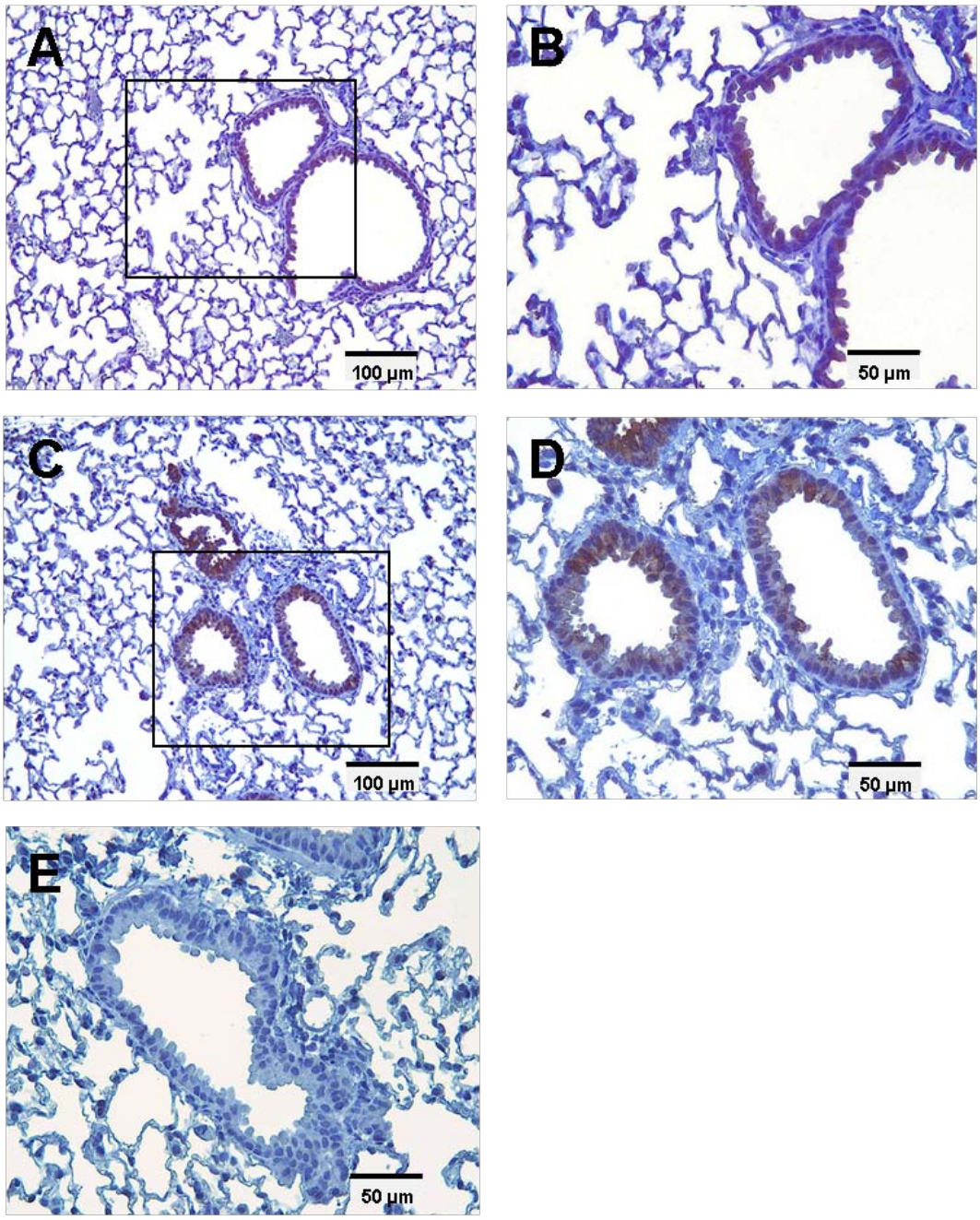

Figure 9. Immunohistological analysis of Wnt3a in lung tissue of uninfected and *M. tuberculosis*-infected mice.
C57BL/6 mice were infected with 100 CFU *M. tuberculosis* via the aerosol route. For microscopical analysis layers of 2 µm were cut from paraffin embedded lung tissue derived from **(A, B)** uninfected mice or **(C, D)** infected mice (day 42 post-infection). Immunohistochemical staining was performed by the sequential use of monoclonal rat anti-Wnt3a antibody, biotin conjugated goat anti-rat IgG and HRP conjugated streptavidin. For detection the cells were incubated with 3,3'-diaminobenzidine (DAB) substrate solution. **(E)** As staining control, sections of infected mice were stained in the absence of the anti-Wnt3a antibody. Tissue sections were counterstained using haematoxylin staining solution. Representative preparations from one out of four infected mice or uninfected mice are shown (magnification 200 x, 400 x).

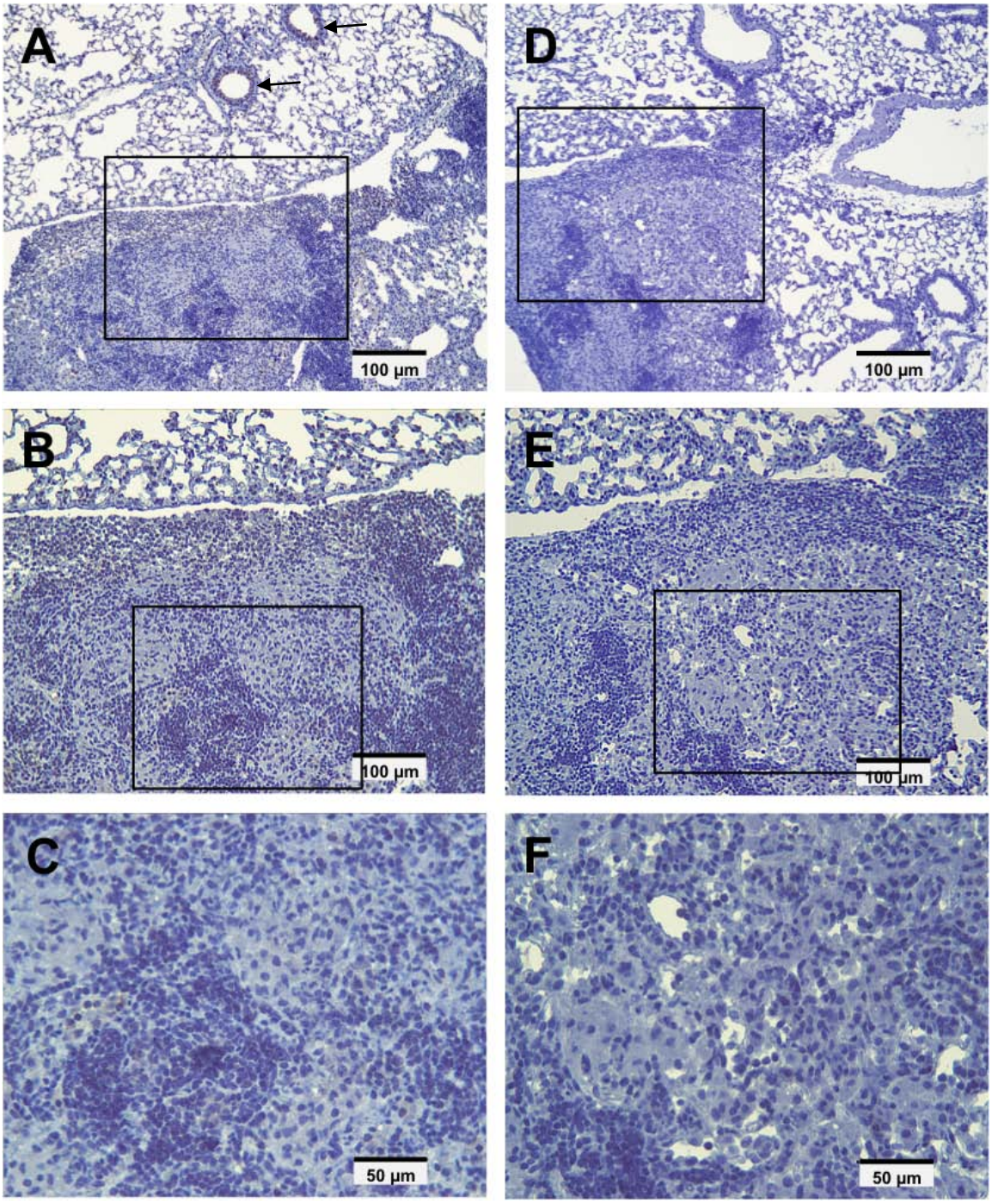

Figure 10. Immunohistological analysis of Wnt3a localization in granulomatous lesions of *M. tuberculosis*-infected mice.
C57BL/6 mice were infected with 100 CFU *M. tuberculosis* via the aerosol route and sacrificed on day 42 post-infection. **(A - C)** For microscopical analysis layers of 2 µm were cut from paraffin embedded lung tissue. Immunohistochemical staining was performed by the sequential use of monoclonal rat anti-Wnt3a antibody, biotin conjugated goat anti-rat IgG and HRP conjugated streptavidin. Positive staining (arrowheads, see also Fig. 9) was indicated by a dark brown reaction product due to HRP-mediated oxidation of DAB substrate solution. **(D - F)** As staining control, sections of infected mice were stained in the absence of the anti-Wnt3a antibody. Tissue sections were counterstained using haematoxylin staining solution. Representative preparations from one out of four infected mice are shown (magnification 100x, 200 x, 400 x).

3.1.7 Analysis of β-catenin stabilization and target gene expression

The β-catenin pathway is the best characterized Wnt/Fzd signaling pathway and known to be involved in the maintenance of the lung homeostasis[76;178;179]. Yet, little is known about its activation during bacterial infections. For that reason lung homogenates of *M. tuberculosis*-infected mice were analyzed to monitor a putative regulation of β-catenin signaling. Lung homogenates were generated and total RNA was extracted to analyze the expression of *Axin2*, which is a β-catenin dependent target gene and negative feed-back regulator of the Wnt/β-catenin pathway[180]. After reverse transcription transcripts of Axin2 were detected by quantitative real-time PCR. Figure 11A demonstrates that in response to mycobacterial infection Axin2 expression was significantly reduced by 70%.

These findings were further corroborated by the detection of overall β-catenin protein levels in lung homogenates. After isolation of total protein from lung homogenates, it was observed by immuno blot experiments that the β-catenin levels were decreased on day 21 and day 42 post-infection. β-catenin was detected indicating a band of approx. 90 kDa (Fig. 11B).

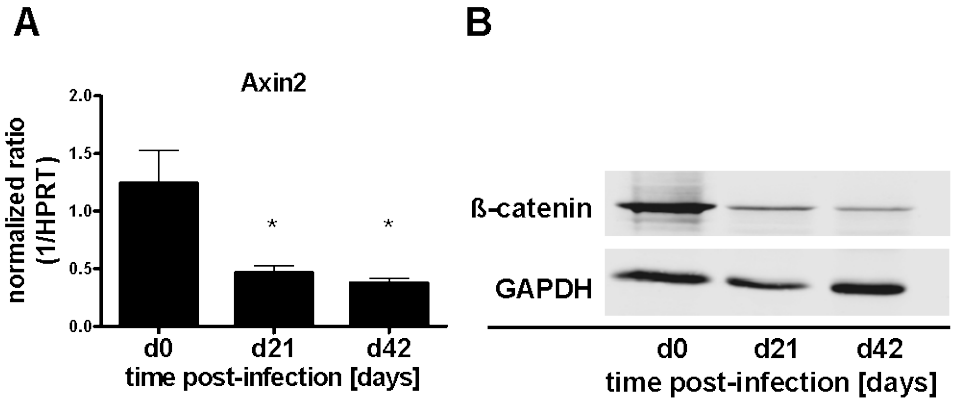

Figure 11. Analysis of Axin2 transcription and β-catenin protein levels in lung homogenates of *M. tuberculosis*-infected mice.
(A) C57BL/6 mice were infected with *M. tuberculosis* by aerosol infection using 100 CFU per lung. For each experiment four mice matching in sex and age were sacrificed at indicated time points. Total RNA was isolated from lung homogenates and reverse transcribed. mRNA expression of Axin2 was determined by quantitative real-time PCR analysis (*Taq*Man® assay), showing the normalized ratio of target gene and reference gene (HPRT). The results represent the mean ± SEM of four mice. Statistical analysis was performed by the Mann-Whitney-u-test defining differences between uninfected (d0) and infected mice as significant (*$p < 0.05$).
(B) Lungs of *M. tuberculosis*-infected C57BL/6 mice and uninfected mice were isolated at indicated time points (see above). Equal concentrations of total protein of five mice per indicated time point were pooled and electrophoretically separated by SDS-PAGE. After protein transfer to a nitrocellulose membrane the blot was incubated with primary β-catenin or GAPDH antibody. After treatment with secondary antibodies the blot was analyzed in an Odyssey near-infrared detection system. Additional immuno blot analysis of GAPDH was performed to ensure equal loading of protein.

Summary 3.1

- *Aerosol infection*: *M. tuberculosis*-infected mice (100 CFU) showed a 5 log increase in the bacterial burden on day 21 and day 42 post-infection. This was paralleled by an increased expression of TNF and IFN-γ mRNA, as well as NOS2 protein, indicating an inflammatory phenotype.
- *Cell composition*: During the course of infection, transcripts of lymphoid and myeloid marker genes (*Lck*, *LysM*) were significantly increased, indicating enhanced T cell and myeloid cell numbers within the lung. In contrast, a strong reduction in the expression of epithelial marker genes *Sftpc* and *Scgb* was observed, indicating a reduction of alveolar type 2 epithelial cell and clara cell numbers.
- *Fzd receptors*: In lung homogenates of *M.tuberculosis*-infected mice Fzd1 and Fzd5 mRNA were found to be significantly up-regulated during the course of infection, whereas Fzd homologs -4, -7, -8, -9 and -10 were decreased. Total Fzd1 protein was reduced in response to *M. tuberculosis* infection. Using $Fzd1^{+/LacZ}$ reporter mice, Fzd1 promoter activity was localized in cells of the vasculature, bronchioles and single cells within alveoli.
- *Wnt ligands*: During the course of infection mRNA levels of Fzd1 ligand Wnt3a were constitutively expressed in lung homogenates, whereas the expression of the Wnt homolog 7b was found to be significantly increased. By immunohistochemical analysis Wnt3a protein was found constitutively expressed in the bronchiolar epithelium and was not detected in alveolar or granulomatous tissue of *M. tuberculosis*-infected mice.
- *Wnt/β-catenin pathway*: During the course of infection β-catenin signaling was decreased in lung homogenates of *M. tuberculosis*-infected mice as measured by the decreased expression of Axin2 mRNA and β-catenin protein levels.

3.2 Fzd1 mRNA expression in murine macrophages after stimulation with mycobacteria and conserved bacterial structures

The ability to recognize a wide range of microorganims and conserved structures through membrane or cytosolic receptors is central to macrophage functions. Thereby, macrophages and closely related myeloid cells initiate responses that contribute to the maintenance of homeostasis, innate effector functions and the induction of acquired immunity[99]. Macrophages are the preferred target cells of *M. tuberculosis*, in which the pathogen may survive and replicate[181]. First *in vivo* experiments have shown that Fzd1 mRNA expression was increased in response to *M. tuberculosis* infection. Thus, further *in vitro* studies were performed to analyze, whether microbial stimulation leads to the induction of Fzd1 mRNA expression in murine macrophages.

3.2.1 Fzd1 transcription in response to increasing doses of mycobacteria and LPS

To analyze the influence of mycobacteria on Fzd1 mRNA expression, bone marrow-derived macrophages (BMDM) were infected with increasing multiplicities of infection (bacteria per macrophage, MOI) of *M. tuberculosis* (*M. tuberculosis*, strain H37Rv) or *M. avium* (*M. avium*, strain SE01) for 4 hours. In an additional approach, BMDM were stimulated for 4 hours with increasing concentrations of lipopolysaccharide (LPS) to monitor Fzd1 transcription in response to conserved bacterial structures derived from Gram-negative bacteria. Quantitative real-time PCR based on a SYBR green assay was performed to examine the induction of Fzd1 and TNF mRNA transcription.

A dose dependent up-regulation of Fzd1 mRNA expression in response to *M. tuberculosis* and *M. avium* by 15- to 60-fold was detected. Following LPS-treatment Fzd1 transcription was increased by 25- to 45-fold reaching a plateau at 1 ng/ml LPS (Fig. 12A). In parallel TNF mRNA expression was analyzed as stimulation control and an indicator of macrophage activation. Fzd1 transcription correlated with a dose dependent increase in TNF mRNA expression (Fig. 12B) in response to *M. tuberculosis* and *M. avium* (35- to 750-fold) or LPS (100- to 375-fold).

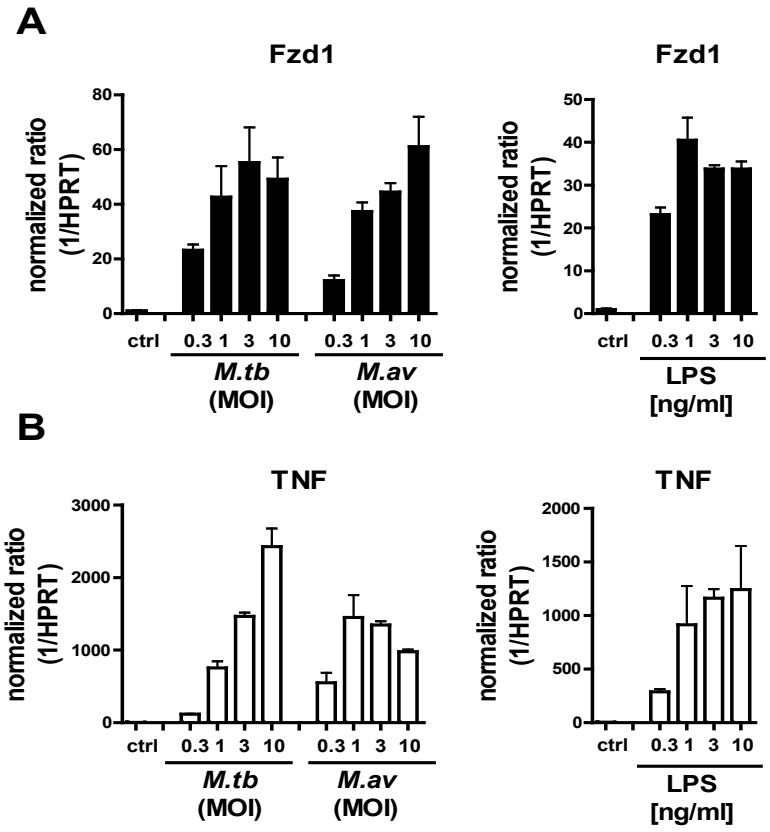

Figure 12. Mycobacteria- and LPS-induced Fzd1 and TNF mRNA expression in murine macrophages.
C57BL/6 bone marrow-derived macrophages (BMDM) were incubated with increasing multiplicities of infection (MOI) of mycobacteria (*M. tuberculosis, M. avium*) per macrophage and increasing concentrations of LPS. After 4 hours of stimulation cells were lysed and total RNA was isolated. Following reverse transcription the mRNA expression of Fzd1 **(A)** and TNF **(B)** was analyzed by quantitative real-time PCR (SYBR green assay). To calculate the normalized ratio of Fzd1 and TNF, the ratio between target gene and reference gene HPRT was formed. BMDM of three mice were pooled. Results are means ± SEM of triplicate measurements.

3.2.2 Time course of Fzd1 transcription in response to mycobacteria and LPS

To monitor the time course of Fzd1 mRNA expression in murine macrophages, cells were stimulated with *M. tuberculosis* (0.5 bacteria per macrophage), *M. avium* (3 bacteria per macrophage) or LPS (10 ng/ml). Cells were lysed at indicated time-points and prepared for analysis by quantitative real-time PCR using a SYBR green assay.

Already 1 hour (*M. avium*, LPS) to 2 hours (*M. tuberculosis*) after stimulation increased Fzd1 transcripts were detected, which remained increased for 8 hours. Independent of the stimulatory agents used, macrophage Fzd1 mRNA expression displayed a maximum after 4 hours post-infection, whereas 24 hours after infection Fzd1 mRNA had decreased to the detection limit (Fig. 13A). In the same samples up-

regulation of TNF mRNA was detected. However, compared to the kinetics of Fzd1, TNF mRNA expression peaked at an earlier time point. TNF was strongly induced after 1 hour (*M. avium*, LPS) and 2 hours (*M. tuberculosis*) post-infection and decreased after 8 hours. In correlation to Fzd1 expression TNF transcripts were reduced to a minimum 24 hours post-infection (Fig. 13B).

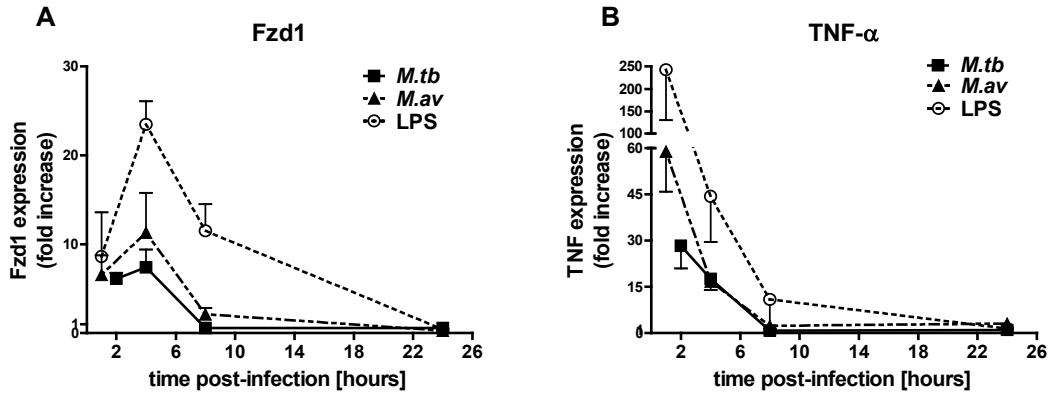

Figure 13. Kinetics of mycobacteria- and LPS-induced Fzd1 and TNF mRNA expression in murine macrophages.
(A, B) C57BL/6 bone marrow-derived macrophages (BMDM) were stimulated at an infection ratio of 0.5 (*M. tuberculosis)* or 3 mycobacteria (*M. avium*) per macrophage and 10 ng/ml LPS, respectively. At indicated time points the cells were lysed and total RNA was isolated. After reverse transcription mRNA expression of Fzd1 and TNF was analyzed by quantitative real-time PCR (SYBR green assay). To calculate the fold induction of Fzd1 and TNF mRNA expression the normalized ratio between target gene and reference gene (HPRT) was normalized to the corresponding control of a given time point. Shown is one out of two independent experiments. Results are means ± SEM of duplicate measurements.

3.2.3 Induction of Fzd1 mRNA expression in murine macrophages:

3.2.3.1 Role of TLR2 and MyD88

In murine macrophages the induction of Fzd1 transcription was triggered in response to mycobacteria and lipopolysaccharide (LPS). Conserved structures of bacteria are recognized by pattern recognition receptors (PRR) in particular by members of the Toll-like receptor family (TLR)[182].

To elucidate if Fzd1 transcription was dependent on the presence of TLR2, BMDM isolated from TLR2-deficient mice and wild type mice were stimulated with *M. tuberculosis*, *M. avium* (3 bacteria per macrophage) and the synthetic lipopeptide Pam_3CSK_4 (100 ng/ml). As a TLR2 independent control, macrophages were treated with LPS (10 ng/ml), which was used as a known agonist of TLR4 dependent signaling. After 4 hours of stimulation the cells were lysed and prepared for

quantification of Fzd1 transcripts by real-time PCR. Due to the advantage of a higher specificity as compared to the SYBR green assay (see figure 12 and 13), the following real-time PCR experiments were performed by *Taq*Man® assay (Fig. 14A). In TLR2-deficient macrophages treated with *M. avium* or synthetic TLR2 agonist Pam_3CSK_4, Fzd1 expression was decreased by 70% (*M. avium*) to 85% (Pam_3CSK_4) as compared to wild type derived cells. In contrast, exposure to *M. tuberculosis* indicated that both BMDM derived from wild type mice and $TLR2^{-/-}$ mice showed no differences in the transcription of Fzd1. These results were below the mRNA expression level of Fzd1 as depicted in figure 12, which was due to the change of the qRT-PCR protocol as well as the use of a freshly cultured *M. tuberculosis* H37Rv strain. This isolate was obtained from the American Type Culture Collection and showed a significantly lower activation potential (as was tested in the Division of the Microbial Interface Biology). In addition to mycobacteria or synthetic lipopeptide, LPS, a known TLR4 ligand, was used as control. The results showed that the treatment of macrophages with LPS did not differ between $TLR2^{-/-}$ and wild type cells.

TNF mRNA expression correlated with the induction of Fzd1 (Fig. 14B). In TLR2-deficient cells the TNF mRNA expression was significantly reduced in response to TLR2 stimuli. The treatment with LPS led to a high induction of TNF expression in $TLR2^{-/-}$ cells and wild type derived cells.

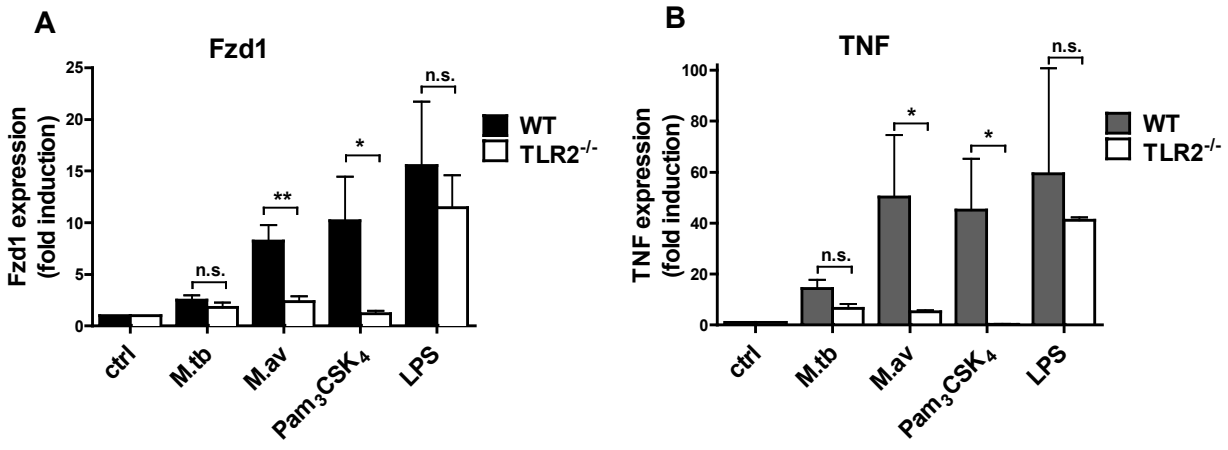

Figure 14. Analysis of Fzd1 and TNF transcription in macrophages of $TLR2^{-/-}$ mice.
BMDM from wild type and TLR2-deficient mice were incubated with an infection ratio of 3 mycobacteria per macrophage (*M. tuberculosis*, *M. avium*), 100 ng/ml of synthetic TLR2 agonist Pam_3CSK_4 and 10 ng/ml LPS. 4 hours post-stimulation cells were lysed for total RNA extraction to monitor the fold induction of **(A)** Fzd1 mRNA and **(B)** TNF mRNA by quantitative real-time PCR (*Taq*Man® assay). Shown is the normalized ratio between target gene and reference gene (HPRT) normalized to the untreated control. The results are means ± SEM of three independent experiments performed in technical duplicates. For statistical analysis the data were log transformed and analyzed by Student's two tailed, paired *t*-test defining differences between wild type and knockout derived cells as significant (*$p < 0.05$).

The downstream signaling pathways initiated through Toll-like receptors are orchestrated by multiple adaptor proteins, kinases and transcription factors[97]. Downstream of TLR2 and TLR4 the influence of adaptor protein myeloid differentiation primary response gene 88 (MyD88) on Fzd1 induction was analyzed. BMDM from MyD88-deficient mice and wild type mice were stimulated with an infection ratio of 3 mycobacteria per macrophage (*M. tuberculosis*, *M. avium*) or LPS (10 ng/ml) for 4 hours and prepared as described above to determine mRNA expression by quantitative real-time PCR (TaqMan® assay).

In MyD88-deficient macrophages treated with mycobacteria a significant reduction of Fzd1 mRNA expression by 75% (*M. tuberculosis*) to 95% (*M. avium*) was observed when compared to wild type cells. Stimulation with LPS led to a significant decrease of Fzd1 transcripts by more than 60% in MyD88-deficient macrophages (Fig. 15A). These findings also correlated with the expression of TNF transcripts, which served as a control for macrophage activation (Fig. 15B). Infection with mycobacteria led to a significant reduction of TNF mRNA levels by 80% (*M. tuberculosis*) and 95% (*M.avium*) in MyD88$^{-/-}$ cells. Stimulation with LPS resulted in a decrease of TNF transcripts by 50%. As a control for MyD88-independent signal transduction macrophages were treated for 4 hours with 50 ng/ml of recombinant TNF and were afterwards analyzed by quantitative real-time PCR. Detection of Fzd1 mRNA expression revealed no differences between BMDM derived from MyD88 knockout mice and wild type mice (Fig. 15C). In correlation with Fzd1, the analysis of TNF mRNA expression also showed no differences between MyD88-deficient macrophages and wild type macrophages (Fig. 15D).

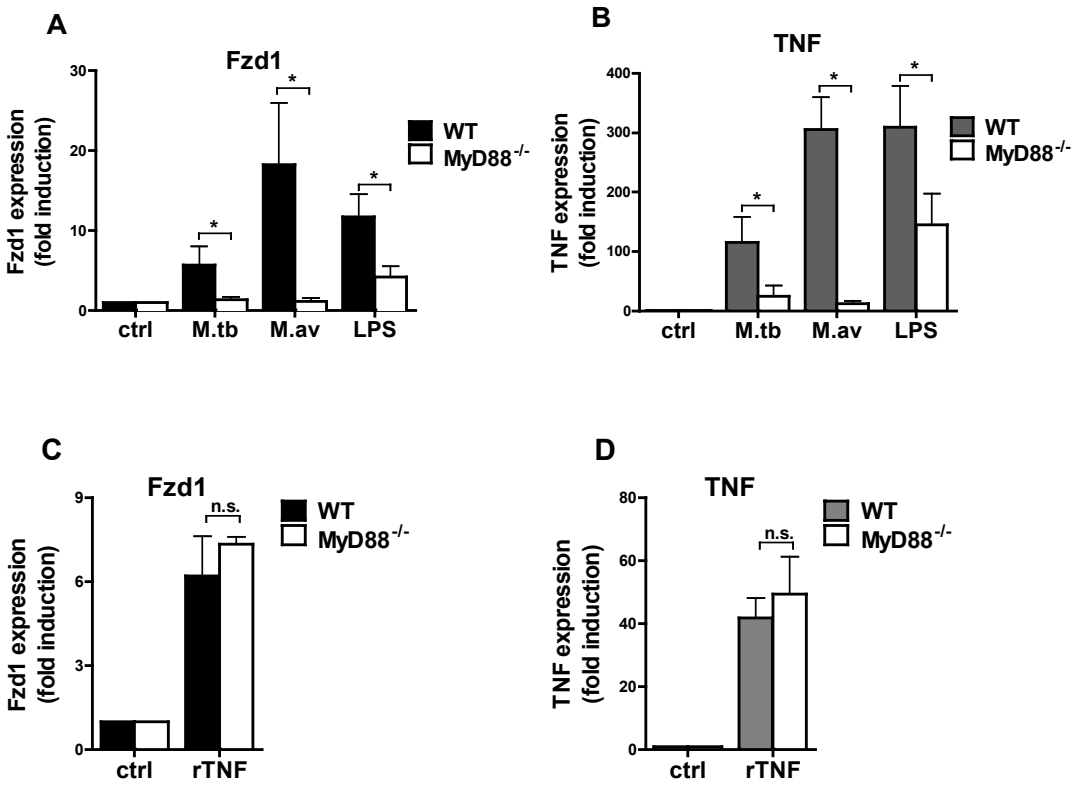

Figure 15. Analysis of Fzd1 and TNF transcription in macrophages of MyD88$^{-/-}$ mice.
BMDM from wild type and MyD88-deficient mice were incubated with an infection ratio of 3 mycobacteria per macrophage (*M. tuberculosis*, *M. avium*), 10 ng/ml LPS or 50 ng/ml recombinant TNF (rTNF). 4 hours post-stimulation cells were lysed for total RNA extraction followed by reverse transcription to monitor the fold induction of Fzd1 mRNA **(A, C)** and TNF mRNA **(B, D)** by quantitative real-time PCR (*Taq*Man® assay). Shown is the normalized ratio between target gene and reference gene (HPRT) normalized to the untreated control. The results are means ± SEM of three independent experiments performed in technical duplicates. For statistical analysis the data were log transformed and analyzed by Student's two tailed, paired *t*-test defining differences between wild type and knockout derived cells as significant (*$p < 0.05$).

3.2.3.2 Involvement of the NF-κB pathway

The activation of the transcription factor nuclear factor-kappaB (NF-κB) in antigen presenting cells is essential for a broad spectrum of cellular responses involved in innate and adaptive immunity[183]. To examine the influence of the NF-κB pathway on Fzd1 mRNA expression, BMDM were infected with *M. tuberculosis*, *M. avium* at a ratio of 3 mycobacteria per macrophage or 10 ng/ml LPS in the presence of inhibitor BAY11-7082 (3 µM), which blocks phosphorylation of IκBα (inhibitor of NF-κB)[157]. After 4 hours of stimulation the expression of Fzd1 and TNF mRNA was analyzed by quantitative real-time PCR. Figure 16A shows that in the presence of the inhibitor, *M. tuberculosis* and *M. avium* infected cells displayed a strong reduction of Fzd1

transcripts by 60% (*M. tuberculosis*) to more than 70% (*M. avium*) as compared to control cells stimulated in the presence of 0.03% DMSO (solvent control). Similar results were obtained in LPS stimulated cells. The presence of the inhibitory compound led to a significant decrease (70%) in Fzd1 expression. However, in case of LPS treated cells the TNF transcription was hardly affected in the presence of 3 µM BAY 11-7082 (Fig. 16B).

The examination of the activation of transcription factor NF-κB was a prerequisite for TNF-induced Fzd1 mRNA expression, cells were treated in parallel with 50 ng/ml of recombinant TNF in the presence or absence of 3 µM BAY 11-7082 (Fig. 16C). The results demonstrated that Fzd1 transcripts were decreased by 70% in the presence of the inhibitor. Examination of the TNF expression indicated a 60% reduction in response to recombinant TNF in the presence of BAY 11-7082 (Fig. 16D).

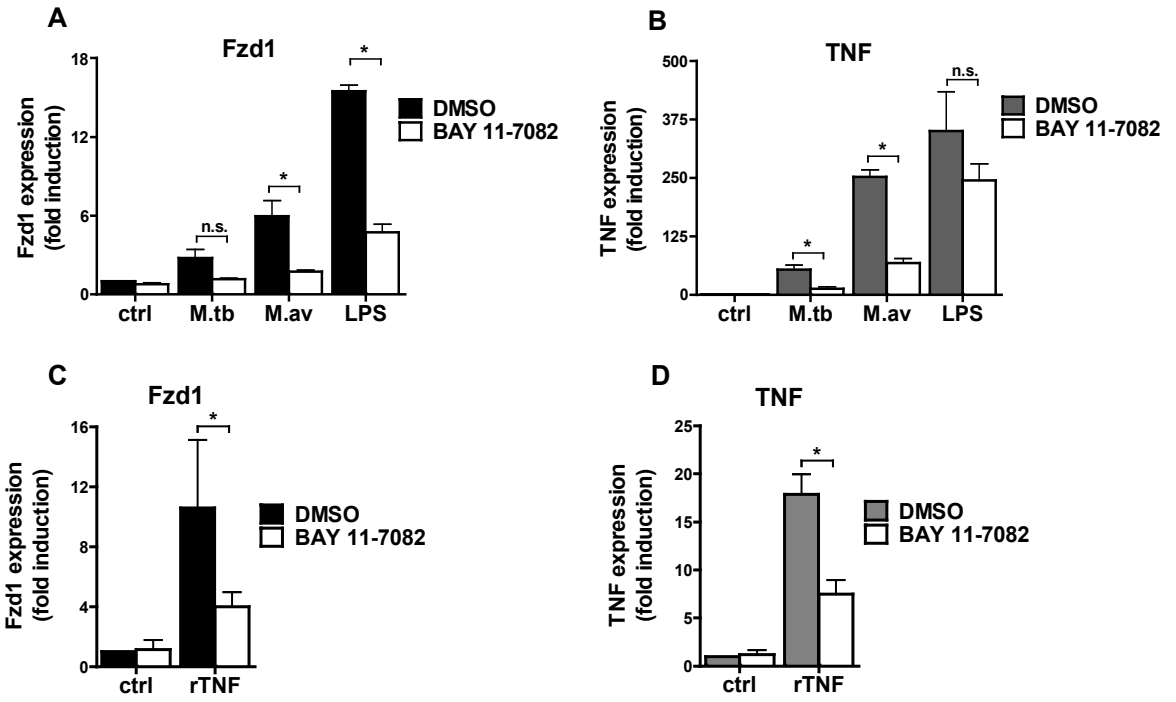

Figure 16. Analysis of macrophage Fzd1 and TNF transcription in the presence of compound BAY 11-7082.

BMDM treated with Iκ-Bα inhibitor (BAY 11-7082, 3 µM) or DMSO (0.03%) were incubated at an infection ratio of 3 mycobacteria (*M. tuberculosis*, *M. avium*) per macrophage, 10 ng/ml LPS or 50 ng/ml recombinant TNF. After 4 hours of stimulation cells were lysed for total RNA extraction and reverse transcribed. The fold induction of Fzd1 mRNA **(A, C)** and TNF mRNA **(B, D)** was analyzed by quantitative real-time PCR (*Taq*Man® assay). Shown is the normalized ratio between target gene and reference gene (HPRT) normalized to the solvent treated control. The results are means ± SEM of three independent experiments performed in technical duplicates. For statistical analysis the data were log transformed and analyzed by Student's two tailed, paired *t*-test defining differences between DMSO and BAY 11-7082 treated cells as significant (*$p < 0.05$).

During all experiments the presence of 0.03% DMSO had no effect on the induction of Fzd1 or TNF transcription as compared to untreated macrophages, to which no solvent was added (data not shown).

3.2.3.3 Influence of TNF and IL-10

In experiments shown above, the Fzd1 mRNA expression correlated with the expression of TNF in macrophages activated by TLR agonists. It was also shown that recombinant TNF alone was sufficient to induce Fzd1 transcription (Fig. 15C, 16C). Due to the fact that TNF is a critical cytokine in the regulation of immune cells and inflammation, the impact of TNF on the expression of Fzd1 mRNA was analyzed. For that reason BMDM derived from TNF-deficient mice and wild type mice were stimulated for 4 hours with 3 mycobacteria (*M. tuberculosis*, *M. avium*) per macrophage, 10 ng/ml LPS or 50 ng/ml recombinant TNF.

Transcription analysis by quantitative real-time PCR demonstrated that in TNF-deficient macrophages stimulated with mycobacteria or LPS, the Fzd1 mRNA levels were strongly reduced when compared to wild type cells (Fig. 17A). This effect could partially be restored through the addition of recombinant TNF (Fig. 17B). To test the integrity of TNF knockout mice, TNF protein concentrations derived from the supernatant of mycobacteria and LPS stimulated cells were measured by ELISA (Fig. 17C). The results indicated that TNF was not detectable in TNF-deficient cells treated with mycobacteria or LPS.

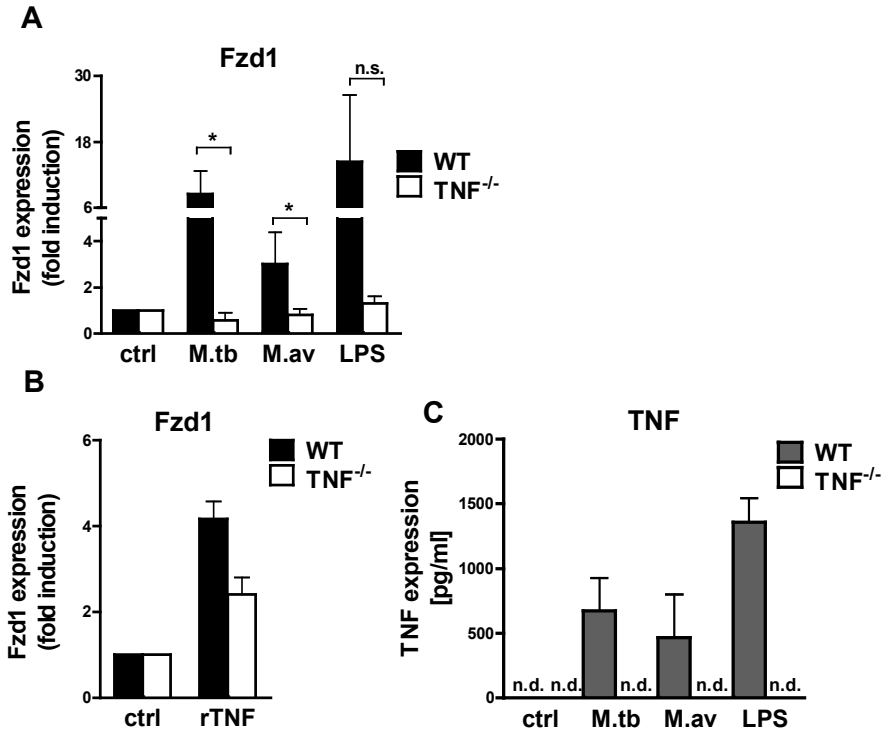

Figure 17. Analysis of Fzd1 and TNF transcription in macrophages of TNF$^{-/-}$ mice.
BMDM from wild type and TNF-deficient mice were incubated with an infection ratio of 3 mycobacteria per macrophage (*M. tuberculosis*, *M. avium*), 10 ng/ml LPS and 50 ng/ml recombinant TNF. 4 hours post-stimulation cells were lysed for total RNA extraction and reverse transcribed for quantitative real-time PCR analysis. The fold induction of Fzd1 mRNA **(A, B)** is shown representing the normalized ratio between target gene and reference gene (HPRT) normalized to the untreated control. **(A)** The results are means ± SEM of three independent experiments performed in technical duplicates. For statistical analysis the data were log transformed and analyzed by Student's two tailed, paired *t*-test defining differences between wild type and knockout derived cells as significant (*$p < 0.05$).
(B,C) The results represent means ± SEM of two independent experiments performed in technical duplicates (n.d., non-detectable). **(C)** The cytokine concentration of supernatant-derived TNF was determined by ELISA.

To examine the modulation of Fzd1 mRNA expression in response to anti-inflammatory cytokines, BMDM were pre-incubated with 25 ng/ml recombinant IL-10 and subsequently stimulated with an infection ratio of 3 mycobacteria (*M. avium*) per macrophage or 10 ng/ml LPS. After 4 hours of stimulation cells were prepared for quantitative real-time PCR analysis as described above. The results indicated that the addition of IL-10 led to a decreased Fzd1 transcription by 75% in response to *M. avium.* However, the results did not prove to be statistically significant (Fig. 18A). In contrast, cells stimulated with LPS showed Fzd1 mRNA induction also in the presence of recombinant IL-10 (Fig. 18A). TNF transcription was strongly reduced in

response to mycobacteria and LPS, if the macrophages were pre-incubated with recombinant IL-10 (Fig. 18B).

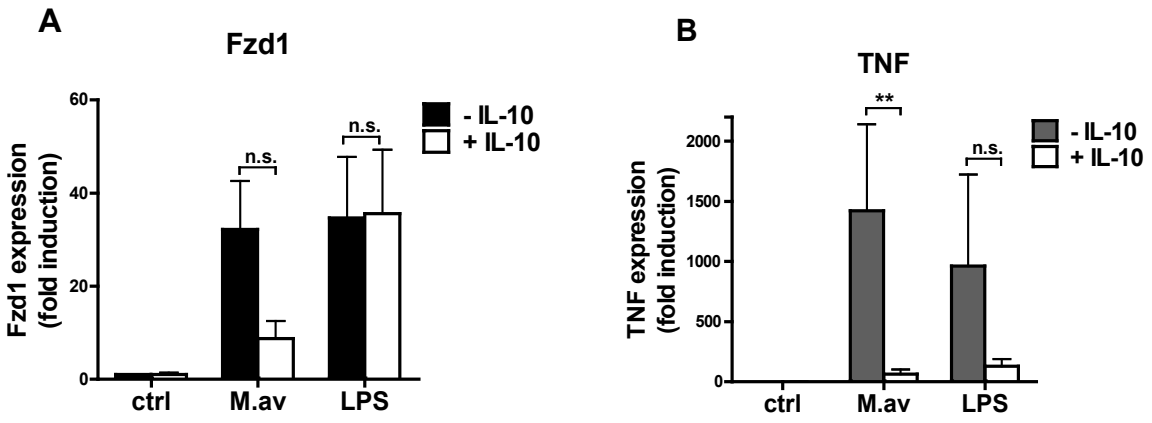

Figure 18. Analysis of macrophage Fzd1 and TNF mRNA expression in the presence of IL-10. BMDM were pre-incubated with recombinant IL-10 (25 ng/ml) for 24 hours, followed by stimulation with *M. avium* at an infection ratio of 3 mycobacteria (*M. avium*) per macrophage or 10 ng/ml LPS. 4 hours post-stimulation cells were lysed for isolation of total RNA. **(A, B)** The fold induction of Fzd1 and TNF mRNA was analyzed by quantitative real-time PCR (SYBR green assay). Shown is the normalized ratio between target gene and reference gene (HPRT) normalized to unstimulated control. The results are means ± SEM of three independent experiments performed in technical duplicates. For statistical analysis the data were log transformed and analyzed by Student's two tailed, paired *t*-test defining differences between IL-10-treated cells and control cells as significant (** $p < 0.005$).

Summary 3.2

- Fzd1 mRNA expression in murine bone marrow- derived macrophages was dose-dependently up-regulated in response to *M. tuberculosis*, *M. avium* and LPS.
- Fzd1 transcription was detected after 1 hour post-infection and lasted up to 8 hours during the course of infection.
- Fzd1 mRNA was most prominently increased 4 hours post-infection, whereas after 24 hours Fzd1 transcripts were reduced to detection limit.
- In murine macrophages Fzd1 mRNA expression was induced depending on the presence of TLR2, MyD88 and activation of the NF-κB pathway.
- The induction of Fzd1 mRNA expression was critically dependent on TNF.

3.3 Fzd1 protein expression in response to mycobacterial infection *in vitro*

It was observed that Fzd1 mRNA expression in murine macrophages was induced by pro-inflammatory TLR/NF-κB signaling. To examine Fzd1 on the protein level, cells were treated with mycobacteria, LPS and interferon gamma (IFN-γ). In the following experiments macrophages were analyzed by flow cytometric measurements for the presence of the receptor on the cell surface. Additional immuno blot experiments were applied to detect the expression of total Fzd1 protein. Based on recent reports that Fzd homologs frequently traffick between cellular compartments, further analyses were performed to monitor the dynamics of Fzd1 expression. To reveal whether Fzd1 was differentially expressed on the cell surface as compared with total Fzd1 protein, stimulated macrophages were analyzed by extracellular versus intracellular flow cytometric measurements.

3.3.1 Influence of mycobacteria and IFN-γ on Fzd1 protein expression:

3.3.1.1 *In vitro* differentiated macrophages

BMDM were pre-incubated with IFN-γ (250U/ml, 24 hours) and treated with an infection ratio of 0.5 mycobacteria (*M. tuberculosis*) per macrophage or LPS (10 ng/ml) for 24 hours. Subsequently, the macrophages were stained using monoclonal anti-Fzd1 and anti-F4/80 antibodies to analyze surface expression of Fzd1 and F4/80 by flow cytometry. Cells were gated by forward, side scatter profile and the percentage of Fzd1/F4/80 positive cells was determined based on isotype controls.

Two major cell populations were detected: macrophages that stained negative for Fzd1 ($Fzd1^{-}/F4/80^{+}$) and macrophages that stained highly positive for Fzd1 ($Fzd1^{high}/F4/80^{+}$). Compared to the untreated cells the percentage of $Fzd1^{high}/F4/80^{+}$ macrophages had increased in response to *M. tuberculosis* infection from 13.7% to 26.5%. Macrophages stimulated with LPS showed an increase in the $Fzd1^{high}/F4/80^{+}$ population from 13.0% to 21.4% (Fig. 19A).

Lymphocyte derived interferon gamma (IFN-γ) plays a pivotal role during macrophage effector functions against mycobacteria[143;144]. For that reason *in vitro* and *in vivo* differentiated macrophages were additionally pre-incubated with IFN-γ to analyze the influence of macrophage-activating factor on Fzd1 expression. It was observed that the addition of IFN-γ and *M. tuberculosis* further doubled the $Fzd1^{high}/F4/80^{+}$ population from 26.5% to 50.8%. Co-stimulation with LPS in the

presence of IFN-γ enhanced the percentage of Fzd1^{high}/F4/80^{+} cells by approx. 2 fold from 21.4% to 37.7%. In contrast, the presence of IFN-γ alone had no influence on the Fzd1^{high}/F4/80 positive population (Fig. 19A). The results of a representative experiment are shown in figure 19B.

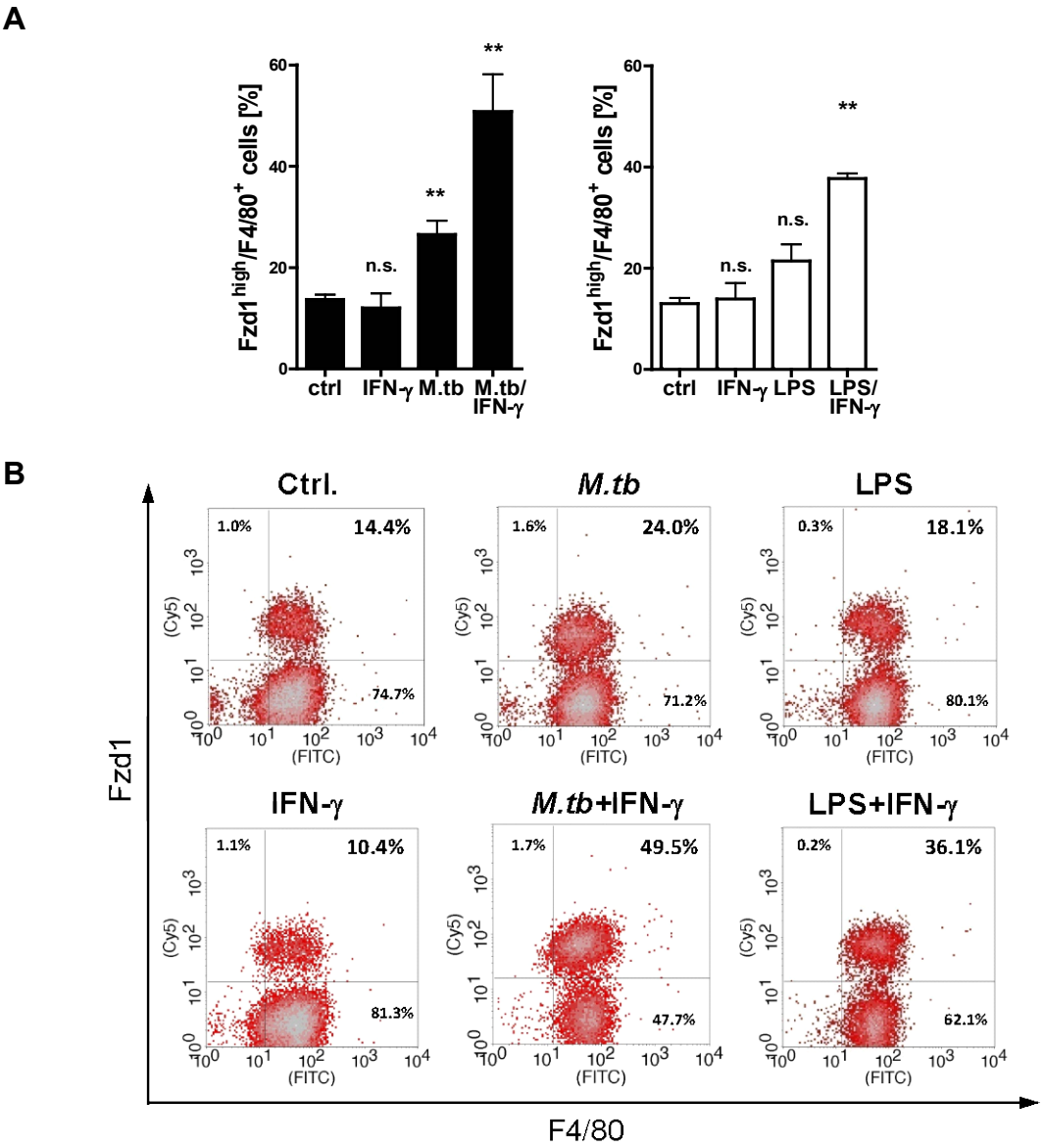

Figure 19. Fzd1 surface expression on BMDM after co-stimulation with IFN-γ and *M. tuberculosis* or LPS.

BMDM incubated in the presence or absence of IFN-γ (250 U/ml, 24 hours prior to stimulation) were stimulated with an infection ratio of 0.5 mycobacteria (*M. tuberculosis*) per macrophage or 10 ng/ml LPS for 24 hours. The cells were stained with anti-Fzd1 and anti-F4/80 monoclonal antibodies and analyzed by flow cytometric measurements. The macrophage population was determined by gating on forward (FSC) and side scatter (SSC) profile. Isotype controls were used to determine the percentage of Fzd1/F4/80 positive cells by quadrant plot analysis. **(A)** Shown are the means ± SEM of the percentage of Fzd1/F4/80 positive cells, summarizing the results of five (*M. tuberculosis*) and three (LPS) independent experiments, **(B)** of which one representative experiment is depicted.
For statistical analysis the data were log transformed and analyzed by Student's two tailed, paired *t*-test defining differences between control and stimulated cells as significant (**$p < 0.005$).

3.3.1.2 *In vivo* differentiated macrophages

To monitor Fzd1 expression on *in vivo* differentiated macrophages, peritoneal exudate cells (PEC) were stimulated with *M. avium* (3 mycobacteria per macrophage) or LPS (10 ng/ml) in the presence or absence of 250 U/ml IFN-γ. PEC were double stained using a monoclonal anti-Fzd1 and an anti-CD86 antibody to analyze Fzd1/CD86 expressing cells. The expression of CD86 was monitored to differentiate between myeloid and activated myeloid cells (Fig. 20).

Following stimulation, two major cell populations were distinguished: $Fzd1^-/CD86^+$ cells and $Fzd1^+/CD86^+$ cells. Taken as a marker of cellular activation, the $CD86^+$ cell population could further be subdivided into highly activated cells ($CD86^{high}$) and cells of low activation ($CD86^{low}$). Stimulation of PEC with *M. avium* and LPS led to an up-regulation of $Fzd1^+/CD86^+$ cells by nearly 3- (*M. avium*) and 2.5-fold (LPS). After co-stimulation with IFN-γ the percentage of $Fzd1^+/CD86^+$ cells was further enhanced by 2.5- (LPS/IFN-γ) to 3-fold (*M. avium*/IFN-γ). PEC that were treated with IFN-γ alone, showed an increase of $Fzd1^+/CD86^+$ cells by 5.5-fold.

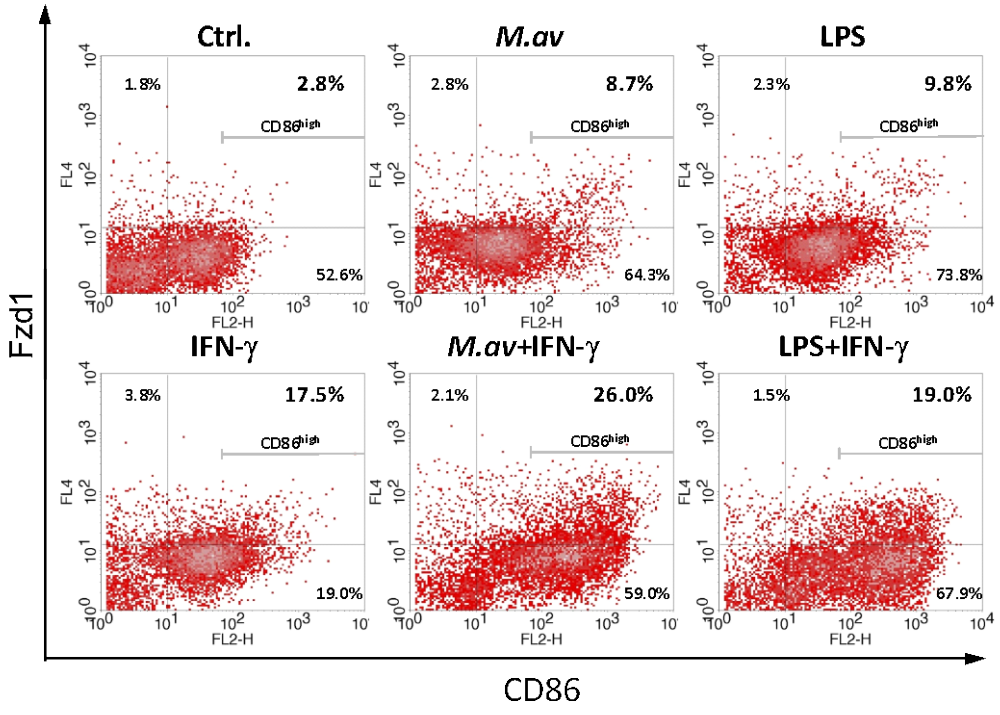

Figure 20. Fzd1 surface expression on PEC after co-stimulation with IFN-γ and *M. tuberculosis* or LPS.

PEC incubated in the presence or absence of IFN-γ (250 U/ml, 24 hours prior to stimulation) were stimulated with an infection ratio of 0.5 mycobacteria (*M. tuberculosis*) per macrophage or 10 ng/ml LPS for 24 hours. The cells were stained with anti-Fzd1 and anti-CD86 monoclonal antibodies for flow cytometric measurements. The macrophage population was determined by gating on forward (FSC) and side scatter (SSC) profile. Isotype controls were used to determine the percentage of Fzd1/CD86 positive cells, as indicated by quadrant plot analysis. The results are representative for one out of two independent experiments.

With regard to cellular activation, an increase in the Fzd1 positive population was primarily detected in highly activated cells ($Fzd1^{+}/CD86^{high}$; Fig. 20).

3.3.2. Fzd1 protein detection by Western Blot compared to FACS analysis

To examine the expression of total Fzd1 protein, BMDM were stimulated with LPS (10 ng/ml) or pre-activated in the presence or absence of IFN-γ (250 U/ml) and sequentially infected with *M. tuberculosis* (0.5 mycobacteria per macrophage). At indicated time points cells were lysed for analysis by Western blot. Using an anti-Fzd1 antibody, a double band of approx. 70 kDa was detected, which corresponded to the theoretical mass of Fzd1 (71 kDa). In addition the antibody also detected a recombinant Fzd1/Fc fusion protein known to be approx. 55 kDa in size, which demonstrated the specificity of the antibody used.

Stimulation of macrophages with LPS showed no differences in the expression of Fzd1 protein after 2 to 48 hours (Fig. 21A). In addition, neither macrophages infected with *M. tuberculosis* nor cells treated with *M. tuberculosis*/IFN-γ showed differences in Fzd1 expression at indicated time points (Fig. 21B). In contrast, the induction of nitric oxide synthase 2 (NOS2) was analyzed as a control of macrophage activation[184-186]. Using a monoclonal anti-NOS2 antibody, the results indicated a single band of approx. 125 kDa, which was detected 12 to 32 hours post-infection (Fig. 21B). The blots were stripped and incubated with anti-GAPDH antibody to ensure an equal loading of protein. Staining with anti-GAPDH resulted in a single band of approx. 35 kDa (Fig. 21).

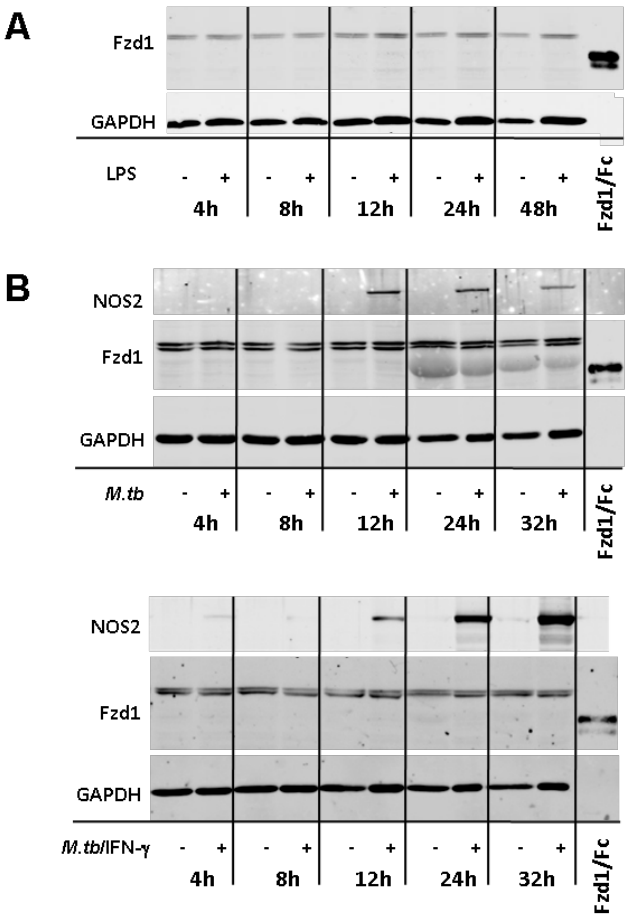

Figure 21. Western blot analysis of Fzd1 and NOS2 protein levels in macrophages. BMDM were stimulated with 10 ng/ml LPS or pre-incubated in the presence or absence of IFN-γ (250 U/ml, 24 hours) followed by *M. tuberculosis*-treatment (0.5 bacteria per macrophage). The cells were lysed at indicated time points and the lysates electrophoretically separated. The protein was transferred to a nitrocellulose membrane. **(A, B)** The blots were incubated with anti-Fzd1 and **(B)** anti-NOS2 antibodies for the detection of Fzd1 and NOS2 protein. After incubation with secondary reagents the blots were analyzed using an Odyssey near-infrared detection system. 30 ng of a recombinant Fzd1/Fc fusion protein were used to ensure the specificity of monoclonal anti-Fzd1 antibody. Additional Western blot analysis of GAPDH was performed to ensure equal loading of protein. The results are representative for one out of two independent experiments.

To analyze the relation between Fzd1 surface expression and total protein expression, *in vitro* differentiated macrophages were pre-activated in the presence of IFN-γ and sequentially stimulated for 24 hours with *M. tuberculosis* or LPS. Subsequently cells were treated with an anti-Fzd1 antibody for extracellular and intracellular FACS staining.

The overlay in figure 22 shows that after treatment with *M. tuberculosis*/IFN-γ or LPS/IFN-γ an increase of cell surface (extracellular) stained Fzd1 positive cells was detected by flow cytometric measurements. On the contrary, FACS measurements of intracellularly stained cells indicated that the Fzd1 positive population of stimulated macrophages remained almost unchanged as compared to unstimulated cells. The results obtained by flow cytometric measurements of intracellularly stained cells further corroborate the notion, that following stimulation the overall amount of total Fzd1 protein remains constant, as observed by Western blot analyses.

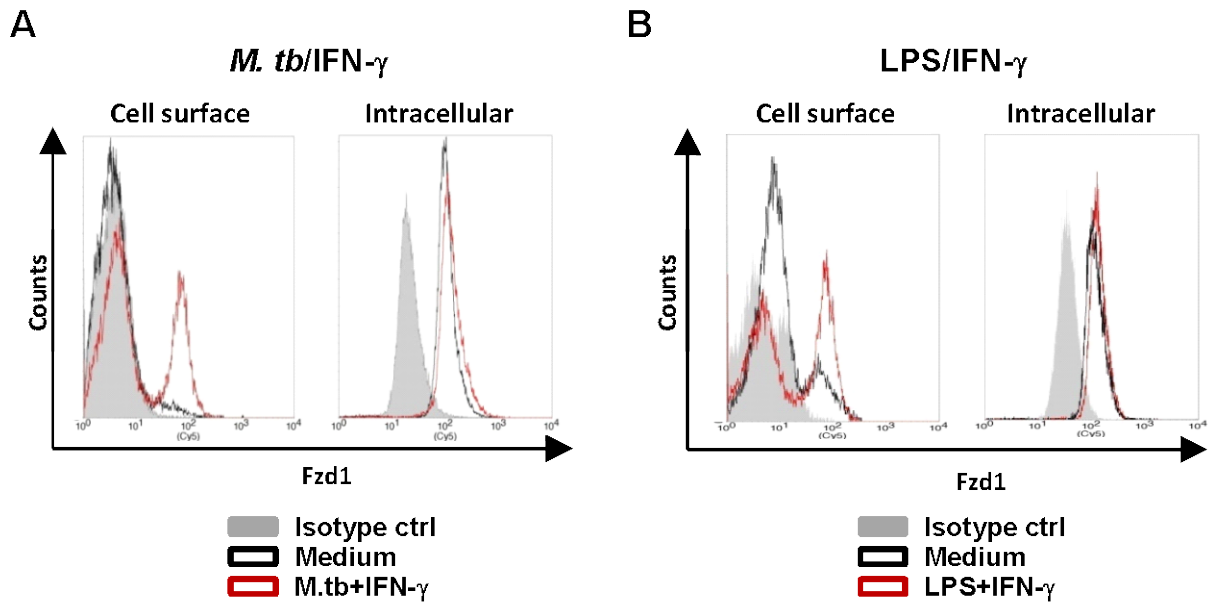

Figure 22. FACS analysis of cell surface and intracellular Fzd1 expression in murine macrophages.
(A) BMDM were pre-incubated in the presence or absence of IFN-γ (250 U/ml, 24 hours) and subsequently stimulated with *M. tuberculosis* (0.5 mycobacteria per macrophage) or **(B)** 10 ng/ml LPS for 24 hours. Using a monoclonal anti-Fzd1 antibody, the cell surface and intracellular (total) Fzd1 expression of murine macrophages was analyzed by flow cytometry. The macrophage population was determined by gating on forward scatter (FSC), side scatter (SSC) profile. Delineated by histograms are relative counts on gated cells. The results are representative for one out of two independent experiments. Open histograms, Fzd1 stained cells; greyfilled histograms, isotype controls.

3.3.3 Kinetics of Fzd1 surface expression

Having detected regulation on the cell surface, the kinetics of Fzd1 expression was analyzed by FACS analysis of surface-stained macrophages. BMDM were co-stimulated with 250 U/ml of IFN-γ and an *M. tuberculosis* infection ratio of 0.5 mycobacteria per macrophage or 10 ng/ml LPS. At the time points indicated the macrophages were placed on ice and subsequently stained with anti-Fzd1 and anti-F4/80 antibodies as described above.

Within 2 to 12 hours post-infection the Fzd1/F4/80 positive population remained unchanged. Following 12 hours post-infection an up-regulation in the Fzd1/F4/80 positive population was observed in both, macrophages treated with *M. tuberculosis*/IFN-γ and cells treated with LPS/IFN-γ (Fig. 23). Highest expression was observed 24 hours post-infection. After 48 hours Fzd1/F4/80 expression was still high in cells challenged with *M. tuberculosis*/IFN-γ (approx. 30%), yet to a lesser extent as compared to 24 hours post-infection (approx. 40%). 48 hours after treatment with

LPS/IFN-γ the Fzd1/F4/80 positive population had decreased from approx. 40% at 24 hours post-stimulation to the expression level of untreated cells (approx. 18%).

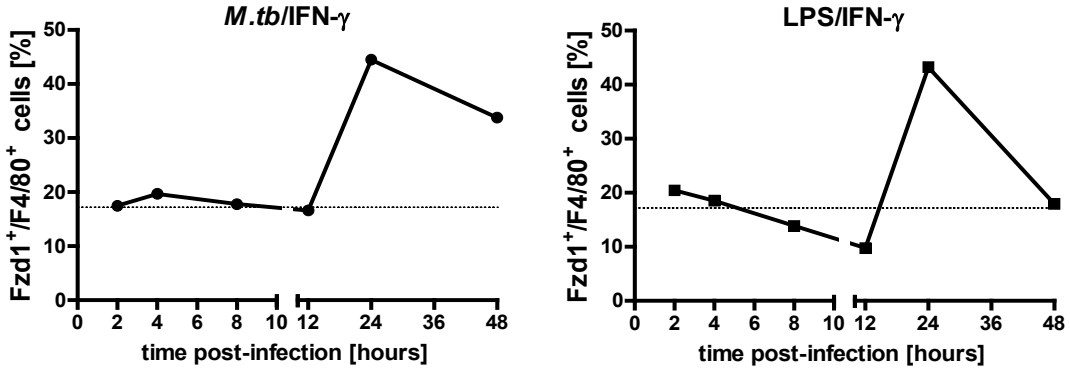

Figure 23. Kinetics of mycobacteria- and LPS-induced Fzd1 surface expression on murine macrophages.
BMDM were pre-incubated with IFN-γ (250 U/ml) for 24 hours and subsequently stimulated with *M. tuberculosis* (0.5 mycobacteria per macrophage) or 10 ng/ml LPS. At indicated time points the cells were stained with anti-Fzd1 and anti-F4/80 monoclonal antibodies to analyze the surface expression of Fzd1 and F4/80 by flow cytometric measurements. The macrophage population was determined by gating on forward (FSC) and side scatter (SSC) profile. Isotype controls were used to determine the percentage of Fzd1/F4/80 positive cells by quadrant plot analysis. The dotted line indicates the mean of the untreated cells. The results are representative for one out of two independent experiments.

Summary 3.3

- Stimulation of bone marrow-derived macrophages with *M. tuberculosis* or LPS led to an increase of Fzd1 surface expression ($Fzd1^{high}$/F4/80 cells), which was synergistically enhanced in the presence of IFN-γ.
- Stimulation of peritoneal exudate cells with *M. avium*/IFN-γ or LPS/IFN-γ resulted in an increased Fzd1 surface expression on activated cells ($CD86^{high}$ positive).
- Stimulation of macrophages with *M. tuberculosis* or LPS in the presence or absence of IFN-γ did not affect the total amount of Fzd1 protein, as observed by Western blot and intracellular FACS analyses.
- Enhanced expression of Fzd1 protein was observed on the plasma membrane by FACS analysis: 24 hours after stimulation with *M. tuberculosis*/IFN-γ or LPS/IFN-γ an increase of Fzd1 that lasted up to 48 hours, was detected on the cell surface of F4/80 positive macrophages. The highest percentage of Fzd1/F4/80 positive gated cells was observed 24 hours post-stimulation.

3.4 Fzd1 expression in human macrophages

In addition to the *in vitro* mouse model of mycobacterial infection, first experiments were performed to analyze the presence of Fzd1 protein in human innate immune cells. To find out whether Fzd1 protein was similarly expressed in human macrophages as observed in murine cells, human monocyte-derived macrophages were infected with mycobacteria and analyzed by immunoblot experiments as well as flow cytometric measurements.

3.4.1 Fzd1 protein detection by Western blot

To examine the presence of Fzd1 protein in *in vitro* differentiated human macrophages, the cells were stimulated with increasing infection ratios of mycobacteria per macrophage (*M. tuberculosis*, strain H37Rv and *M. avium*, strain SE01) and 10 ng/ml LPS. Following 4 and 24 hours of stimulation cells were lysed and prepared for protein detection by Western blot. Using anti-Fzd1 antibodies, a specific double band of approx. 70 kDa was detected (Fig. 24). Yet, in analogy to the findings in murine *in vitro* differentiated macrophages (see Fig. 21), 4 and 24 hours after treatment no differences in Fzd1 protein expression between stimulated and unstimulated cells could be resolved (Fig. 24). To assert that equal amounts of protein were used in the immunoblot experiments, an anti-GAPDH antibody was used to provide a measure for equivalent loading. The detection of GAPDH resulted in a specific band of approx. 35 kDa (Fig. 24).

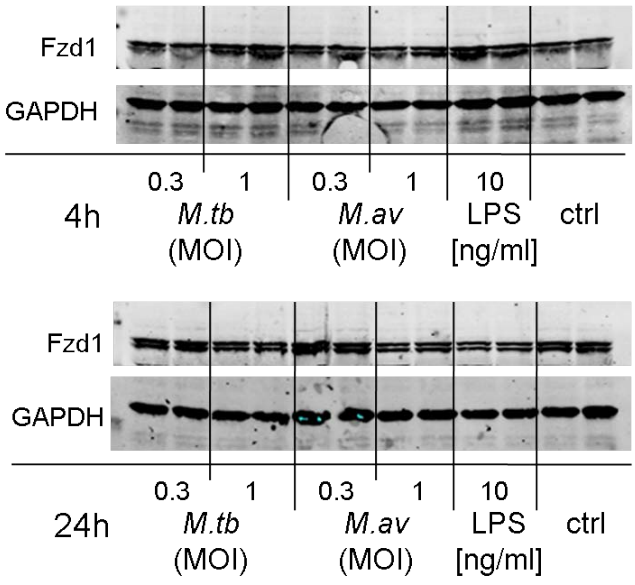

Figure 24. Western blot analysis of Fzd1 protein levels in human macrophages. Human monocyte-derived macrophages were challenged with 0.5 or 1 mycobacteria per macrophage (*M. tuberculosis*, strain H37Rv; *M. avium*, strain SE01) or 10 ng/ml LPS. The cells were lysed 4 hours and 24 hours post-stimulation. The cell lysates were electrophoretically separated and transferred to a nitrocellulose membrane by Western blot. The blots were incubated with an anti-Fzd1 antibody for the detection of Fzd1 protein. After staining with secondary reagents the blots were analyzed using an Odyssey near-infrared detection system. Additional Western blot analysis of GAPDH was performed to ensure equal loading of protein. The results of two independent experiments are shown.

3.4.2 Fzd1 protein detection by FACS analysis

Having detected Fzd1 protein on the surface of *in vitro* and *in vivo* differentiated murine macrophages, Fzd1 expression on human monocyte-derived macrophages was analyzed by FACS analysis. In analogy to murine experiments the cells were stimulated as indicated. For analysis the cells were extracellularly stained with monoclonal anti-Fzd1 and a monoclonal anti-CD14 antibody as a myeloid cell marker. After stimulation of human macrophages two cell populations were of primary interest: $Fzd1^-/CD14^+$ cells and $Fzd1^+/CD14^+$ cells. Based on their degree of Fzd1 protein expression, human macrophages could further be subdivided into $Fzd1^{low}$ and $Fzd1^{high}$ expressing cells (Fig. 25).

Following infection with *M. tuberculosis* a 3.8-fold increase in the percentage of $Fzd1^+/CD14^+$ positive cells was observed as compared to the untreated control. Stimulation with IFN-γ further enhanced the size of this population by 62%. Treatment of human macrophages with LPS caused an up-regulation of $Fzd1^+/CD14^+$ positive gated cells by 2.7-fold. Yet, IFN-γ had no further impact on the percentage of LPS stimulated $Fzd1^+/CD14^+$ cells. Macrophages treated solely with IFN-γ showed no difference in the $Fzd1^+/CD14^+$ population when compared to the unstimulated control. An overall increase of Fzd1 surface expression was primarily due to an increase of the $Fzd1^{low}/CD14^+$ cell population, that was observed to derive from a complete shift of $Fzd1^-/CD14^+$ cells (Fig. 25). The cell population that was high in Fzd1 expression ($Fzd1^{high}/CD14^+$) remained nearly unchanged in response to stimulation.

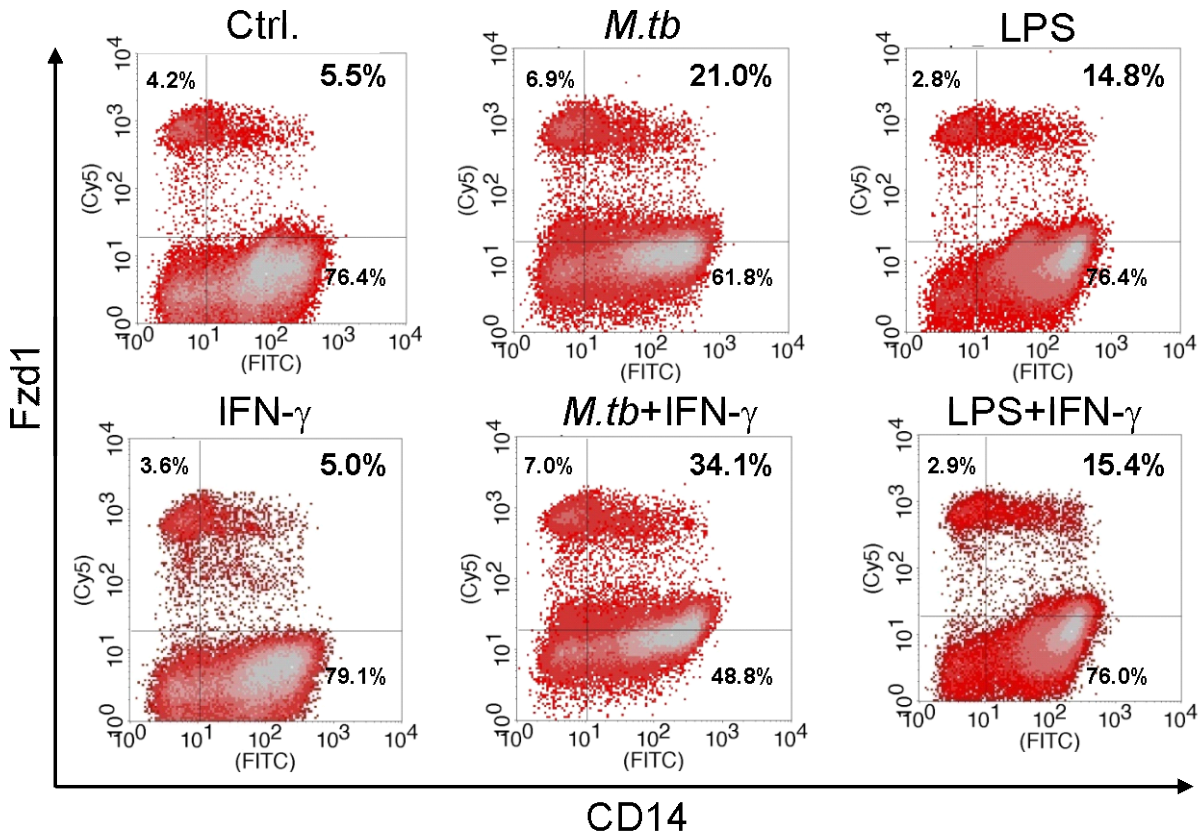

Figure 25. Fzd1 surface expression on human macrophages after co-stimulation with IFN-γ and *M. tuberculosis* or LPS.
Human monocyte-derived macrophages were stimulated with an infection ratio of *M. tuberculosis* at 1 mycobacterium per macrophage or 10 ng/ml LPS for 24 hours. For co-stimulations the cells were incubated in the presence of IFN-γ (250 U/ml) 24 hours prior to and during infection. The macrophages were stained with anti-Fzd1 and anti-CD14 monoclonal antibodies. In flow cytometric measurements the macrophage population was determined by gating on forward, sideward scatter profile. Based on isotype controls the percentage of cells that stained positive for Fzd1 and CD14 was monitored by dot plot analysis. The results are representative for one out of two independent experiments.

Summary 3.4

- Fzd1 protein was detected by Western blot in human macrophages, showing a double band of approx. 70 kDa.
- Stimulation of human macrophages with *M. tuberculosis* or LPS did not affect the total amount of Fzd1 protein, as observed by Western blot.
- Treatment of human macrophages with *M. tuberculosis* or LPS led to an increase of Fzd1 surface expression ($Fzd1^{low}/CD14^{+}$ cells), which was further enhanced in the presence of IFN-γ.

3.5 Functional role of Wnt3a and Fzd1 in murine macrophages

Based on their ability to induce β-catenin signaling, Wnt family members can be divided into two distinct types: transforming Wnts and non-transforming Wnts[187;188]. It was shown that binding of transforming Wnt homolog Wnt3a to its corresponding Frizzled receptor leads to accumulation and translocation of β-catenin into the nucleus inducing the transcription of β-catenin-dependent target genes such as *Axin2* [180;189]. In addition, Fzd1 has been shown to be primarily associated with the activation of the β-catenin pathway[55;190;191]. In the following experiments the influence of transforming Wnt3a on murine macrophages was analyzed.

3.5.1 Influence of Wnt3a on the induction of β-catenin signaling

Binding of Wnt3a to its corresponding Frizzled receptor leads to Wnt/β-catenin signaling in various cell types, but has not been addressed in mature macrophages. To analyze if Wnt3a induces β-catenin signaling in bone marrow-derived macrophages, Wnt3a conditioned media (Wnt3a CM) derived from stably Wnt3a transfected L-929 fibroblasts (LWnt3a cells) were used. The Wnt3a expression levels of lysates from LWnt3a cells, Wnt5a transfected cells (LWnt5a cells) and untransfected L-929 cells were compared by Western blot. Figure 26A shows that incubation with anti-Wnt3a antibody led to the detection of a band of approx. 40 kDa. Compared to L-929 and LWnt5a cells, high amounts of Wnt3a protein were observed in lysates of LWnt3a cells. Recombinant Wnt3a protein (15 ng) was used as positive control to ensure the specificity of the antibody.

BMDM where incubated with Wnt3a CM or control CM (derived from L-929 cells). After 4 hours of treatment the cells were lysed by TriFast reagent (PEQLAB) for the extraction of both, total protein and RNA. Total protein was isolated to analyze accumulation of β-catenin by Western blot. The results indicated stabilization of β-catenin in response to Wnt3a CM showing a band of approx. 90 kDa (Fig. 26B). In parallel RNA was isolated, reverse transcribed and analyzed by quantitative real-time PCR. Macrophages stimulated with Wnt3a CM exhibited a significant increase in Axin2 transcription when compared to the CM control (Fig. 26C).

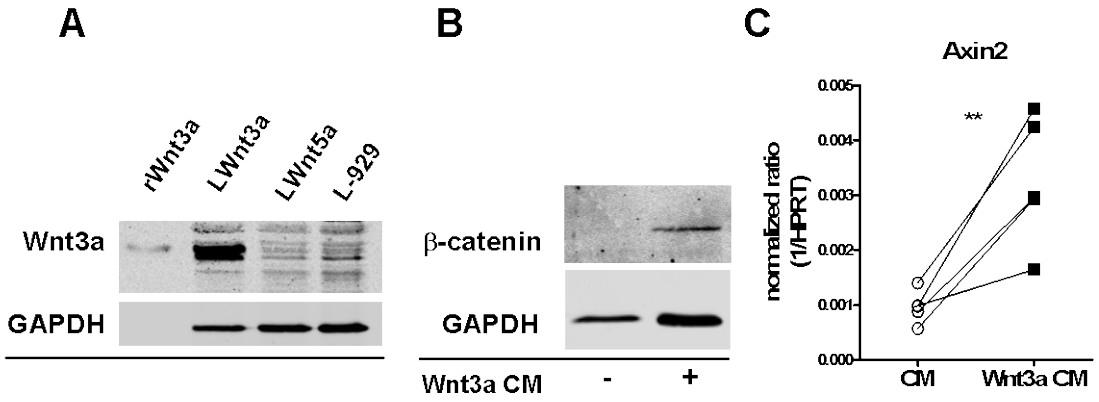

Figure 26. Wnt3a-induced β-catenin stabilization and Axin2 transcription in murine macrophages.
(A) Stably transfected LWnt3a and LWnt5a cell lines as well as L-929 control cells were lysed. The protein was separated by SDS-PAGE and transferred to a nitrocellulose membrane. After incubation with anti-Wnt3a and anti-GAPDH antibodies, secondary antibodies were applied for the analysis in an Odyssey near-infrared detection system. The results represent one out of two independent experiments. **(B, C)** BMDM were exposed to Wnt3a conditioned medium (CM). Following 4 hours of stimulation cells were lysed for isolation of total RNA and total protein from the same sample. **(B)** Cell lysate derived total protein was analyzed by immunoblot using a monoclonal anti-β-catenin antibody. Detection was performed as described above. The results shown are representative for one out of three independent experiments. **(C)** After reverse transcription the normalized ratio of β-catenin-dependent target gene Axin2 and reference gene HPRT was determined by quantitative real-time PCR analysis (*Taq*Man® assay). Indicated are the results of five independent experiments. For statistical analysis the data were log transformed and analyzed by Student's two tailed, paired *t*-test defining differences between CM and Wnt3a CM treated cells as significant (**$p < 0.01$).

3.5.2 Role of Fzd1 in Wnt3a-induced β-catenin signaling

Having detected Wnt3a-induced β-catenin stabilization and transcription of Axin2 in murine macrophages, the role of Fzd1 as a putative receptor for Wnt3a was analyzed.

To find out if Wnt3a-mediated Axin2 expression was dependent on the presence of Fzd1, Wnt3a conditioned medium was incubated for 1 hour with increasing concentrations of a soluble Fzd1/Fc fusion protein. Following incubation the medium was added to primary macrophages. After 4 hours of stimulation the macrophages were lysed and total RNA was isolated for relative quantification of Axin2 expression by real-time PCR analysis. The results demonstrated that Wnt3a CM led to a 4-fold increase in Axin2 transcription compared to cells treated with control medium. This up-regulation was significantly reduced in the presence of 3 µg/ml fusion protein by approx. 90%. In contrast, control medium supplemented with 1 µg/ml and 3 µg/ml of Fzd1/Fc fusion protein caused an increase in Axin2 mRNA expression by approx. 2.5-fold (Fig. 27A). Treatment of cells with Wnt3a conditioned medium and soluble

Fzd1/Fc fusion protein did not influence basal TNF expression in macrophages (Fig. 27B).

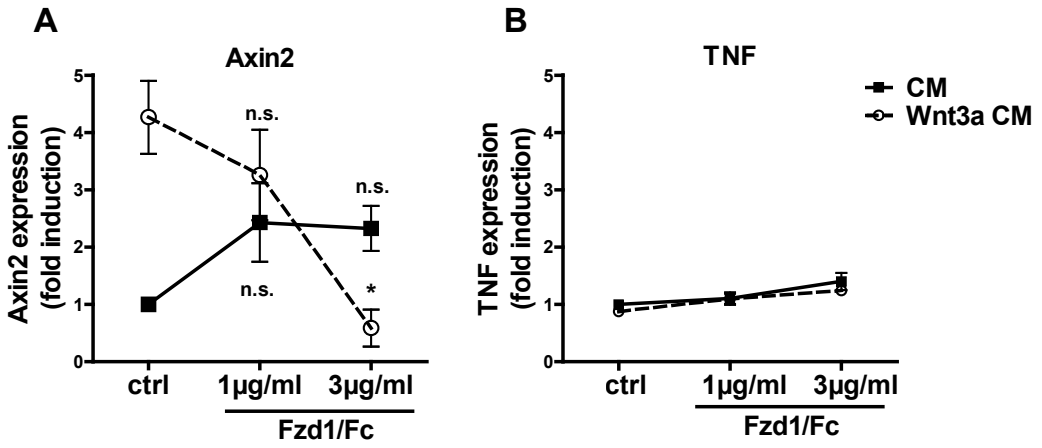

Figure 27. Influence of soluble Fzd1/Fc fusion protein on Wn3a-induced Axin2 expression in murine macrophages.
BMDM were incubated with conditioned medium (Wnt3a CM) derived from Wnt3a transfected L-929 cells (LWnt3a) and supplemented with indicated concentrations of soluble Fzd1/Fc fusion protein. After 4 hours BMDM were lysed for isolation of total RNA and reverse transcribed for quantitative real-time PCR analysis (*Taq*Man® assay). The fold induction of Fzd1 **(A)** and TNF mRNA **(B)** shown represents the normalized ratio between target gene and reference gene (HPRT) normalized to the CM control. The results are means ± SEM of three independent experiments performed in technical duplicates. For statistical analysis the data were log transformed and analyzed by Student's two tailed, paired *t*-test defining differences between untreated and Fzd1/Fc-treated cells as significant (*$p < 0.05$).

Soluble Fzd1/Fc is a chimeric protein composed of the extracellular ligand-binding domain of Fzd1 (Gln 72 – His 248) fused to the Fc region of human IgG1 (Pro 100 – Lys 330). To analyze if soluble Fzd1/Fc protein was devoid of contaminants and to examine if the human Fc region fused to the receptor domain did not lead to macrophage activation through murine Fc-gamma receptor (FcγR)[192], the respiratory burst of murine primary macrophages (BMDM) was measured. Two lots of soluble Fzd1/Fc protein (3 µg/ml) that were applied in the experiments described above were analyzed. In addition, heat inactivated human serum (10 µl) and yeast derived cell wall component zymosan (130 µg/ml) in the presence of human serum were used as negative and positive controls. Prior to the measurements, the macrophages were incubated for 45 min in the presence of 250 µM lucigenine (bis-N-methylacridinium nitrate). Subsequently soluble Fzd1/Fc and control stimuli were added to the cells and the chemiluminiscense activity was determined over a period of 30 min (Fig. 28). Compared to the untreated control, the measurements demonstrated that soluble Fzd1/Fc fusion protein did not induce release of reactive oxygen species (ROS).

Macrophages treated with zymosan/serum strongly accumulated ROS approx. 10 min after treatment. Cells treated with inactivated serum released reactive oxygen species 12 min post-stimulation but to a far lesser degree as compared to the positive control.

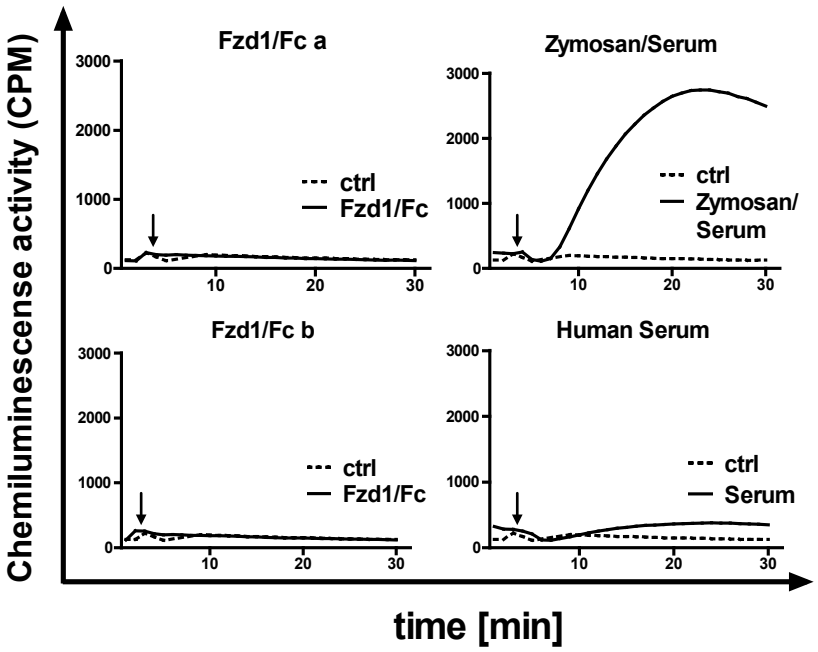

Figure 28. Analysis of soluble Fzd1/Fc fusion protein on the induction of the respiratory burst in murine macrophages.
BMDM were pre-incubated with 250 µM lucigenine for 45 min. After 3 min of blank measurements 3 µg/ml Fzd1/Fc (lot a and lot b), 10 µl heat inactivated human serum and 130 µg/ml zymosan in the presence of human serum were added to the cells. The photon yield resulting from the reaction between reactive oxygen species (ROS) and lucigenine was detected over a period of 30 min by a photomultiplier visualizing the chemiluminescence (CL) activity as counts per minute (CPM). Initial differences in the magnitude of chimiluminescence activity were normalized to a common starting point (0 min) of origin.

3.5.3 Analysis of Wnt3a-mediated modulation of the macrophage response:

3.5.3.1 Influence of Wnt3a on macrophage TNF expression

Having observed defined conditions leading to the induction and regulation of Fzd1, first experiments were performed to examine signaling events mediated by frizzled receptors in an inflammatory and infectious background. Therefore, *M. tuberculosis*-infected macrophages were additionally treated with Wnt3a conditioned medium to monitor whether the Fzd1 ligand Wnt3a may influence effector functions of innate immune cells.

To analyze the influence of Wnt3a on the microbe-induced activation of murine macrophages, BMDM were pre-incubated with Wnt3a conditioned medium (Wnt3a

CM) or control medium. After 1.5 hours the cells were additionally stimulated with *M. tuberculosis* using an infection ratio of 0.5 mycobacteria per macrophage. Supernatants were collected after 12 and 24 hours post-infection and analyzed for the presence of TNF by ELISA (Fig. 29A). Following 12 hours of infection, equal amounts of TNF were detected in supernatant control medium and Wnt3a CM derived from *M. tuberculosis*-infected macrophages (approx. 600 pg/ml). 24 hours post-infection the TNF concentration within the supernatant control medium of *M. tuberculosis*-infected macrophages was further increased, indicating approx. 900 pg/ml. In contrast, 24 hours post-infection the TNF concentration within the Wnt3a CM of macrophages treated with mycobacteria was nearly the same as observed after 12 hours post-infection. When compared to supernatants derived from macrophages that were treated in the presence of control medium and mycobacteria, the TNF concentration was significantly reduced by approx. 45%. TNF was not detected in the supernatants derived from macrophages that were incubated with control medium or Wnt3a CM alone (Fig. 29A).

In a different experimental approach macrophages were infected prior to the addition of Wnt3a CM, by using stimulatory conditions leading to a high surface expression of the Wnt3a receptor Fzd1. For this reason, BMDM were treated with *M. tuberculosis* (0.5 mycobacteria per macrophage) or *M. tuberculosis*/IFN-γ (250 U/ml) for 24 hours. Subsequently, the culture medium was completely removed and the cells were exposed to Wnt3a CM supplemented with *M. tuberculosis* or *M. tuberculosis*/IFN-γ (as described above). After additional 4 hours of incubation the macrophages were lysed and total RNA was isolated for the analysis by quantitative real-time PCR. It was observed that in cells treated with *M. tuberculosis*/IFN-γ the presence of Wnt3a CM led to a significant decrease of TNF mRNA expression by approx. 45% (Fig. 29B). Following infection of macrophages with *M. tuberculosis* alone, the addition of Wnt3a CM had no significant influence on the TNF transcription. In addition, the transcription of other pro-inflammatory mediators and adhesion molecules (IL-12, CXCL1, V-CAM1) as well as anti-inflammatory cytokine IL-10 was examined by quantitative real-time PCR. However, the induction was unaffected by Wnt3a (data not shown).

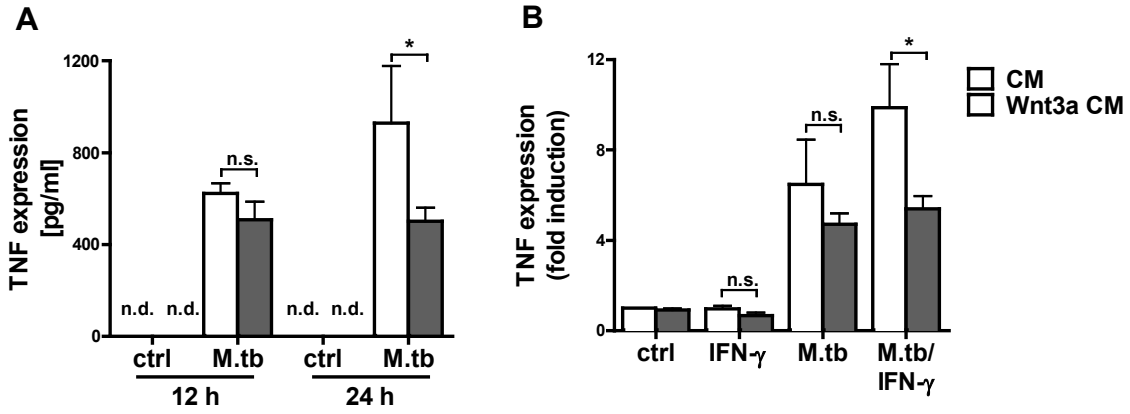

Figure 29. TNF expression in *M. tuberculosis*-infected murine macrophages treated with Wnt3a.
(A) BMDM were pre-activated with Wnt3a CM for 1.5 hours, followed by *M. tuberculosis* treatment with an infection ratio of 0.5 mycobacteria per macrophage. At indicated time points post-infection the TNF concentration in supernatant medium was determined by ELISA. The results represent the mean ± SEM of three independent experiments performed in technical duplicates.
(B) BMDM were pre-incubated in the presence or absence of 250 U/ml IFN-γ for 24 hours and subsequently infected with *M. tuberculosis* (0.5 mycobacteria per macrophage) for another 24 hours. Afterwards the culture medium was completely removed and exchanged against control medium or Wnt3a CM. Subsequently, mycobacteria and IFN-γ were again added to the cells as indicated. After additional 4 hours of incubation the cells were lysed for total RNA extraction, reverse transcribed and analyzed by quantitative real-time PCR (*Taq*Man® assay). Shown is the fold induction of TNF mRNA expression representing the normalized ratio between target gene (TNF) and reference gene (HPRT) normalized to untreated control. The results represent the mean ± SEM of three independent experiments performed in technical duplicates.
(A, B) For statistical analysis the data were log transformed and analyzed by Student's two tailed, paired *t*-test defining differences between CM and Wnt3a CM treated cells as significant (*$p < 0.05$).

3.5.3.2 Influence of Wnt3a on macrophage Arginase1 mRNA expression

Based on predominantly pro- or anti-inflammatory effector functions, macrophages are assigned a M1 or M2 phenotype[193;194]. To analyze whether M2 associated marker gene Arginase1 (*Arg1*) was induced in response to Wnt3a, BMDM were treated for 4 hours with Wnt3a CM and control medium. Subsequently cells were lysed and processed for quantitative real-time PCR (see also Fig. 27A).

Figure 30A shows that Wnt3a CM led to a significant increase of Arg1 transcription in primary macrophages. To analyze the influence of Fzd1 on Arg1 expression, BMDM were treated with Wnt3a CM that was pre-incubated with increasing concentrations of soluble Fzd1/Fc fusion protein (Fig. 30B). After 4 hours of stimulation the cells were lysed. Total mRNA was extracted and processed for quantitative real-time PCR analysis. The results indicated that Wnt3a-induced Arg1 mRNA expression was inhibited in the presence of 1 µg/ml or 3 µg/ml soluble Fzd1/Fc fusion protein. Yet,

the data were statistically not significant. Control medium supplemented with Fzd1/Fc fusion protein had no effect on Arg1 expression.

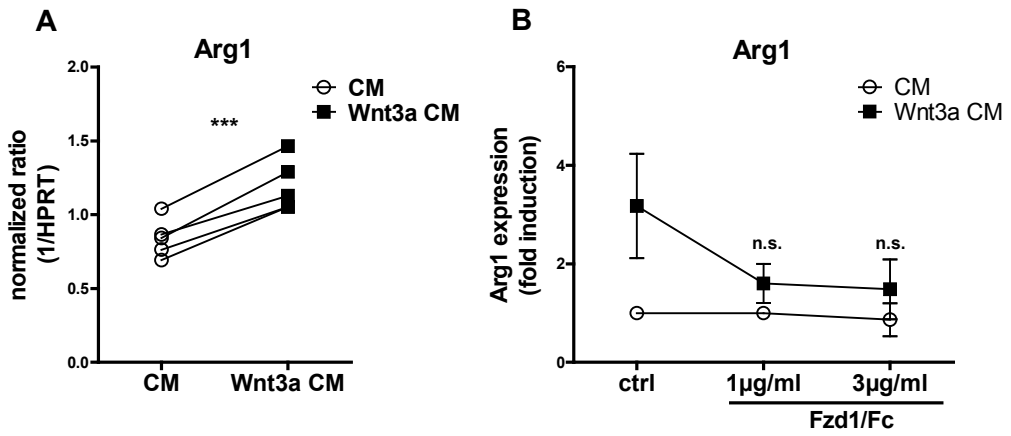

Figure 30. Macrophage Arginase1 transcription in the presence of Wnt3a and soluble Fzd1/Fc fusion protein.
(A) BMDM were incubated with Wnt3a conditioned medium (Wnt3a CM) or control medium (CM). After 4 hours the cells were lysed and total RNA was isolated. Following reverse transcription the normalized ratio of Arg1 and reference gene HPRT was determined by quantitative real-time PCR analysis. Indicated are the results of five independent experiments.
For statistical analysis the data were log transformed and analyzed by Student's two tailed, paired *t*-test defining differences between CM and Wnt3a CM treated cells as significant (***$p < 0.001$).
(B) BMDM were incubated with Wnt3a CM supplemented with increasing concentrations of soluble Fzd1/Fc fusion protein for 4 hours. The fold induction of Arg1 mRNA expression shown represents the normalized ratio between target gene and reference gene (HPRT) normalized to the CM control. The results are means ± SEM of three independent experiments performed in technical duplicates.

Summary 3.5

- Wnt3a CM induced β-catenin stabilization and Axin2 expression in murine macrophages.
- Wnt3a-CM-induced Axin2 expression was dose-dependently inhibited by soluble Fzd1/Fc fusion protein.
- Pre-incubation of macrophages with Wnt3a led to a decreased TNF release following *M. tuberculosis* infection.
- *M. tuberculosis*/IFN-γ-activated macrophages showed a significant decrease in TNF mRNA expression after incubation with Wnt3a.

4. Discussion

The current study gives new insights into the role of Wnt/Fzd signaling in the context of inflammation. As a specific model system, *in vitro* and *in vivo* infection with *M. tuberculosis* in mice was used. With the main focus on the induction and function of Wnt receptor Fzd1, the following major observations were made:
(i) In the lungs of *M. tuberculosis*-infected mice overall Wnt/β-catenin signaling was strongly decreased. The mRNA expression of Frizzled homologs Fzd3, -4, -7, -8, -9 and -10 were significantly down-regulated during the course of *M. tuberculosis* infection, whereas transcripts of Fzd1 and Fzd5 were significantly increased. (ii) In primary macrophages TNF was critical for the expression of Fzd1 mRNA. (iii) Microbe-induced Fzd1 transcription was dependent on the presence of TLR2, MyD88 and activation of the NF-κB pathway. In addition, pre-activation of macrophages with IFN-γ synergistically enhanced the presence of Fzd1 protein in the plasma membrane. (iv) Fzd1 ligand Wnt3a was constitutively expressed in the lungs of *M. tuberculosis*-infected mice. In macrophages Wnt3a-induced β-catenin signaling was blocked in the presence of a soluble Fzd1/Fc fusion protein. (v) Wnt3a promoted a reduced TNF formation after *M. tuberculosis* infection.

Acute lung inflammation is characterized by high levels of pro-inflammatory cytokines and chemokines as well as increased expression of adhesion molecules for the recruitment and activation of immune cells[195]. The release of matrix metalloproteinases (MMPs) enables inflammatory cells to migrate through tissue layers to the site of inflammation[196]. Whereas moderate amounts of pro-inflammatory mediators are efficiently inactivated after local inflammation, the excessive release of effector molecules may contribute to tissue destruction and lung pathology[197;198]. Thus, mechanisms leading to the termination of inflammation are prerequisite to prevent inflammation-induced pathogenesis. These functions are characterized by an increased secretion of anti-inflammatory mediators and processes of wound healing as well as an enhanced proliferation of resident stem cells[199]. Very recently different studies have shown an involvement of Wnt/Fzd signaling pathways in these processes.

Wnt and Fzd homologs were recently demonstrated to directly regulate inflammatory responses of immune cells. Wnt5a and its corresponding receptor Fzd5 were localized in granulomatous lesions of TB patients, and demonstrated to regulate innate and adaptive immune responses in mycobacterial infection[153]. In activated human macrophages interactions between Wnt5a and Fzd5 were identified to enhance the expression of pro-inflammatory cytokines through the Wnt/Ca^{2+}-dependent pathway [46]. Ca^{2+}-dependent Wnt/Fzd signaling was also involved in the recruitment of human T cells, in which Wnt5a and Fzd2 were shown to sensitize the cells to migrate along a chemokine gradient[47]. At the site of inflammation, Wnt/β-catenin signaling was identified to induce extravasation of murine effector T cells [200]. Endothelial cell-derived Wnt1 and Wnt3a activated Fzd5 on human T cells leading to the expression of matrix metalloproteinases, and thereby enabling the cells to cross sub-endothelial layers. The resolution phase after tissue damage is characterized by a decrease of inflammation, tissue recovery, and matrix remodeling. In a mouse model of acute lung injury due to profound oxidative stress, increased epithelial cell proliferation and β-catenin stabilization during the resolution phase was demonstrated. Thus, a role of Wnt/β-catenin signaling was postulated for the termination of inflammation[171]. It was shown that different Wnt/Fzd pathways supported pro- and anti-inflammatory functions, thereby it may tip the balance of immune responses either in one or the other direction. Until recently the role of Wnt/Fzd signaling in the regulation of inflammation has not been reported. The new

findings add a novel meaning to the function of the highly conserved and "developmental" Wnt/Fzd pathways.

To analyze major components of the Wnt/Fzd pathways under chronic inflammatory conditions, mice were infected via the aerosol route with *M. tuberculosis*. Post-infection all mice that were used for analysis showed mycobacterial growth as previously described[201] and a strong inflammatory response as determined by the analysis of TNF, IFN-γ and NOS2[129;143;147;202]. In addition, transcripts of myeloid and lymphoid marker genes (*LysM* and *Lck*) were strongly increased during the course of infection, indicating a strong infiltration of immune cells, which was confirmed by immunohistochemistry. On the contrary, a reduction in the relative expression of bronchiolar and alveolar epithelial cell associated marker genes (*Scgb* and *Sftpc*) was examined. Both, an influx of immune cells and a decrease in the expression of epithelial marker genes indicated a severe alteration of the cellular composition and homeostasis of the respiratory system after *M. tuberculosis* infection. The homeostasis of most organs, including the lung, is known to be maintained by Wnt/Fzd signaling cascades[203], suggesting that Wnt/Fzd pathways may be induced in response to *M. tuberculosis* infection.

A systematic screen of Frizzled receptors in lung homogenates of *M. tuberculosis*-infected mice identified transcripts of Fzd1 and Fzd5 to be significantly up-regulated on day 21 and 42 post-infection, whereas Fzd3, -4, -7, -8, -9 and -10 were significantly decreased. A function of Fzd5 in mycobacterial infection was recently described by Blumenthal et al., showing that human Fzd5 and Wnt5a regulated microbially-induced IL-12 responses of antigen presenting cells and IFN-γ release in activated T cells[153]. The detection of Fzd5 in murine lung homogenates may further support these recent findings, which are still subject of ongoing studies in the Division of Microbial Interface Biology. In contrast to Fzd5, little was known about the regulation and function of Fzd1 in the context of inflammatory and infectious processes. Therefore, the major objective of the current study was the characterization of Fzd1.

To examine Fzd1 expressing cells in the murine lung *in vivo*, $Fzd1^{+/LacZ}$ reporter mice were analyzed using an X-gal staining protocol. Fzd1 promoter activity was detected in vascular tissue and cells of the outer rim of bronchioles. In addition, Fzd1 promoter activity was observed in single cells of the alveolar tissue.

Fzd1 has so far been reported to be primarily expressed in cells of mesenchymal origin such as smooth muscle cells (SMCs)[56;204]. Additional lung mesenchyme derived cells are represented by endothelial cells, pericytes, lipocytes, stromal fibroblasts and alveolar macrophages[205]. Thus, these cells may show Fzd1 promoter activity, of which alveolar macrophages would be of primary interest in the context of mycobacterial infection. Macrophages are the preferred habitat of *M. tuberculosis* and mediate essential effector functions in the control of mycobacterial growth. Therefore, *in vitro* studies were performed on murine macrophages to analyze the role of Fzd1 in inflammation.

Mechanisms leading to the induction of Fzd1 mRNA expression under defined infectious conditions were of special interest. Stimulation of bone marrow-derived macrophages with *M. tuberculosis*, *M. avium* and LPS showed, that transcripts of Fzd1 were up-regulated after treatment with increasing doses of different TLR agonists. The results suggested that murine Fzd1 transcription was induced in a TLR-dependent manner. With regard to the kinetics of Fzd1 mRNA expression, transcripts were most prominently expressed 4 hours post-infection, whereas after 24 hours Fzd1 transcript levels were reduced to detection limit. Recent data corroborated these findings. In a systematic micro-array analysis of G protein-coupled receptor expression in primary mouse macrophages, Lattin et al. identified Fzd1 mRNA to be significantly increased 6 hours after stimulation with LPS[206]. The authors also found that the expression of Fzd1 was strongly reduced 24 hours post-stimulation. In contrast, analyzing rat aortic smooth muscle cells in response to platelet-derived growth factor (PDG-BB) and FGF2, Mao et al. found the kinetics of Fzd1 transcription inversely regulated[207]: whereas Fzd1 transcripts were most prominently down-regulated 2 to 4 hours post-stimulation, mRNA expression was again increased to basal level after 24 hours. Taken together, these observations suggest a cell type and stimulus-specific regulation of Fzd1 transcription. Thus, additional analyses were carried out on murine macrophages to study the influence of TLR-mediated signaling pathways on Fzd1 transcription in response to microbial stimulation.

After binding of pathogen-associated molecular patterns (PAMPs) Toll-like receptors initiate signaling cascades leading to the induction of key inflammatory responses[208].

Downstream of TLRs the signal is mediated by different adaptor proteins, of which myeloid differentiation primary response gene 88 (MyD88) is shared by most TLR homologs except TLR3[209]. The central TLR/MyD88-induced signaling pathway leads to the activation and translocation of transcription factor NF-κB into the nucleus and the expression of NF-κB-dependent target genes[118].

Stimulation of TLR2-deficient macrophages with *M. avium* or Pam_3CSK_4 demonstrated the relevance of TLR2 signaling for the induction of Fzd1. However, after exposure to *M. tuberculosis* Fzd1 expression did not show significant differences between $TLR2^{-/-}$ and wild type cells. These data may suggest the presence of additional pathways leading to Fzd1 transcription. Previous reports indicated that in response to *M. tuberculosis* infection *in vitro*, TLR2 was dispensable in promoting expression of immunologically important genes[210-212]. Comparing the wild type Fzd1 expression with the data observed in the dose response (see Fig. 12), differences in the induction of Fzd1 are noticeable. These differences may be due to a lower activation potential of a freshly cultured H37Rv *M. tuberculosis* strain. In addition, the dose response was analyzed using the SYBR green assay of quantitative real-time PCR, which provides the advantage of an increased flexibility, whereas a more specific RT-PCR protocol based on hydrolysis probes was used for the comparison between WT and KO macrophages. In contrast to TLR2, effective immune responses to *M. tuberculosis* infection critically depended on the presence of MyD88, since knockout mice fail to control mycobacterial growth[213]. The current data show that MyD88 signaling was essential for the induction of Fzd1 mRNA in response to *M. tuberculosis*, *M. avium* and LPS. Downstream of MyD88, inhibition of NF-κB pathway (by using the compound BAY 11-7082 to prevent IκB phosphorylation) indicated that MyD88-induced Fzd1 expression in macrophages also depended on NF-κB-activation, showing a significant decrease in the presence of the inhibitory compound. In addition to these observations, treatment of murine macrophages with recombinant TNF demonstrated that Fzd1 mRNA was also expressed independently of TLR and MyD88. Nevertheless, in response to recombinant TNF, Fzd1 transcription was strongly reduced in the presence of BAY 11-7082, further corroborating a pivotal role of transcription factor NF-κB in the induction of Fzd1. Whereas little is known about the role of MyD88 on the expression of Wnt and Fzd homologs, recent publications support an involvement of TLRs and NF-κB in the modulation of Wnt/Fzd signaling. A study on *Drosophila* provided

evidence that bacteria-induced Toll/Dorsal (TLR/NF-κB homologs) signaling activated expression of ligand WntD [152]. In addition, using a human hepatoblastoma cell line and dealing with the subject of oncogenesis, Sun et al. demonstrated direct binding of the NF-κB-p50 to the Wnt1 promoter region [214]. Yet, direct TLR- or NF-κB-dependent induction was only shown for Wnt homologs. However, Fzd receptors were reported to be induced in response to microbial stimulation and conserved bacterial structures, thereby implying TLR/NF-κB-dependent transcription [46;153;206]. With regard to NF-κB directed activation of Fzd1 RNA expression, recent reports indicated possible modes of induction: Based on sequence analyses Yerges et al. identified a binding site for the transcription factor early growth response protein 1 (Egr1) in the Fzd1 promotor region[215]. Egr1 itself possesses multiple NF-κB binding sites within its promoter region, and its expression was blocked in the presence of BAY 11-7082[216]. In addition, Egr1 is induced by a large number of growth factors, cytokines and injurious stimuli (including LPS), and serves as a critical regulator of multiple developmental and inflammatory functions[217-219]. Thus, analyses on Egr1 expression may provide further insights into direct or indirect induction of Fzd1 mRNA expression.

TNF is a critical mediator for the induction and regulation of diverse inflammatory functions. Especially in the control of mycobacterial infection TNF governs multiple functions such as activation and recruitment of immune cells or granuloma formation[130]. In a positive feedback loop TNF is released in response to NF-κB signaling and induces expression of NF-κB-dependent target genes. To investigate the importance of TNF on Fzd1 expression, macrophages derived from TNF-deficient mice were examined.

The data demonstrated a pivotal role of TNF in the induction of Fzd1. The results imply that TLR/NF-κB signaling activates TNF, which in turn initiates Fzd1 transcription by auto- or paracrine TNF signaling. In consequence the results show that Fzd1 induction is not specific for mycobacteria or other pathogens, but rather expressed in a more general pro-inflammatory context depending on TNF. These observations implicate diverse inflammatory functions in which Fzd1 could be involved. It is known that Wnt ligands and Fzd receptors are up-regulated in chronic inflammatory diseases, such as inflammatory bowel disease, rheumatoid arthritis or psoriasis [151;220;221]. Even though the modes of Wnt and Fzd induction are not fully

understood, the current findings implicate that up-regulation may be due to the presence of TNF in chronic inflammation.

IL-10 is a critical mediator in resolving inflammation by counteracting pro-inflammatory responses induced by TNF and other cytokines. One functional mechanism of IL-10 is to block IκBα phosphorylation and to prevent NF-κB dependent target gene expression[222]. In the present work, wild type derived macrophages were pre-incubated with recombinant IL-10 to examine its function on Fzd1 transcription. It was shown that in response to *M. avium*-infection IL-10 negatively regulated Fzd1 expression, further supporting an inflammation-induced role of Fzd1. On the one hand this observation could be due to a direct modulation of Fzd1 expression by IL-10. On the other hand, considering that IL-10 blocks TNF expression and inhibits activation of NF-κB, it may also support the central role of TNF and NF-κB in promoting Fzd1 transcription. Similar findings were described by Pereira et al., who demonstrated an active role of Wnt5a signaling in the inflammatory macrophage response. In addition, the authors showed that IL-10 decreased Wnt5a expression in activated murine macrophages[46]. However, an influence of IL-10 on the expression of Fzd receptors has not been described to date.

Having examined modes leading to the induction of Fzd1 transcription in mature macrophages, studies were performed analyzing the impact of macrophage activation on Fzd1 protein expression.

Little is known about the protein expression of Fzd1. Up-regulation of the receptor was detected by immunohistochemistry in patients of reflux esophagitis and Alzheimer's disease. In addition, Fzd1 was identified at the invasion front of different types of tumors. To date, Fzd1 protein expression has not been reported in mature macrophages. By Western blot analyses Tickenbrock et al. identified Fzd1 in protein lysates of human monocytes, strongly indicating that Fzd1 might also be expressed in fully differentiated macrophages[223].

In the current study Fzd1 protein expression was identified at the surface of *in vitro* and *in vivo* differentiated murine macrophages by FACS measurements, and was increased on the plasma membrane after stimulation with mycobacteria or LPS. Further analyses were carried out to investigate the impact of cytokines released by activated lymphocytes on Fzd1 expression. In particular IFN-γ is known to play an essential role in macrophage activation and to mediate protective immunity against

mycobacterial infection[143]. By FACS analyses it was demonstrated that pre-activation of BMDM with IFN-γ synergistically triggered Fzd1 surface expression in response to *M. tuberculosis* or LPS. Fzd1/CD86 staining of peritoneal exudate cells additionally implied that Fzd1 was primarily increased on highly activated macrophages ($Fzd1^{+}/CD86^{high}$). The data suggest that Fzd1 surface expression corresponded to TLR stimulation and increased macrophage activation through IFN-γ. Thus, the results may suggest a role of the receptor in inflammatory processes. In addition to these novel findings, further analyses on the dynamics of Fzd1 protein expression were carried out.

Fzd1 was detected by Western blot experiments showing a double band of approx. 70 kDa that may reflect different glycosylation forms of the receptor[224]. Analysis of total protein revealed no differences in the Fzd1 expression between treated or untreated macrophages. However, comparison of TLR/IFN-γ activated macrophages by extra- and intracellular flow cytometric measurements indicated a shift of Fzd1 from intracellular compartments to the plasma membrane. The results imply that the transportation of Fzd1 towards the cell surface is up-regulated, whereas the total amount of Fzd1 protein remains unchanged. The kinetics of Fzd1 surface expression showed a strong increase 24 hours post-stimulation, indicating that upon stimulation Fzd1 may functionally be most accessible at later time points. Yet, additional analyses of the Fzd1 turnover would bring a more profound insight about the regulation of Fzd1 on protein level. Recent publications demonstrated frequent trafficking and a very dynamic regulation of Fzd homologs. Bryja et al. showed that inhibition of endocytosis in murine neuronal cells led to a shift in the distribution of GFP-tagged Fzd4 from cytosolic compartments towards the plasma membrane[225], implicating a continuous uptake of Fzd4 into the cell. In an additional report, Terabayashi et al. demonstrated that the amount of Fzd5 within the plasma membrane was regulated through endocytosis and lysosomal degradation[226]. Binding of a Wnt homolog to its Fzd receptor may also induce receptor-mediated endocytosis[227], thus greatly affecting the presence and regulation of Fzd (surface) expression. In this context, clathrin-mediated endocytosis was demonstrated to be a prerequisite for Wnt/Fzd signaling and suggested to attenuate signaling through lysosomal degradation of Wnt ligands and receptors[227].

To elucidate whether a similar regulation of Fzd1 protein expression as observed in mouse macrophages may also be found in human cells, further analyses were performed on human macrophages. Western blot analyses of human monocyte-derived macrophages revealed that Fzd1 protein is also present in human cells. Yet, a regulation of total Fzd1 protein was not observed at different stimulatory conditions. Extracellular FACS analysis of human macrophages after treatment with *M. tuberculosis*, LPS, or IFN-γ indicated that Fzd1 was similarly up-regulated to the cell surface as demonstrated for murine macrophages. The data showed comparable modes of Fzd1 protein expression in human macrophages as observed in the mouse model.

The Wnt homologs Wnt3a and Wnt7b have been reported to bind to Fzd1[55;56]. Wnt3a was shown to induce β-catenin signaling in various human and murine cell lines transfected with Fzd1[55;72]. In addition, based on *in vitro* coimmunoprecipitation assays Wnt7b was demonstrated to interact with Fzd1 and to activate the β-catenin pathway in Fzd1 transfected human embryonic kidney cells[56]. In the current study transcripts of Fzd1 ligands Wnt3a and Wnt7b were detected in lung homogenates of *M. tuberculosis*-infected mice. Wnt7b expression was shown to be significantly up-regulated during the course of infection. In previous reports it was demonstrated that Wnt7b greatly affects lung development[177]. Different from Wnt7b, Wnt3a mRNA was found constitutively expressed in response to *M. tuberculosis* infection. By immunohistochemical analyses Wnt3a was localized in cells of the bronchiolar epithelium, but not in granulomatous lung tissue of infected mice. In a recent report both Wnt3a and Wnt7b were shown to be expressed in the lung of idiopathic pulmonary fibrosis (IPF) patients. The authors detected increased transcript levels of Wnt7b in primary AT2 cells derived from IPF patients, whereas Wnt3a was localized by immunohistochemistry in AT2 cells and in ciliated bronchial epithelial cells[228]. The fact that Wnt3a and Wnt7b were expressed in the lungs of *M. tuberculosis*-infected mice may indicate possible interactions with Fzd1 *in vivo*.

For practical reasons this study focused on ligand Wnt3a to further analyze the role of putative Fzd1-mediated signal transduction. Wnt3a is one of the best characterized Wnt homologs and features a great availability of valuable research tools, such as: the availability of a Wnt3a expressing cell line (LWnt3a), recombinant Wnt3a protein and monoclonal anti-Wnt3a antibodies.

Wnt3a is located on murine chromosome 11. Deletion leads to an embryonic lethal phenotype. Mice deficient for Wnt3a exhibit a truncated anterior-posterior axis, defects in somitogenesis, paraxial mesoderm and laterality, as well as dysmorphologies in the central nerve system and hypoplasic development of the hippocampus[229-232]. In an overall picture on cellular Wnt3a functions, it is mostly associated with the recruitment and differentiation of self-renewal cells[233-236]. Yet, to date the issue whether and how Wnt3a-induced signaling may influence macrophage responses has not been addressed. Three different reports have shown Wnt3a-mediated functions on myeloid cells: Spencer et al. indicated that Wnt3a inhibited osteoclastogenesis, when mouse primary mononuclear cells were co-cultured with primary osteoblasts[237]. With regard to hematopoesis in mice, Wnt3a was shown to affect development of myeloid progenitor cells and thymocytes[238]. In addition, Tickenbrock et al. demonstrated that Wnt3a induced β-catenin signaling in human monocytes, leading to a reduced migration through an endothelial layer[223].
Here it was demonstrated that mature mouse macrophages activated β-catenin signaling in response to Wnt3a conditioned medium. This effect was inhibited in the presence of a soluble Fzd1/Fc fusion protein, giving an indirect evidence that Wnt3a may induce β-catenin signaling through Fzd1. Yet, additional experiments, such as co-immunoprecipitation of Wnt3a and Fzd1 are needed to demonstrate a direct interaction. In addition, the inhibition of β-catenin signaling by Fzd1/Fc fusion protein strongly suggests the binding of Wnt3a to Fzd1, but does not exclude interactions between Wnt3a and additional Fzd homologs.

Even though Wnt3a has been well characterized, only few reports have directly linked Wnt3a to immunologic processes. Wnt3a was demonstrated to be involved in the recruitment of hematopoietic cells[239], and generation of multipotent $CD8^+$ memory stem cells[240]. In a murine model of type II diabetes, Wnt3a has been shown to contribute to aortic calcification. In this context, the authors observed an up-regulation of Wnt3a transcripts in aortic myofibroblasts treated with TNF[241].
In the current study, pre-incubation of murine macrophages with Wnt3a conditioned medium led to a decreased TNF release in response to *M. tuberculosis*. Moreover, activation of macrophages with *M. tuberculosis* and IFN-γ 24 hours prior to the addition of Wnt3a conditioned medium significantly decreased TNF mRNA

expression. The results indicated an anti-inflammatory function of Wnt3a on murine macrophages that may be mediated through Fzd1. The results suggest that Wnt3a-induced signaling may affect the extent of chronic inflammation. Recently Chacón et al. demonstrated Wnt3a/Fzd1-dependent protection of neuronal PC12 cells from apoptosis[72]. In response to Aβ oligomers, which is believed to be the causative agent of Alzheimer's disease, Wnt3a-induced activation of β-catenin signaling caused a negative regulation of caspase3. These observations further corroborate a putative function of Wnt3a (/Fzd1) -induced β-catenin signaling in fully differentiated cells.

Due to the inflammatory gene expression profile and effector functions in response to bacterial infection, macrophages have been classified into two groups: M1 and M2 macrophages[193]. Based on a given micro environment, M1 macrophages conduct microbicidal and pro-inflammatory functions, whereas M2 macrophages are less microbicidal and involved the resolution of inflammation[242]. Lymphocytes contribute to the polarization of macrophages. IFN-γ is a critical mediator in the activation of macrophages enhancing NOS2 expression and release of reactive nitrogen intermediates, whereas alternative macrophage activation through Th2-type cytokines IL-4 and IL-13 results in an M2 phenotype[194]. A common marker for alternative macrophage activation is the expression of Arginase1 (Arg1), which counteracts NOS2 functions by competing for its substrate L-arginine. In macrophages Arg1 activity catalyzes the production of urea and L-ornithine[243]. Metabolites of L-ornithine are associated with the induction of cell proliferation and collagen synthesis[243].

It was observed that Wnt3a-treated macrophages negatively regulate TNF expression when infected with *M. tuberculosis*. To analyze if Wnt3a had any influence on macrophage polarization, expression of Arg1 was examined. Initial results indicated increased Arg1 transcription after Wnt3a treatment, which could be inhibited in the presence of a soluble Fzd1/Fc fusion protein. These observations suggest that Wnt3a may promote alternative macrophage activation. It is intriguing to speculate that Wnt3a-induced β-catenin signaling may influence anti-inflammatory functions through macrophage polarization in an infectious context. However, additional studies are needed to confirm and corroborate these initial observations.

The role of β-catenin signaling in inflammation is becoming more evident to be closely connected to the NF-κB pathway. In recent cancer studies a direct regulation of the β-catenin pathway through IκB kinases α and β (IKKα, β) or interaction with NF-κB has been reported[244-247]. Constitutive β-catenin signaling was shown to inhibit NF-κB activation and target gene expression of TRAF1, Fas, or NOS2[246;248]. Vice versa, activation of the NF-κB pathway led to phosphorylation and degradation of β-catenin. Two independent reports on *Salmonella*-induced inflammation have demonstrated that β-catenin signaling was down-regulated during acute inflammation, whereas constitutive activation of the β-catenin pathway negatively regulated inflammatory responses[249;250]. In a model of acute lung injury Douglas et al. demonstrated reduction of β-catenin signaling during inflammatory responses, whereas epithelial proliferation and resolution of inflammation was paralleled by an enhanced β-catenin expression[171]. Idiopathic pulmonary fibrosis (IPF) has recently been associated with Wnt/β-catenin signaling. Königshoff et al. summarize these findings, arguing that the chronic lung disease is due to a dysfunctional regeneration signal of the damaged epithelium[251]. Thus, it is suggested that Wnt/β-catenin signaling is involved in the restoration of the physiological equilibrium of the lung tissue.

The examination of lung homogenates of *M. tuberculosis*-infected mice showed that major effectors and regulators of the β-catenin pathway were negatively regulated under pro-inflammatory conditions. The data demonstrated a down-regulation of β-catenin-dependent target gene Axin2 during the course of infection and a reduction of β-catenin protein levels. In agreement with previous reports[247;249], these observations suggest that activation of the NF-κB pathway may be inversely correlated to the activation of the β-catenin pathway. In consequence, activation of the NF-κB pathway during *M. tuberculosis* infection may directly inhibit β-catenin stabilization and target gene expression. In addition to Wnt/β-catenin signaling, the overall protein levels of Fzd1 in lungs of *M. tuberculosis*-infected mice were reduced during the course of infection. The results further indicate a close connection between β-catenin signaling and Fzd1 protein expression at the level of the entire lung. Compared to increased mRNA levels of Fzd1, the data implicate that Fzd1 protein was differentially regulated during the course of infection. Further investigations need to be done to clarify this observation in more detail. Yet, a

massive influx of immune cells negative for Fzd1 protein may have caused a "dilution" and an apparent reduction of total Fzd1 protein levels within lung homogenates. Strong infiltration of immune cells, especially lymphocytes, was detected by the expression of marker genes and by immunohistochemistry. In addition, the difference between an increased Fzd1 transcription and reduced expression of Fzd1 protein may be indicative for a high turnover of the receptor. Different reports have shown that Wnt/Fzd signaling was subject to diverse modes of inhibition, including internalization and degradation of Fzd receptors[226;252-254]. In this context, it was reported that co-receptor LRP1 interacts with the CRD of human Fzd1 and thereby blocking β-catenin signaling[255]. LRP1 has also been characterized to facilitate retrograde trafficking towards the lysosomal compartment[256;257], suggesting that repressive effects of LRP1 are amplified by an enhanced Fzd1 internalization and lysosomal degradation. First experiments have indicated that transcripts of LRP1 were increased during the course of infection (data not shown). For that reason a reduction of Fzd1 protein in response to *M. tuberculosis* infection may be explained by an increased expression of its inhibitor LRP1. Lysosomal degradation of Fzd receptors is a regulatory mechanism that has been well described in Drosophila[258;259]. Similar to β-catenin, which is in a non-signaling-state frequently targeted to the proteasome, Fzd1 may be frequently targeted to the lysosomal compartment or down-regulated after transcription. A high turnover of Fzd1 or β-catenin would allow the cells to rapidly adapt to changes in the inflammatory environment and to initiate further immune regulatory functions once Wnt/β-catenin signaling is activated.

Based on the current study, the following scenario can be developed (Fig. 31):
Mycobacteria and conserved bacterial structures activate TNF release (Fig. 31a). Fzd1 mRNA expression is up-regulated on murine macrophages in response to TLR/NF-κB dependent stimulation. This increase correlates with the expression of TNF, which is essential for the induction of Fzd1 transcription (Fig. 31b). These observations suggest that pathways leading to a differential regulation of TNF might have an indirect impact on Fzd1 expression. On the cell surface of macrophages the presence of Fzd1 protein is increased upon activation with mycobacteria or LPS. This effect is synergistically enhanced in the presence of IFN-γ, suggesting that adaptive immune responses might contribute to Fzd1 mediated functions (Fig. 31b). Increased

levels of the Fzd1 receptor enhances its availability for external agonists. Wnt3a that may be derived from epithelial cells, binds to Fzd receptors and induces β-catenin signaling in murine macrophages (Fig. 31c). Wnt3a-induced β-catenin signaling is blocked in the presence of a soluble Fzd1/Fc fusion protein, suggesting that Wnt3a activates the Wnt/β-catenin pathway through Fzd1 (Fig. 31c). In the presence of Wnt3a, macrophages that are activated with *M. tuberculosis* and IFN-γ selectively reduce TNF expression, resulting in a negative feedback inhibition of Fzd1 (Fig. 31d). This Wnt3a-mediated mechanism may function on the one hand to negatively regulate TNF expression and on the other hand to maintain macrophage effector functions but with reduced pathologic side effects of TNF[198].

The involved pathways leading to the reduction of TNF are presently not clear. Treatment of murine macrophages with Wnt3a resulted in the induction of Arginase1, suggesting that Wnt3a might promote alternative macrophage activation. IL-4 and IL-13 are best known to induce alternative activation of macrophages and to selectively inhibit macrophage effector functions. It was shown that in LPS/IFN-γ treated macrophages IL-4 and IL-13 moderately reduced the expression of pro-inflammatory cytokines and NOS2 as compared with potent inhibition by IL-10[260;261]. However, Wnt3a indicated had no impact on the NOS2 expression in macrophages treated with mycobacteria and IFN-γ as analyzed by Western blot (data not shown).

The traditional view, namely that Wnt/Fzd signaling is merely involved in cell differentiation and tissue regeneration may have to be expanded: Wnt/Fzd signaling emerges as a regulatory component of the inflammatory response to infectious agents and may thus be seen as yet another feedback mechanism to maintain tissue function in conditions of environmental stress.

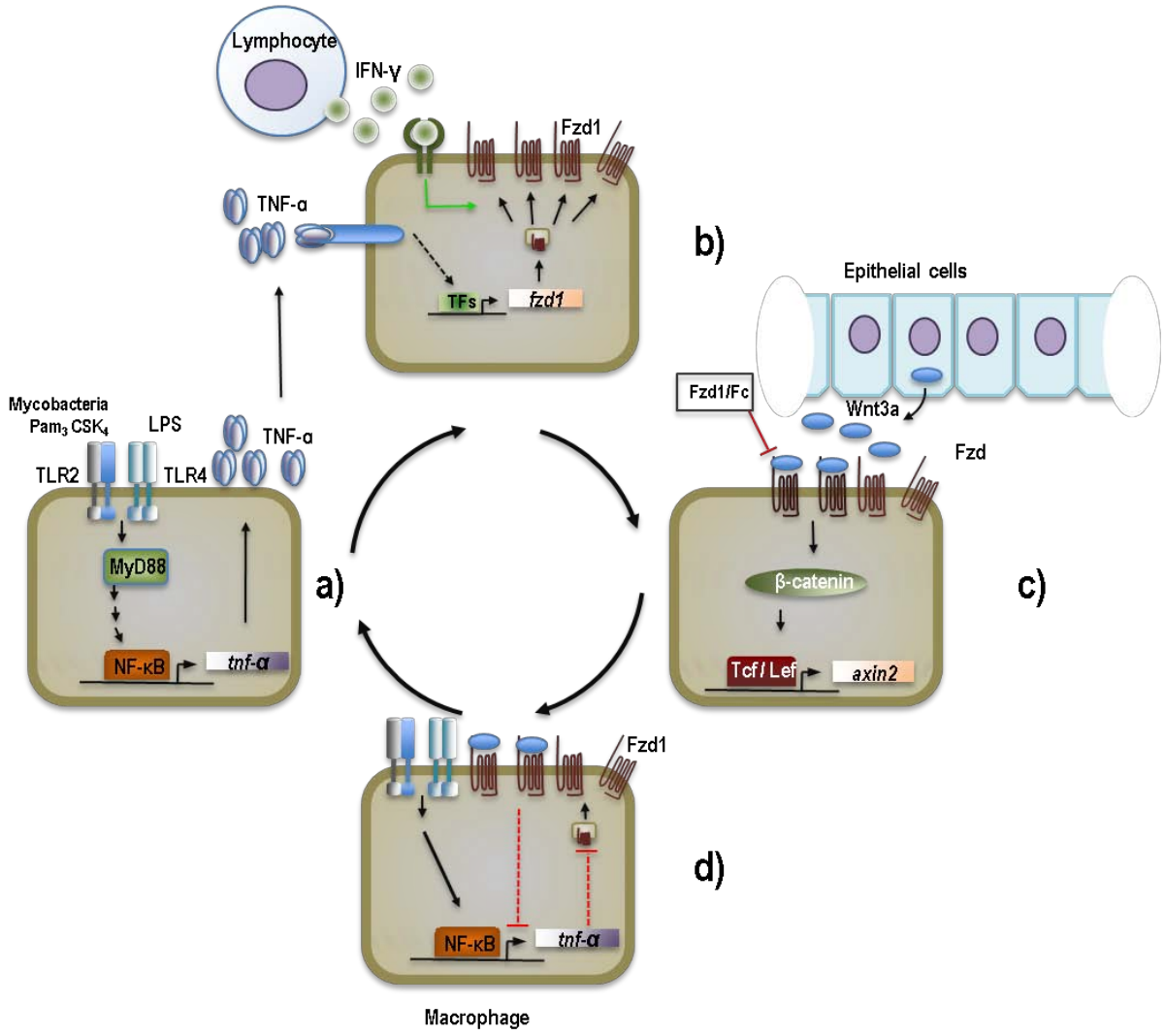

Figure 31. Working model on the involvement of Fzd1 and Wnt3a-induced β-catenin signaling in macrophage effector functions and inflammatory processes.
a) Mycobacteria and conserved bacterial structures activate TNF release, that **b)** in an auto- or paracrine manner triggers the induction of Fzd1 mRNA. Synergistic effects between IFN-γ (secreted by activated lymphocytes) and inflammatory macrophages further enhance the presence of Fzd1 within the plasma membrane. **c)** Wnt3a (primarily expressed by epithelial cells) binds to macrophage Fzd receptors, inducing a β-catenin signaling cascade that can be blocked in the presence of soluble Fzd1 (Fzd1/Fc). **d)** Wnt3a affects macrophage effector functions by selectively decreasing TNF mRNA expression and protein release causing a feed back loop that negatively regulates the expression of Fzd1.

The data derived from murine *in vitro* experiments suggest that Wnt3a selectively induces anti-inflammatory functions in murine macrophages. These functions may be activated through Fzd1-mediated β-catenin signaling. In macrophages Fzd1 was expressed in response to TLR/NF-κB signaling pathways and was further modulated by pro- and anti-inflammatory cytokines. It was implied that following *M. tuberculosis* infection a decrease in β-catenin signaling *in vivo* was in advantage of pro-inflammatory responses. Mycobacterial infection leads to severe inflammation and

lung pathology. The destruction of lung tissue due to severe pathological processes is counteracted by the recovery of epithelial cells, that are recruited from bronchioalveolar stem cell niches. In the alveolar stem cell niche, the proliferation of type 2 epithelial cells into type 1 pneumocytes was demonstrated to be activated by β-catenin[262-264]. This process of tissue-renewal is of major importance, since type 1 pneumocytes represent the bulk of the alveolar surface area. In addition, multipotent mesenchymal cells were identified to reside within the lung. It was shown that these progenitor cells significantly contributed to injury repair and tissue regeneration of the otherwise slowly renewing lung epithelium[265-267]. Mesenchymal stem cells were reported to conduct self-renewal and differentiation programs in response to Wnt3a-mediated β-catenin stabilization[268].

In the current study it was shown that Wnt3a was present within the lung before and after mycobacterial infection. In a more general sense, Wnt3a-induced β-catenin signaling may contribute to anti-inflammatory functions and processes involved in wound healing and tissue remodeling through different ways: on the one hand through the selective reduction of TNF release by macrophages, and on the other hand through differentiation and self-renewal of alveolar and mesenchymal stem cell populations. In the current model of *M. tuberculosis* infection, the murine immune system is not able to overcome chronic inflammation, which leads to lethal tissue destruction and organ failure. Thus, potential anti-inflammmatory effects of Wnt/β-catenin signaling *in vivo* may be suppressed in support of pro-inflammatory responses. To study protective functions of Wnt/Fzd signaling pathways during the resolution phase of mycobacteria-induced inflammation, a model of anti-mycobacterial drug therapy may provide deeper insights. Due to the effects of drug treatment mice would be able to recover from *M. tuberculosis* infection. A reduction of the bacterial burden may be paralleled by processes of wound healing and tissue remodeling. These functions may be marked and supported by an increased activation of the Wnt/β-catenin pathway.

Wnt/Fzd and TLR pathways were shown to intersect in Drosophila, zebrafish, mice and humans, indicating an evolutionarily conserved interplay[152;153;269;270]. Recent reports have demonstrated that Wnt/Fzd signaling was functionally involved in bridging innate and adaptive immunity to microbial infection[46;152;153;197]. The current study indicates that the Fzd1 ligand Wnt3a selectively induces anti-inflammatory

functions in *M. tuberculosis*-infected murine macrophages. It may be hypothesized that Wnt3a-mediated signaling in innate immune cells is involved in protective cellular functions that prevent inflammation-induced pathology. Thus, Wnt3a may counteract pro-inflammatory suppression of the β-catenin pathway, and may support the regeneration of organ homeostasis.

5. Abstract

Elements of the highly conserved Wnt/Frizzled signaling pathways, which are known to be essential in developmental processes, have recently been identified as regulators of the inflammatory immune response.

Using the established mouse model of experimental *Mycobacterium tuberculosis* infection the current study identifies Frizzled1 and its ligand Wnt3a as novel factors modulating immune cell function. Mice infected with *M. tuberculosis* via the aerosol route showed a dramatic increase in the bacterial burden on day 21 and day 42 post-infection, which was paralleled by a massive inflammatory response, as measured by an increased expression of TNF and IFN-γ mRNA, and the expression of inducible nitric oxide synthase. A systematic screen of Fzd homologs in lung homogenates of infected mice identified Fzd1 and Fzd5 mRNA to be significantly up-regulated during the course of infection, whereas Fzd homologs -4, -7, -8, -9 and -10 were decreased. Similarly the Wnt/ß-catenin signaling pathway, as measured by β-catenin levels and transcripts of the ß-catenin dependent target gene *Axin2*, appeared down-regulated during *M. tuberculosis*-infection. Using Fzd1 reporter mice, Fzd1 promoter activity was localized in cells of the vasculature, bronchioles and single cells within alveoli. In infected mice the Fzd1 ligand Wnt3a was constitutively expressed on the mRNA and protein level. Immunohistochemical analysis localized Wnt3a in the bronchiolar epithelium.

In vitro infection of murine macrophages led to a significant induction of Fzd1 mRNA in response to *M. tuberculosis*, *M. avium* and conserved bacterial structures, which was dependent on TLR2, MyD88, and the NF-κB pathway. TNF was characterized as a pivotal mediator of microbially induced Fzd1 transcription. Surface expression of Fzd1 protein on murine macrophages was increased in response to *M. tuberculosis* infection and synergistically enhanced in the presence of IFN-γ. Addition of Wnt3a induced Wnt/β-catenin signaling in murine macrophages, which was inhibited in the presence of a soluble Fzd1/Fc fusion protein. Furthermore, Wnt3a reduced TNF transcription and release, suggesting that Wnt3a selectively promotes anti-inflammatory functions in murine macrophages.

The current study extends the role of Wnt/Fzd signaling in regulating innate effector functions: It identifies a potential feedback mechanism, in which induction of the Wnt/β-catenin pathway may fine tune the activation status of antigen presenting cells, thereby protecting the immune cell from hyperactivation during microbe-induced inflammation.

6. Zusammenfassung

Faktoren des hoch konservierten Wnt/Frizzled Signalwegs, der vor allem in entwicklungsbiologischen Prozessen gut charakterisiert ist, wurden kürzlich als Regulatoren der inflammatorischen Immunantwort identifiziert.

Im etablierten Mausmodell der experimentellen *M. tuberculosis*-Infektion wurden in der vorliegenden Arbeit neue Funktionen der Faktoren Frizzled1 (Fzd1) und Wnt3a gezeigt, die die Funktion von Immunzellen modulieren: Am Tag 21 und Tag 42 nach Aerosolinfektion wiesen Mäuse einen dramatischen Anstieg der bakteriellen Keimlast auf, der mit einer erhöhten Transkription von TNF und IFN-γ sowie mit der Expression der induzierbaren Stickoxidsynthase einherging. In einer gezielten Untersuchung aller Fzd-Homologe in Lungenhomogenaten infizierter Mäuse waren Transkripte der Homologe Fzd1 und Fzd5 signifikant hochreguliert, während die mRNA-Expression von Fzd4, -7, -8, -9 und -10 signifikant vermindert war. Ähnlich verhielt es sich mit einer Herunterregulierung des Wnt/Fzd-induzierten β-Catenin-Signalwegs, der nach Infektion mit *M. tuberculosis* in Lungenhomogenaten auf das Vorkommen von β-Catenin Protein und die Transkription des Zielgens *Axin*2 untersucht wurde. Durch Fzd1-Reportermäuse wurde eine Aktivität des Fzd1-Promoters in Zellen des Blutgefäßsystems, den Bronchiolen und in einzelnen Zellen der Alveolen lokalisiert. Der Fzd1-Ligand Wnt3a wurde in infizierten Mäusen auf mRNA- und Proteinebene konstitutiv exprimiert und durch immunhistochemische Untersuchungen im bronchiolaren Epithel lokalisiert.

In vitro führte die Infektion von murinen Makrophagenm mit *M. tuberculosis*, *M. avium* und konservierten bakteriellen Strukturen zu einer signifikanten Induktion von Fzd1 mRNA. Es wurde gezeigt, dass diese abhängig von TLR2, MyD88 und dem NF-κB-Signalweg ist. TNF wurde dabei als ein essentieller Mediator der mikrobiell induzierten Fzd1 mRNA-Expression charakterisiert. Auf der Zelloberfläche bewirkte die Infektion mit *M. tuberculosis* einen Anstieg der Fzd1 Proteinexpression, die in Gegenwart von IFN-γ synergistisch gesteigert wurde. Die Stimulation mit Wnt3a führte in Makrophagen zur Induktion des Wnt/β-Catenin-Signalwegs, der in Gegenwart von einem löslichen Fzd1/Fc-Fusionsprotein inhibiert wurde. Ferner beeinflusste Wnt3a die Effektorfunktionen von Makrophagen, indem es eine Verminderung der TNF-Transkription sowie der TNF-Freisetzung bewirkte. Diese Ergebnisse implizieren, dass Wn3a selektiv anti-inflammatorische Funktionen in murinen Makrophagen auslöst.

Die vorliegende Arbeit erweitert das Wissen über Wnt/Fzd-Signalwege und deren Funktion in der Regulierung des angeborenen Immunsystems: Es wird ein potentieller Rückkopplungsmechanismus identifiziert, der durch die Induktion des Wnt/β-Catenin-Signalwegs den Aktivierungsstatus antigenpräsentierender Zellen herabsenken und dadurch zum Schutz der Immunzellen vor einer Hyperaktivierung mikrobiell induzierter Entzündungsreaktionen beitragen könnte.

7. References

1. Srivastava,M., E.Begovic, J.Chapman, N.H.Putnam, U.Hellsten, T.Kawashima, A.Kuo, T.Mitros, A.Salamov, M.L.Carpenter, A.Y.Signorovitch, M.A.Moreno, K.Kamm, J.Grimwood, J.Schmutz, H.Shapiro, I.V.Grigoriev, L.W.Buss, B.Schierwater, S.L.Dellaporta, and D.S.Rokhsar. 2008. The Trichoplax genome and the nature of placozoans. *Nature* 454:955-960.

2. Wodarz,A. and R.Nusse. 1998. Mechanisms of Wnt signaling in development. *Annu.Rev.Cell Dev.Biol.* 14:59-88.

3. Clevers,H. 2006. Wnt/beta-catenin signaling in development and disease. *Cell* 127:469-480.

4. Qureshi,S.T. and R.Medzhitov. 2003. Toll-like receptors and their role in experimental models of microbial infection. *Genes Immun.* 4:87-94.

5. Janssens,S. and R.Beyaert. 2003. Role of Toll-like receptors in pathogen recognition. *Clin.Microbiol.Rev.* 16:637-646.

6. Nusslein-Volhard,C. and E.Wieschaus. 1980. Mutations affecting segment number and polarity in Drosophila. *Nature* 287:795-801.

7. Nusse,R., A.van Ooyen, D.Cox, Y.K.Fung, and H.Varmus. 1984. Mode of proviral activation of a putative mammary oncogene (int-1) on mouse chromosome 15. *Nature* 307:131-136.

8. Nusse,R. and H.E.Varmus. 1982. Many tumors induced by the mouse mammary tumor virus contain a provirus integrated in the same region of the host genome. *Cell* 31:99-109.

9. Miller,J.R. 2002. The Wnts. *Genome Biol.* 3:REVIEWS3001.1-3001.15.

10. Willert,K., J.D.Brown, E.Danenberg, A.W.Duncan, I.L.Weissman, T.Reya, J.R.Yates, III, and R.Nusse. 2003. Wnt proteins are lipid-modified and can act as stem cell growth factors. *Nature* 423:448-452.

11. Mikels,A.J. and R.Nusse. 2006. Purified Wnt5a protein activates or inhibits beta-catenin-TCF signaling depending on receptor context. *PLoS.Biol.* 4:e115.

12. Takada,R., Y.Satomi, T.Kurata, N.Ueno, S.Norioka, H.Kondoh, T.Takao, and S.Takada. 2006. Monounsaturated fatty acid modification of Wnt protein: its role in Wnt secretion. *Dev.Cell* 11:791-801.

13. Zhai,L., D.Chaturvedi, and S.Cumberledge. 2004. Drosophila wnt-1 undergoes a hydrophobic modification and is targeted to lipid rafts, a process that requires porcupine. *J.Biol.Chem.* 279:33220-33227.

14. Smolich,B.D., J.A.McMahon, A.P.McMahon, and J.Papkoff. 1993. Wnt family proteins are secreted and associated with the cell surface. *Mol.Biol.Cell* 4:1267-1275.

15. Komekado,H., H.Yamamoto, T.Chiba, and A.Kikuchi. 2007. Glycosylation and palmitoylation of Wnt-3a are coupled to produce an active form of Wnt-3a. *Genes Cells* 12:521-534.

16. Kurayoshi,M., H.Yamamoto, S.Izumi, and A.Kikuchi. 2007. Post-translational palmitoylation and glycosylation of Wnt-5a are necessary for its signalling. *Biochem.J.* 402:515-523.

17. Bartscherer,K., N.Pelte, D.Ingelfinger, and M.Boutros. 2006. Secretion of Wnt ligands requires Evi, a conserved transmembrane protein. *Cell.* 125:523-533.

18. Bartscherer,K. and M.Boutros. 2008. Regulation of Wnt protein secretion and its role in gradient formation. *EMBO Rep.* 9:977-982.

19. Zecca,M., K.Basler, and G.Struhl. 1996. Direct and long-range action of a wingless morphogen gradient. *Cell* 87:833-844.

20. Chen,M.H., Y.J.Li, T.Kawakami, S.M.Xu, and P.T.Chuang. 2004. Palmitoylation is required for the production of a soluble multimeric Hedgehog protein complex and long-range signaling in vertebrates. *Genes Dev.* 18:641-659.

21. Zeng,X., J.A.Goetz, L.M.Suber, W.J.Scott, Jr., C.M.Schreiner, and D.J.Robbins. 2001. A freely diffusible form of Sonic hedgehog mediates long-range signalling. *Nature* 411:716-720.

22. Neumann,S., D.Y.Coudreuse, D.R.van der Westhuyzen, E.R.Eckhardt, H.C.Korswagen, G.Schmitz, and H.Sprong. 2009. Mammalian Wnt3a is released on lipoprotein particles. *Traffic.* 10:334-343.

23. Lin,X. 2004. Functions of heparan sulfate proteoglycans in cell signaling during development. *Development* 131:6009-6021.

24. Bhanot,P., M.Brink, C.H.Samos, J.C.Hsieh, Y.Wang, J.P.Macke, D.Andrew, J.Nathans, and R.Nusse. 1996. A new member of the frizzled family from Drosophila functions as a Wingless receptor. *Nature* 382:225-230.

25. Dann,C.E., J.C.Hsieh, A.Rattner, D.Sharma, J.Nathans, and D.J.Leahy. 2001. Insights into Wnt binding and signalling from the structures of two Frizzled cysteine-rich domains. *Nature* 412:86-90.

26. Povelones,M. and R.Nusse. 2005. The role of the cysteine-rich domain of Frizzled in Wingless-Armadillo signaling. *EMBO J.* 24:3493-3503.

27. Chen,C.M., W.Strapps, A.Tomlinson, and G.Struhl. 2004. Evidence that the cysteine-rich domain of Drosophila Frizzled family receptors is dispensable for transducing Wingless. *Proc.Natl.Acad.Sci.U.S.A.* 101:15961-15966.

28. Yamamoto,A., T.Nagano, S.Takehara, M.Hibi, and S.Aizawa. 2005. Shisa promotes head formation through the inhibition of receptor protein maturation for the caudalizing factors, Wnt and FGF. *Cell* 120:223-235.

29. Rulifson,E.J., C.H.Wu, and R.Nusse. 2000. Pathway specificity by the bifunctional receptor frizzled is determined by affinity for wingless. *Mol.Cell* 6:117-126.

30. Schulte,G. and V.Bryja. 2007. The Frizzled family of unconventional G-protein-coupled receptors. *Trends Pharmacol.Sci.* 28:518-525.

31. Wong,H.C., A.Bourdelas, A.Krauss, H.J.Lee, Y.Shao, D.Wu, M.Mlodzik, D.L.Shi, and J.Zheng. 2003. Direct binding of the PDZ domain of Dishevelled to a conserved internal sequence in the C-terminal region of Frizzled. *Mol.Cell* 12:1251-1260.

32. Foord,S.M., T.I.Bonner, R.R.Neubig, E.M.Rosser, J.P.Pin, A.P.Davenport, M.Spedding, and A.J.Harmar. 2005. International Union of Pharmacology. XLVI. G protein-coupled receptor list. *Pharmacol.Rev.* 57:279-288.

33. Katanaev,V.L., R.Ponzielli, M.Semeriva, and A.Tomlinson. 2005. Trimeric G protein-dependent frizzled signaling in Drosophila. *Cell* 120:111-122.

34. Bikkavilli,R.K., M.E.Feigin, and C.C.Malbon. 2008. G alpha o mediates WNT-JNK signaling through dishevelled 1 and 3, RhoA family members, and MEKK 1 and 4 in mammalian cells. *J.Cell Sci.* 121:234-245.

35. Liu,X., J.S.Rubin, and A.R.Kimmel. 2005. Rapid, Wnt-induced changes in GSK3beta associations that regulate beta-catenin stabilization are mediated by Galpha proteins. *Curr.Biol.* 15:1989-1997.

36. Slusarski,D.C., V.G.Corces, and R.T.Moon. 1997. Interaction of Wnt and a Frizzled homologue triggers G-protein-linked phosphatidylinositol signalling. *Nature* 390:410-413.

37. Liu,X., T.Liu, D.C.Slusarski, J.Yang-Snyder, C.C.Malbon, R.T.Moon, and H.Wang. 1999. Activation of a frizzled-2/beta-adrenergic receptor chimera promotes Wnt signaling and differentiation of mouse F9 teratocarcinoma cells via Galphao and Galphat. *Proc.Natl.Acad.Sci.U.S.A* 96:14383-14388.

38. Liu,T., X.Liu, H.Wang, R.T.Moon, and C.C.Malbon. 1999. Activation of rat frizzled-1 promotes Wnt signaling and differentiation of mouse F9 teratocarcinoma cells via pathways that require Galpha(q) and Galpha(o) function. *J.Biol.Chem.* 274:33539-33544.

39. Kikuchi A, Yamamoto H, and Kishida S. 2006. Multiplicity of the interactions of Wnt proteins and their receptors. *Cell Signal.* 19:659-71.

40. Sheldahl,L.C., D.C.Slusarski, P.Pandur, J.R.Miller, M.Kuhl, and R.T.Moon. 2003. Dishevelled activates Ca2+ flux, PKC, and CamKII in vertebrate embryos. *J.Cell Biol.* 161:769-777.

41. Gwak,J., M.Cho, S.J.Gong, J.Won, D.E.Kim, E.Y.Kim, S.S.Lee, M.Kim, T.K.Kim, J.G.Shin, and S.Oh. 2006. Protein-kinase-C-mediated beta-catenin phosphorylation negatively regulates the Wnt/beta-catenin pathway. *J.Cell Sci.* 119:4702-4709.

42. Saneyoshi,T., S.Kume, Y.Amasaki, and K.Mikoshiba. 2002. The Wnt/calcium pathway activates NF-AT and promotes ventral cell fate in Xenopus embryos. *Nature* 417:295-299.

43. Ishitani,T., S.Kishida, J.Hyodo-Miura, N.Ueno, J.Yasuda, M.Waterman, H.Shibuya, R.T.Moon, J.Ninomiya-Tsuji, and K.Matsumoto. 2003. The TAK1-NLK mitogen-activated protein kinase cascade functions in the Wnt-5a/Ca(2+) pathway to antagonize Wnt/beta-catenin signaling. *Mol.Cell Biol.* 23:131-139.

44. Adhikari,A., M.Xu, and Z.J.Chen. 2007. Ubiquitin-mediated activation of TAK1 and IKK. *Oncogene* 26:3214-3226.

45. Veeman,M.T., J.D.Axelrod, and R.T.Moon. 2003. A second canon. Functions and mechanisms of beta-catenin-independent Wnt signaling. *Dev.Cell.* 5:367-377.

46. Pereira,C., D.J.Schaer, E.B.Bachli, M.O.Kurrer, and G.Schoedon. 2008. Wnt5A/CaMKII signaling contributes to the inflammatory response of macrophages and is a target for the antiinflammatory action of activated protein C and interleukin-10. *Arterioscler.Thromb.Vasc.Biol.* 28:504-510.

47. Ghosh,M.C., G.D.Collins, B.Vandanmagsar, K.Patel, M.Brill, A.Carter, A.Lustig, K.G.Becker, W.W.Wood, III, C.D.Emeche, A.D.French, M.P.O'Connell, M.Xu, A.T.Weeraratna, and D.D.Taub. 2009. Activation of Wnt5A signaling is required for CXCL12-mediated T-cell migration. *Blood 114:1366-1373*.

48. Seifert,J.R. and M.Mlodzik. 2007. Frizzled/PCP signalling: a conserved mechanism regulating cell polarity and directed motility. *Nat.Rev.Genet.* 8:126-138.

49. Kohn,A.D. and R.T.Moon. 2005. Wnt and calcium signaling: beta-catenin-independent pathways. *Cell Calcium.* 38:439-446.

50. Unterseher,F., J.A.Hefele, K.Giehl, E.M.De Robertis, D.Wedlich, and A.Schambony. 2004. Paraxial protocadherin coordinates cell polarity during convergent extension via Rho A and JNK. *EMBO J.* 23:3259-3269.

51. Oishi,I., H.Suzuki, N.Onishi, R.Takada, S.Kani, B.Ohkawara, I.Koshida, K.Suzuki, G.Yamada, G.C.Schwabe, S.Mundlos, H.Shibuya, S.Takada, and Y.Minami. 2003. The receptor tyrosine kinase Ror2 is involved in non-canonical Wnt5a/JNK signalling pathway. *Genes Cells* 8:645-654.

52. Inoue,T., H.S.Oz, D.Wiland, S.Gharib, R.Deshpande, R.J.Hill, W.S.Katz, and P.W.Sternberg. 2004. C. elegans LIN-18 is a Ryk ortholog and functions in parallel to LIN-17/Frizzled in Wnt signaling. *Cell* 118:795-806.

53. Yoshikawa,S., R.D.McKinnon, M.Kokel, and J.B.Thomas. 2003. Wnt-mediated axon guidance via the Drosophila Derailed receptor. *Nature* 422:583-588.

54. Yao,R., T.Maeda, S.Takada, and T.Noda. 2001. Identification of a PDZ domain containing Golgi protein, GOPC, as an interaction partner of frizzled. *Biochem.Biophys.Res.Commun.* 286:771-778.

55. Gao,Y. and H.Y.Wang. 2006. Casein kinase 2 Is activated and essential for Wnt/beta-catenin signaling. *J.Biol.Chem.* 281:18394-18400.

56. Wang,Z., W.Shu, M.M.Lu, and E.E.Morrisey. 2005. Wnt7b activates canonical signaling in epithelial and vascular smooth muscle cells through interactions with Fzd1, Fzd10, and LRP5. *Mol.Cell Biol.* 25:5022-5030.

57. Liu,T., A.J.DeCostanzo, X.Liu, H.Wang, S.Hallagan, R.T.Moon, and C.C.Malbon. 2001. G protein signaling from activated rat frizzled-1 to the beta-catenin-Lef-Tcf pathway. *Science* 292:1718-1722.

58. Cong,F., L.Schweizer, and H.Varmus. 2004. Wnt signals across the plasma membrane to activate the beta-catenin pathway by forming oligomers containing its receptors, Frizzled and LRP. *Development.* 131:5103-5115.

59. Liu,T., X.Liu, H.Wang, R.T.Moon, and C.C.Malbon. 1999. Activation of rat frizzled-1 promotes Wnt signaling and differentiation of mouse F9 teratocarcinoma cells via pathways that require Galpha(q) and Galpha(o) function. *J.Biol.Chem.* 274:33539-33544.

60. DELTAGEN knockout mice phenotypic data summary. http://www.informatics.jax.org/external/ko/deltagen/670.html.

61. van Amerongen,R. and A.Berns. 2006. Knockout mouse models to study Wnt signal transduction. *Trends Genet.* 22:678-689.

62. Chan,S.D., D.B.Karpf, M.E.Fowlkes, M.Hooks, M.S.Bradley, V.Vuong, T.Bambino, M.Y.Liu, C.D.Arnaud, G.J.Strewler, and . 1992. Two homologs of the Drosophila polarity gene frizzled (fz) are widely expressed in mammalian tissues. *J.Biol.Chem.* 267:25202-25207.

63. Kulkarni,N.H., D.L.Halladay, R.R.Miles, L.M.Gilbert, C.A.Frolik, R.J.Galvin, T.J.Martin, M.T.Gillespie, and J.E.Onyia. 2005. Effects of parathyroid hormone on Wnt signaling pathway in bone. *J.Cell Biochem.* 95:1178-1190.

64. Roman-Roman,S., D.L.Shi, V.Stiot, E.Hay, B.Vayssiere, T.Garcia, R.Baron, and G.Rawadi. 2004. Murine Frizzled-1 behaves as an antagonist of the canonical Wnt/beta-catenin signaling. *J.Biol.Chem.* 279:5725-5733.

65. Yang,L., K.Yamasaki, Y.Shirakata, X.Dai, S.Tokumaru, Y.Yahata, M.Tohyama, Y.Hanakawa, K.Sayama, and K.Hashimoto. 2006. Bone morphogenetic protein-2 modulates Wnt and frizzled expression and enhances the canonical pathway of Wnt signaling in normal keratinocytes. *J.Dermatol.Sci.* 42:111-119.

66. Zerlin,M., M.A.Julius, and J.Kitajewski. 2008. Wnt/Frizzled signaling in angiogenesis. *Angiogenesis.* 11:63-69.

67. Hsieh,M., M.A.Johnson, N.M.Greenberg, and J.S.Richards. 2002. Regulated expression of Wnts and Frizzleds at specific stages of follicular development in the rodent ovary. *Endocrinology.* 143:898-908.

68. Ferrell,C.M., S.T.Dorsam, H.Ohta, R.K.Humphries, M.K.Derynck, C.Haqq, C.Largman, and H.J.Lawrence. 2005. Activation of stem-cell specific genes by HOXA9 and HOXA10 homeodomain proteins in CD34+ human cord blood cells. *Stem Cells* 23:644-655.

69. Milovanovic,T., K.Planutis, A.Nguyen, J.L.Marsh, F.Lin, C.Hope, and R.F.Holcombe. 2004. Expression of Wnt genes and frizzled 1 and 2 receptors in normal breast epithelium and infiltrating breast carcinoma. *Int.J.Oncol.* 25:1337-1342.

70. Holcombe,R.F., J.L.Marsh, M.L.Waterman, F.Lin, T.Milovanovic, and T.Truong. 2002. Expression of Wnt ligands and Frizzled receptors in colonic mucosa and in colon carcinoma. *Mol.Pathol.* 55:220-226.

71. You,X.J., P.J.Bryant, F.Jurnak, and R.F.Holcombe. 2007. Expression of Wnt pathway components frizzled and disheveled in colon cancer arising in patients with inflammatory bowel disease. *Oncol.Rep.* 18:691-694.

72. Chacon,M.A., L.Varela-Nallar, and N.C.Inestrosa. 2008. Frizzled-1 is involved in the neuroprotective effect of Wnt3a against Abeta oligomers. *J.Cell Physiol.* 217:215-227.

73. Haegel,H., L.Larue, M.Ohsugi, L.Fedorov, K.Herrenknecht, and R.Kemler. 1995. Lack of beta-catenin affects mouse development at gastrulation. *Development* 121:3529-3537.

74. Huelsken,J., R.Vogel, V.Brinkmann, B.Erdmann, C.Birchmeier, and W.Birchmeier. 2000. Requirement for beta-catenin in anterior-posterior axis formation in mice. *J.Cell Biol.* 148:567-578.

75. Schneider,S., H.Steinbeisser, R.M.Warga, and P.Hausen. 1996. Beta-catenin translocation into nuclei demarcates the dorsalizing centers in frog and fish embryos. *Mech.Dev.* 57:191-198.

76. Grigoryan,T., P.Wend, A.Klaus, and W.Birchmeier. 2008. Deciphering the function of canonical Wnt signals in development and disease: conditional loss- and gain-of-function mutations of beta-catenin in mice. *Genes Dev.* 22:2308-2341.

77. Cardoso,W.V. and J.Lu. 2006. Regulation of early lung morphogenesis: questions, facts and controversies. *Development* 133:1611-1624.

78. Logan,C.Y. and R.Nusse. 2004. The Wnt signaling pathway in development and disease. *Annu.Rev.Cell Dev.Biol.* 20:781-810.

79. Hill,T.P., M.M.Taketo, W.Birchmeier, and C.Hartmann. 2006. Multiple roles of mesenchymal beta-catenin during murine limb patterning. *Development* 133:1219-1229.

80. Strigini,M. and S.M.Cohen. 2000. Wingless gradient formation in the Drosophila wing. *Curr.Biol.* 10:293-300.

81. Neumann,C. and S.Cohen. 1997. Morphogens and pattern formation. *Bioessays* 19:721-729.

82. Staal,F.J. and J.M.Sen. 2008. The canonical Wnt signaling pathway plays an important role in lymphopoiesis and hematopoiesis. *Eur.J.Immunol.* 38:1788-1794.

83. Reya,T. and H.Clevers. 2005. Wnt signalling in stem cells and cancer. *Nature* 434:843-850.

84. Westendorf,J.J., R.A.Kahler, and T.M.Schroeder. 2004. Wnt signaling in osteoblasts and bone diseases. *Gene* 341:19-39.

85. Nusse R. (http://www.stanford.edu/~rnusse/wntwindow.html).

86. Takahashi,K. and S.Yamanaka. 2006. Induction of pluripotent stem cells from mouse embryonic and adult fibroblast cultures by defined factors. *Cell* 126:663-676.

87. Takahashi,K., K.Tanabe, M.Ohnuki, M.Narita, T.Ichisaka, K.Tomoda, and S.Yamanaka. 2007. Induction of pluripotent stem cells from adult human fibroblasts by defined factors. *Cell* 131:861-872.

88. Ling,L., V.Nurcombe, and S.M.Cool. 2009. Wnt signaling controls the fate of mesenchymal stem cells. *Gene* 433:1-7.

89. Le Blanc,K. and O.Ringden. 2005. Immunobiology of human mesenchymal stem cells and future use in hematopoietic stem cell transplantation. *Biol.Blood Marrow Transplant.* 11:321-334.

90. Dazzi,F., R.Ramasamy, S.Glennie, S.P.Jones, and I.Roberts. 2006. The role of mesenchymal stem cells in haemopoiesis. *Blood Rev.* 20:161-171.

91. Staal,F.J., T.C.Luis, and M.M.Tiemessen. 2008. WNT signalling in the immune system: WNT is spreading its wings. *Nat.Rev.Immunol.* 8:581-593.

92. Yang,S.H., M.J.Park, I.H.Yoon, S.Y.Kim, S.H.Hong, J.Y.Shin, H.Y.Nam, Y.H.Kim, B.Kim, and C.G.Park. 2009. Soluble mediators from mesenchymal stem cells suppress T cell proliferation by inducing IL-10. *Exp.Mol.Med.* 41:315-324.

93. Andoh,A., S.Bamba, M.Brittan, Y.Fujiyama, and N.A.Wright. 2007. Role of intestinal subepithelial myofibroblasts in inflammation and regenerative response in the gut. *Pharmacol.Ther.* 114:94-106.

94. Thiele,A., M.Wasner, C.Müller, K.Engeland, and S.Hauschildt. 2001. Regulation and possible function of beta-catenin in human monocytes. *J.Immunol.* 167:6786-6793.

95. Monick,M.M., A.B.Carter, P.K.Robeff, D.M.Flaherty, M.W.Peterson, and G.W.Hunninghake. 2001. Lipopolysaccharide activates Akt in human alveolar macrophages resulting in nuclear accumulation and transcriptional activity of beta-catenin. *J.Immunol.* 166:4713-4720.

96. Beutler,B. and E.T.Rietschel. 2003. Innate immune sensing and its roots: the story of endotoxin. *Nat.Rev.Immunol.* 3:169-176.

97. Lee MS and Kim YJ. 2007. Signaling pathways downstream of pattern-recognition receptors and their cross talk. *Annu.Rev.Biochem.* 76:447-80.

98. Schlesinger,L.S., C.G.Bellinger-Kawahara, N.R.Payne, and M.A.Horwitz. 1990. Phagocytosis of Mycobacterium tuberculosis is mediated by human monocyte complement receptors and complement component C3. *J.Immunol.* 144:2771-2780.

99. Taylor,P.R., L.Martinez-Pomares, M.Stacey, H.H.Lin, G.D.Brown, and S.Gordon. 2005. Macrophage receptors and immune recognition. *Annu.Rev.Immunol.* 23:901-44.

100. Siren,J., T.Imaizumi, D.Sarkar, T.Pietila, D.L.Noah, R.Lin, J.Hiscott, R.M.Krug, P.B.Fisher, I.Julkunen, and S.Matikainen. 2006. Retinoic acid inducible gene-I and mda-5 are involved in influenza A virus-induced expression of antiviral cytokines. *Microbes.Infect.* 8:2013-2020.

101. Kaparakis,M., D.J.Philpott, and R.L.Ferrero. 2007. Mammalian NLR proteins; discriminating foe from friend. *Immunol.Cell Biol.* 85:495-502.

102. Lee,M.S. and Y.J.Kim. 2007. Signaling pathways downstream of pattern-recognition receptors and their cross talk. *Annu.Rev.Biochem.* 76:447-480.

103. Tenor,J.L. and A.Aballay. 2008. A conserved Toll-like receptor is required for Caenorhabditis elegans innate immunity. *EMBO Rep.* 9:103-109.

104. Akira,S., S.Uematsu, and O.Takeuchi. 2006. Pathogen recognition and innate immunity. *Cell* 124:783-801.

105. Beutler,B. 2004. Inferences, questions and possibilities in Toll-like receptor signalling. *Nature* 430:257-263.

106. Ozinsky,A., D.M.Underhill, J.D.Fontenot, A.M.Hajjar, K.D.Smith, C.B.Wilson, L.Schroeder, and A.Aderem. 2000. The repertoire for pattern recognition of pathogens by the innate immune system is defined by cooperation between toll-like receptors. *Proc.Natl.Acad.Sci.U.S.A* 97:13766-13771.

107. Gilleron,M., V.F.Quesniaux, and G.Puzo. 2003. Acylation state of the phosphatidylinositol hexamannosides from Mycobacterium bovis bacillus Calmette Guerin and mycobacterium tuberculosis H37Rv and its implication in Toll-like receptor response. *J.Biol.Chem.* 278:29880-29889.

108. Schröder,N.W., S.Morath, C.Alexander, L.Hamann, T.Hartung, U.Zähringer, U.B.Gobel, J.R.Weber, and R.R.Schumann. 2003. Lipoteichoic acid (LTA) of Streptococcus pneumoniae and Staphylococcus aureus activates immune cells via Toll-like receptor (TLR)-2, lipopolysaccharide-binding protein (LBP), and CD14, whereas TLR-4 and MD-2 are not involved. *J.Biol.Chem.* 278:15587-15594.

109. Becker,I., N.Salaiza, M.Aguirre, J.Delgado, N.Carrillo-Carrasco, L.G.Kobeh, A.Ruiz, R.Cervantes, A.P.Torres, N.Cabrera, A.Gonzalez, C.Maldonado, and A.Isibasi. 2003. Leishmania lipophosphoglycan (LPG) activates NK cells through toll-like receptor-2. *Mol.Biochem.Parasitol.* 130:65-74.

110. Underhill,D.M., A.Ozinsky, A.M.Hajjar, A.Stevens, C.B.Wilson, M.Bassetti, and A.Aderem. 1999. The Toll-like receptor 2 is recruited to macrophage phagosomes and discriminates between pathogens. *Nature* 401:811-815.

111. Aliprantis,A.O., R.B.Yang, M.R.Mark, S.Suggett, B.Devaux, J.D.Radolf, G.R.Klimpel, P.Godowski, and A.Zychlinsky. 1999. Cell activation and apoptosis by bacterial lipoproteins through toll-like receptor-2. *Science* 285:736-739.

112. Bessler,W., K.Resch, E.Hancock, and K.Hantke. 1977. Induction of lymphocyte proliferation and membrane changes by lipopeptide derivatives of the lipoprotein from the outer membrane of Escherichia coli. *Z.Immunitatsforsch.Immunobiol.* 153:11-22.

113. Zähringer,U., B.Lindner, S.Inamura, H.Heine, and C.Alexander. 2008. TLR2 - promiscuous or specific? A critical re-evaluation of a receptor expressing apparent broad specificity. *Immunobiology* 213:205-224.

114. Travassos,L.H., S.E.Girardin, D.J.Philpott, D.Blanot, M.A.Nahori, C.Werts, and I.G.Boneca. 2004. Toll-like receptor 2-dependent bacterial sensing does not occur via peptidoglycan recognition. *EMBO Rep.* 5:1000-1006.

115. Takada,H., Y.Kawabata, R.Arakaki, S.Kusumoto, K.Fukase, Y.Suda, T.Yoshimura, S.Kokeguchi, K.Kato, T.Komuro, and . 1995. Molecular and structural requirements of a lipoteichoic acid from Enterococcus hirae ATCC 9790 for cytokine-inducing, antitumor, and antigenic activities. *Infect.Immun.* 63:57-65.

116. Jin,M.S., S.E.Kim, J.Y.Heo, M.E.Lee, H.M.Kim, S.G.Paik, H.Lee, and J.O.Lee. 2007. Crystal structure of the TLR1-TLR2 heterodimer induced by binding of a tri-acylated lipopeptide. *Cell* 130:1071-1082.

117. Alexander,C. and E.T.Rietschel. 2001. Bacterial lipopolysaccharides and innate immunity. *J.Endotoxin.Res.* 7:167-202.

118. Barton,G.M. and R.Medzhitov. 2003. Toll-like receptor signaling pathways. *Science* 300:1524-1525.

119. Gay,N.J., M.Gangloff, and A.N.Weber. 2006. Toll-like receptors as molecular switches. *Nat.Rev.Immunol.* 6:693-698.

120. Kawai,T. and S.Akira. 2006. TLR signaling. *Cell Death.Differ.* 13:816-825.

121. Chen,Z.J., V.Bhoj, and R.B.Seth. 2006. Ubiquitin, TAK1 and IKK: is there a connection? *Cell Death.Differ.* 13:687-692.

122. Wirth,T., F.Hildebrand, C.Allix-Beguec, F.Wolbeling, T.Kubica, K.Kremer, D.van Soolingen, S.Rusch-Gerdes, C.Locht, S.Brisse, A.Meyer, P.Supply, and

S.Niemann. 2008. Origin, spread and demography of the Mycobacterium tuberculosis complex. *PLoS.Pathog.* 4:e1000160.

123. Glassroth,J. 2008. Pulmonary disease due to nontuberculous mycobacteria. *Chest* 133:243-251.

124. Horsburgh,C.R., Jr. 1996. Epidemiology of disease caused by nontuberculous mycobacteria. *Semin.Respir.Infect.* 11:244-251.

125. Parrish,S.C., J.Myers, and A.Lazarus. 2008. Nontuberculous mycobacterial pulmonary infections in Non-HIV patients. *Postgrad.Med.* 120:78-86.

126. NTM Info & Research, Inc. http://www.ntminfo.org.

127. Ridley,M.J., C.J.Heather, I.Brown, and D.A.Willoughby. 1983. Experimental epithelioid cell granulomas, tubercle formation and immunological competence: an ultrastructural analysis. *J.Pathol.* 141:97-112.

128. Egen,J.G., A.G.Rothfuchs, C.G.Feng, N.Winter, A.Sher, and R.N.Germain. 2008. Macrophage and T cell dynamics during the development and disintegration of mycobacterial granulomas. *Immunity.* 28:271-284.

129. Flynn,J.L., M.M.Goldstein, J.Chan, K.J.Triebold, K.Pfeffer, C.J.Lowenstein, R.Schreiber, T.W.Mak, and B.R.Bloom. 1995. Tumor necrosis factor-alpha is required in the protective immune response against Mycobacterium tuberculosis in mice. *Immunity.* 2:561-572.

130. Lin,P.L., H.L.Plessner, N.N.Voitenok, and J.L.Flynn. 2007. Tumor necrosis factor and tuberculosis. *J.Investig.Dermatol.Symp.Proc.* 12:22-25.

131. Flynn,J.L. and J.Chan. 2001. Immunology of tuberculosis. *Annu.Rev.Immunol.* 19:93-129.

132. Grosset,J. 2003. Mycobacterium tuberculosis in the extracellular compartment: an underestimated adversary. *Antimicrob.Agents Chemother.* 47:833-836.

133. Pieters,J. 2001. Entry and survival of pathogenic mycobacteria in macrophages. *Microbes.Infect.* 3:249-255.

134. Zhang,Y., M.Doerfler, T.C.Lee, B.Guillemin, and W.N.Rom. 1993. Mechanisms of stimulation of interleukin-1 beta and tumor necrosis factor-alpha by Mycobacterium tuberculosis components. *J.Clin.Invest.* 91:2076-2083.

135. Rom,W.N., N.Schluger, K.Law, R.Condos, Y.Zhang, M.Weiden, T.Harkin, and K.M.Tchou-Wong. 1995. Human host response to Mycobacterium tuberculosis. *Schweiz.Med.Wochenschr.* 125:2178-2185.

136. Osborn,L. 1990. Leukocyte adhesion to endothelium in inflammation. *Cell* 62:3-6.

137. Bevilacqua,M.P. 1993. Endothelial-leukocyte adhesion molecules. *Annu.Rev.Immunol.* 11:767-804.

138. Luster,A.D. 1998. Chemokines--chemotactic cytokines that mediate inflammation. *N.Engl.J.Med.* 338:436-445.

139. Peters,W., H.M.Scott, H.F.Chambers, J.L.Flynn, I.F.Charo, and J.D.Ernst. 2001. Chemokine receptor 2 serves an early and essential role in resistance to Mycobacterium tuberculosis. *Proc.Natl.Acad.Sci.U.S.A* 98:7958-7963.

140. Hölscher,C. 2004. The power of combinatorial immunology: IL-12 and IL-12-related dimeric cytokines in infectious diseases. *Med.Microbiol.Immunol.* 193:1-17.

141. Caruso,A.M., N.Serbina, E.Klein, K.Triebold, B.R.Bloom, and J.L.Flynn. 1999. Mice deficient in CD4 T cells have only transiently diminished levels of IFN-gamma, yet succumb to tuberculosis. *J.Immunol.* 162:5407-5416.

142. Scanga,C.A., V.P.Mohan, K.Yu, H.Joseph, K.Tanaka, J.Chan, and J.L.Flynn. 2000. Depletion of CD4(+) T cells causes reactivation of murine persistent tuberculosis despite continued expression of interferon gamma and nitric oxide synthase 2. *J.Exp.Med.* 192:347-358.

143. Cooper,A.M., D.K.Dalton, T.A.Stewart, J.P.Griffin, D.G.Russell, and I.M.Orme. 1993. Disseminated tuberculosis in interferon gamma gene-disrupted mice. *J.Exp.Med.* 178:2243-2247.

144. Flynn,J.L., J.Chan, K.J.Triebold, D.K.Dalton, T.A.Stewart, and B.R.Bloom. 1993. An essential role for interferon gamma in resistance to Mycobacterium tuberculosis infection. *J.Exp.Med.* 178:2249-2254.

145. Ding,A.H., C.F.Nathan, and D.J.Stuehr. 1988. Release of reactive nitrogen intermediates and reactive oxygen intermediates from mouse peritoneal macrophages. Comparison of activating cytokines and evidence for independent production. *J.Immunol.* 141:2407-2412.

146. Nathan,C. and M.U.Shiloh. 2000. Reactive oxygen and nitrogen intermediates in the relationship between mammalian hosts and microbial pathogens. *Proc.Natl.Acad.Sci.U.S.A* 97:8841-8848.

147. MacMicking,J.D., R.J.North, R.LaCourse, J.S.Mudgett, S.K.Shah, and C.F.Nathan. 1997. Identification of nitric oxide synthase as a protective locus against tuberculosis. *Proc.Natl.Acad.Sci.U.S.A* 94:5243-5248.

148. Harris,J., S.A.De Haro, S.S.Master, J.Keane, E.A.Roberts, M.Delgado, and V.Deretic. 2007. T helper 2 cytokines inhibit autophagic control of intracellular Mycobacterium tuberculosis. *Immunity.* 27:505-517.

149. Gutierrez,M.G., S.S.Master, S.B.Singh, G.A.Taylor, M.I.Colombo, and V.Deretic. 2004. Autophagy is a defense mechanism inhibiting BCG and Mycobacterium tuberculosis survival in infected macrophages. *Cell* 119:753-766.

150. MacMicking,J.D., G.A.Taylor, and J.D.McKinney. 2003. Immune control of tuberculosis by IFN-gamma-inducible LRG-47. *Science* 302:654-659.

151. Sen,M., K.Lauterbach, H.El Gabalawy, G.S.Firestein, M.Corr, and D.A.Carson. 2000. Expression and function of wingless and frizzled homologs in rheumatoid arthritis. *Proc.Natl.Acad.Sci.U.S.A* 97:2791-2796.

152. Gordon,M.D., M.S.Dionne, D.S.Schneider, and R.Nusse. 2005. WntD is a feedback inhibitor of Dorsal/NF-kappaB in Drosophila development and immunity. *Nature.* 437:746-749.

153. Blumenthal,A., S.Ehlers, J.Lauber, J.Buer, C.Lange, T.Goldmann, H.Heine, E.Brandt, and N.Reiling. 2006. The Wingless homolog WNT5A and its receptor Frizzled-5 regulate inflammatory responses of human mononuclear cells induced by microbial stimulation. *Blood.* 108:965-973.

154. George,S.J. 2008. Wnt pathway: a new role in regulation of inflammation. *Arterioscler.Thromb.Vasc.Biol.* 28:400-402.

155. Hänsch,H.C., D.A.Smith, M.E.Mielke, H.Hahn, G.J.Bancroft, and S.Ehlers. 1996. Mechanisms of granuloma formation in murine Mycobacterium avium infection: the contribution of CD4+ T cells. *Int.Immunol.* 8:1299-1310.

156. Takeuchi,O., S.Sato, T.Horiuchi, K.Hoshino, K.Takeda, Z.Dong, R.L.Modlin, and S.Akira. 2002. Cutting edge: role of Toll-like receptor 1 in mediating immune response to microbial lipoproteins. *J.Immunol.* 169:10-14.

157. Pierce,J.W., R.Schoenleber, G.Jesmok, J.Best, S.A.Moore, T.Collins, and M.E.Gerritsen. 1997. Novel inhibitors of cytokine-induced IkappaBalpha phosphorylation and endothelial cell adhesion molecule expression show anti-inflammatory effects in vivo. *J.Biol.Chem.* 272:21096-21103.

158. Shibamoto,S., K.Higano, R.Takada, F.Ito, M.Takeichi, and S.Takada. 1998. Cytoskeletal reorganization by soluble Wnt-3a protein signalling. *Genes Cells* 3:659-670.

159. Kishida,M., S.Koyama, S.Kishida, K.Matsubara, S.Nakashima, K.Higano, R.Takada, S.Takada, and A.Kikuchi. 1999. Axin prevents Wnt-3a-induced accumulation of beta-catenin. *Oncogene* 18:979-985.

160. Austin,T.W., G.P.Solar, F.C.Ziegler, L.Liem, and W.Matthews. 1997. A role for the Wnt gene family in hematopoiesis: expansion of multilineage progenitor cells. *Blood* 89:3624-3635.

161. Boyum,A. 1968. Isolation of mononuclear cells and granulocytes from human blood. Isolation of monuclear cells by one centrifugation, and of granulocytes by combining centrifugation and sedimentation at 1 g. *Scand.J.Clin.Lab Invest Suppl.* 97:77-89.

162. Contreras,T.J., J.F.Jemionek, H.C.Stevenson, V.M.Hartwig, and A.S.Fauci. 1980. An improved technique for the negative selection of large numbers of human lymphocytes and monocytes by counterflow centrifugation--elutriation. *Cell Immunol.* 54:215-229.

163. Andreesen,R., J.Picht, and G.W.Lohr. 1983. Primary cultures of human blood-born macrophages grown on hydrophobic teflon membranes. *J.Immunol.Methods* 56:295-304.

164. Becker,S., M.K.Warren, and S.Haskill. 1987. Colony-stimulating factor-induced monocyte survival and differentiation into macrophages in serum-free cultures. *J.Immunol.* 139:3703-3709.

165. Gill,G.W., J.K.Frost, and K.A.Miller. 1974. A new formula for a half-oxidized hematoxylin solution that neither overstains nor requires differentiation. *Acta Cytol.* 18:300-311.

166. Taboas,J.O. and R.J.Ceremsak. 1967. A rapid hematoxylin and eosin stain. *Tech.Bull.Regist.Med.Technol.* 37:119-120.

167. Longnecker,D.S. 1966. A program for automated hematoxylin and eosin staining. *Am.J.Clin.Pathol.* 45:229.

168. Laemmli,U.K. 1970. Cleavage of structural proteins during the assembly of the head of bacteriophage T4. *Nature* 227:680-685.

169. Willems,E., L.Leyns, and J.Vandesompele. 2008. Standardization of real-time PCR gene expression data from independent biological replicates. *Anal.Biochem.* 379:127-129.

170. Nusse,R. 2005. Wnt signaling in disease and in development. *Cell Res.* 15:28-32.

171. Douglas,I.S., d.Diaz, V, R.A.Winn, and N.F.Voelkel. 2006. Beta-catenin in the fibroproliferative response to acute lung injury. *Am.J.Respir.Cell Mol.Biol.* 34:274-285.

172. Michels,C.E., H.E.Scales, K.A.Saunders, S.McGowan, F.Brombracher, J.Alexander, and C.E.Lawrence. 2009. Neither interleukin-4 receptor alpha expression on CD4+ T cells, or macrophages and neutrophils is required for protective immunity to Trichinella spiralis. *Immunology* 128:385-394.

173. Mucenski,M.L., S.E.Wert, J.M.Nation, D.E.Loudy, J.Huelsken, W.Birchmeier, E.E.Morrisey, and J.A.Whitsett. 2003. beta-Catenin is required for specification of proximal/distal cell fate during lung morphogenesis. *J.Biol.Chem.* 278:40231-40238.

174. Shu,W., S.Guttentag, Z.Wang, T.Andl, P.Ballard, M.M.Lu, S.Piccolo, W.Birchmeier, J.A.Whitsett, S.E.Millar, and E.E.Morrisey. 2005. Wnt/beta-catenin signaling acts upstream of N-myc, BMP4, and FGF signaling to regulate proximal-distal patterning in the lung. *Dev.Biol.* 283:226-239.

175. Mulugeta,S. and M.F.Beers. 2006. Surfactant protein C: its unique properties and emerging immunomodulatory role in the lung. *Microbes.Infect.* 8:2317-2323.

176. Rawlins,E.L., T.Okubo, Y.Xue, D.M.Brass, R.L.Auten, H.Hasegawa, F.Wang, and B.L.Hogan. 2009. The role of Scgb1a1+ Clara cells in the long-term

maintenance and repair of lung airway, but not alveolar, epithelium. *Cell Stem Cell* 4:525-534.

177. Rajagopal,J., T.J.Carroll, J.S.Guseh, S.A.Bores, L.J.Blank, W.J.Anderson, J.Yu, Q.Zhou, A.P.McMahon, and D.A.Melton. 2008. Wnt7b stimulates embryonic lung growth by coordinately increasing the replication of epithelium and mesenchyme. *Development* 135:1625-1634.

178. Hendrickx,M. and L.Leyns. 2008. Non-conventional Frizzled ligands and Wnt receptors. *Dev.Growth Differ.* 50:229-243.

179. Torday,J.S. and V.K.Rehan. 2007. The evolutionary continuum from lung development to homeostasis and repair. *Am.J.Physiol Lung Cell Mol.Physiol.* 292:608-611.

180. Jho,E.H., T.Zhang, C.Domon, C.K.Joo, J.N.Freund, and F.Costantini. 2002. Wnt/beta-catenin/Tcf signaling induces the transcription of Axin2, a negative regulator of the signaling pathway. *Mol.Cell Biol.* 22:1172-1183.

181. Russell,D.G. 2007. Who puts the tubercle in tuberculosis? *Nat.Rev.Microbiol.* 5:39-47.

182. Akira,S., S.Uematsu, and O.Takeuchi. 2006. Pathogen recognition and innate immunity. *Cell.* 124:783-801.

183. Ghosh,S. and M.S.Hayden. 2008. New regulators of NF-kappaB in inflammation. *Nat.Rev.Immunol.* 8:837-848.

184. Stuehr,D.J. and M.A.Marletta. 1985. Mammalian nitrate biosynthesis: mouse macrophages produce nitrite and nitrate in response to Escherichia coli lipopolysaccharide. *Proc.Natl.Acad.Sci.U.S.A* 82:7738-7742.

185. MacMicking,J., Q.W.Xie, and C.Nathan. 1997. Nitric oxide and macrophage function. *Annu.Rev.Immunol.* 15:323-50.:323-350.

186. Löwenstein,C.J. and E.Padalko. 2004. iNOS (NOS2) at a glance. *J.Cell Sci.* 117:2865-2867.

187. Kuhl,M., L.C.Sheldahl, M.Park, J.R.Miller, and R.T.Moon. 2000. The Wnt/Ca2+ pathway: a new vertebrate Wnt signaling pathway takes shape. *Trends Genet.* 16:279-283.

188. Kikuchi,A. and H.Yamamoto. 2008. Tumor formation due to abnormalities in the beta-catenin-independent pathway of Wnt signaling. *Cancer Sci.* 99:202-208.

189. Feigin,M.E. and C.C.Malbon. 2007. RGS19 regulates Wnt-beta-catenin signaling through inactivation of Galpha(o). *J.Cell Sci.* 120:3404-3414.

190. Liu,T., A.J.DeCostanzo, X.Liu, H.Wang, S.Hallagan, R.T.Moon, and C.C.Malbon. 2001. G protein signaling from activated rat frizzled-1 to the beta-catenin-Lef-Tcf pathway. *Science.* 292:1718-1722.

191. Flahaut,M., R.Meier, A.Coulon, K.A.Nardou, F.K.Niggli, D.Martinet, J.S.Beckmann, J.M.Joseph, A.Muhlethaler-Mottet, and N.Gross. 2009. The Wnt receptor FZD1 mediates chemoresistance in neuroblastoma through activation of the Wnt/beta-catenin pathway. *Oncogene*. 28:2245-2256.

192. Mosser,D.M. 1994. Receptors on phagocytic cells involved in microbial recognition. *Immunol.Ser.* 60:99-114.

193. Benoit,M., B.Desnues, and J.L.Mege. 2008. Macrophage polarization in bacterial infections. *J.Immunol.* 181:3733-3739.

194. Gordon,S. 2003. Alternative activation of macrophages. *Nat.Rev.Immunol.* 3:23-35.

195. Lewis,C.C., J.Y.Yang, X.Huang, S.K.Banerjee, M.R.Blackburn, P.Baluk, D.M.McDonald, T.S.Blackwell, V.Nagabhushanam, W.Peters, D.Voehringer, and D.J.Erle. 2008. Disease-specific gene expression profiling in multiple models of lung disease. *Am.J.Respir.Crit Care Med.* 177:376-387.

196. Warner,R.L., C.S.Lewis, L.Beltran, E.M.Younkin, J.Varani, and K.J.Johnson. 2001. The role of metalloelastase in immune complex-induced acute lung injury. *Am.J.Pathol.* 158:2139-2144.

197. Gibbs,D.F., T.P.Shanley, R.L.Warner, H.S.Murphy, J.Varani, and K.J.Johnson. 1999. Role of matrix metalloproteinases in models of macrophage-dependent acute lung injury. Evidence for alveolar macrophage as source of proteinases. *Am.J.Respir.Cell Mol.Biol.* 20:1145-1154.

198. Mukhopadhyay,S., J.R.Hoidal, and T.K.Mukherjee. 2006. Role of TNFalpha in pulmonary pathophysiology. *Respir.Res.* 7:125.:125.

199. Kotton,D.N. and A.Fine. 2008. Lung stem cells. *Cell Tissue Res.* 331:145-156.

200. Wu B, Crampton SP, and Hughes CC. 2007. Wnt signaling induces matrix metalloproteinase expression and regulates T cell transmigration. *Immunity.* 26:227-39.

201. Schaefer,M., N.Reiling, C.Fessler, J.Stephani, I.Taniuchi, F.Hatam, A.O.Yildirim, H.Fehrenbach, K.Walter, J.Ruland, H.Wagner, S.Ehlers, and T.Sparwasser. 2008. Decreased pathology and prolonged survival of human DC-SIGN transgenic mice during mycobacterial infection. *J.Immunol.* 180:6836-6845.

202. Roach,D.R., A.G.Bean, C.Demangel, M.P.France, H.Briscoe, and W.J.Britton. 2002. TNF regulates chemokine induction essential for cell recruitment, granuloma formation, and clearance of mycobacterial infection. *J.Immunol.* 168:4620-4627.

203. Aoki,K. and M.M.Taketo. 2008. Tissue-specific transgenic, conditional knockout and knock-in mice of genes in the canonical Wnt signaling pathway. *Methods Mol.Biol.* 468:307-331.

204. Deutscher,E. and Y.H.Hung-Chang. 2007. Essential roles of mesenchyme-derived beta-catenin in mouse Müllerian duct morphogenesis. *Dev.Biol.* 307:227-236.

205. De Langhe,S.P., G.Carraro, D.Tefft, C.Li, X.Xu, Y.Chai, P.Minoo, M.K.Hajihosseini, J.Drouin, V.Kaartinen, and S.Bellusci. 2008. Formation and differentiation of multiple mesenchymal lineages during lung development is regulated by beta-catenin signaling. *PLoS.ONE.* 3:1516.

206. Lattin,J.E., K.Schröder, A.I.Su, J.R.Walker, J.Zhang, T.Wiltshire, K.Saijo, C.K.Glass, D.A.Hume, S.Kellie, and M.J.Sweet. 2008. Expression analysis of G Protein-Coupled Receptors in mouse macrophages. *Immunome.Res.* 4:5.

207. Mao,C., O.T.Malek, M.E.Pueyo, P.G.Steg, and F.Soubrier. 2000. Differential expression of rat frizzled-related frzb-1 and frizzled receptor fz1 and fz2 genes in the rat aorta after balloon injury. *Arterioscler.Thromb.Vasc.Biol.* 20:43-51.

208. Iwasaki,A. and R.Medzhitov. 2004. Toll-like receptor control of the adaptive immune responses. *Nat.Immunol.* 5:987-995.

209. Meylan,E., K.Burns, K.Hofmann, V.Blancheteau, F.Martinon, M.Kelliher, and J.Tschopp. 2004. RIP1 is an essential mediator of Toll-like receptor 3-induced NF-kappa B activation. *Nat.Immunol.* 5:503-507.

210. Jang,S., S.Uematsu, S.Akira, and P.Salgame. 2004. IL-6 and IL-10 induction from dendritic cells in response to Mycobacterium tuberculosis is predominantly dependent on TLR2-mediated recognition. *J.Immunol.* 173:3392-3397.

211. Shi,S., A.Blumenthal, C.M.Hickey, S.Gandotra, D.Levy, and S.Ehrt. 2005. Expression of many immunologically important genes in Mycobacterium tuberculosis-infected macrophages is independent of both TLR2 and TLR4 but dependent on IFN-alphabeta receptor and STAT1. *J.Immunol.* 175:3318-3328.

212. Fremond,C.M., D.Togbe, E.Doz, S.Rose, V.Vasseur, I.Maillet, M.Jacobs, B.Ryffel, and V.F.Quesniaux. 2007. IL-1 receptor-mediated signal is an essential component of MyD88-dependent innate response to Mycobacterium tuberculosis infection. *J.Immunol.* 179:1178-1189.

213. Hölscher,C., N.Reiling, U.E.Schaible, A.Hölscher, C.Bathmann, D.Korbel, I.Lenz, T.Sonntag, S.Kröger, S.Akira, H.Mossmann, C.J.Kirschning, H.Wagner, M.Freudenberg, and S.Ehlers. 2008. Containment of aerogenic Mycobacterium tuberculosis infection in mice does not require MyD88 adaptor function for TLR2, -4 and -9. *Eur.J.Immunol.* 38:680-694.

214. Sun,C.S., K.T.Wu, H.H.Lee, Y.H.Uen, Y.F.Tian, C.C.Tzeng, A.H.Wang, C.J.Cheng, and S.L.Tsai. 2008. Anti-sense morpholino oligonucleotide assay shows critical involvement for NF-kappaB activation in the production of Wnt-1 protein by HepG2 cells: oncology implications. *J.Biomed.Sci.* 15:633-643.

215. Yerges,L.M., Y.Zhang, J.A.Cauley, C.M.Kammerer, C.S.Nestlerode, V.W.Wheeler, A.L.Patrick, C.H.Bunker, S.P.Moffett, R.E.Ferrell, and J.M.Zmuda. 2009. Functional characterization of genetic variation in the

Frizzled 1 (FZD1) promoter and association with bone phenotypes: more to the LRP5 story? *J.Bone Miner.Res.* 24:87-96.

216. Hasan,R.N. and A.I.Schafer. 2008. Hemin upregulates Egr-1 expression in vascular smooth muscle cells via reactive oxygen species ERK-1/2-Elk-1 and NF-kappaB. *Circ.Res.* 102:42-50.

217. Fu,M., X.Zhu, J.Zhang, J.Liang, Y.Lin, L.Zhao, M.U.Ehrengruber, and Y.E.Chen. 2003. Egr-1 target genes in human endothelial cells identified by microarray analysis. *Gene* 315:33-41.

218. Khachigian,L.M. 2006. Early growth response-1 in cardiovascular pathobiology. *Circ.Res.* 98:186-191.

219. Coleman,D.L., A.H.Bartiss, V.P.Sukhatme, J.Liu, and H.D.Rupprecht. 1992. Lipopolysaccharide induces Egr-1 mRNA and protein in murine peritoneal macrophages. *J.Immunol.* 149:3045-3051.

220. Reischl,J., S.Schwenke, J.M.Beekman, U.Mrowietz, S.Sturzebecher, and J.F.Heubach. 2007. Increased expression of Wnt5a in psoriatic plaques. *J.Invest Dermatol.* 127:163-169.

221. You J, Nguyen AV, Albers CG, Lin F, and Holcombe RF. 2008. Wnt Pathway-Related Gene Expression in Inflammatory Bowel Disease. *Dig.Dis.Sci.* 53:1013-1019.

222. Shames,B.D., C.H.Selzman, D.R.Meldrum, E.J.Pulido, H.A.Barton, X.Meng, A.H.Harken, and R.C.McIntyre, Jr. 1998. Interleukin-10 stabilizes inhibitory kappaB-alpha in human monocytes. *Shock* 10:389-394.

223. Tickenbrock,L., J.Schwable, A.Strey, B.Sargin, S.Hehn, M.Baas, C.Choudhary, V.Gerke, W.E.Berdel, C.Müller-Tidow, and H.Serve. 2006. Wnt signaling regulates transendothelial migration of monocytes. *J.Leukoc.Biol.* 79:1306-1313.

224. Wang,H.Y., T.Liu, and C.C.Malbon. 2006. Structure-function analysis of Frizzleds. *Cell Signal.* 18:934-941.

225. Bryja,V., L.Cajanek, A.Grahn, and G.Schulte. 2007. Inhibition of endocytosis blocks Wnt signalling to beta-catenin by promoting dishevelled degradation. *Acta Physiol (Oxf)* 190:55-61.

226. Terabayashi,T., Y.Funato, M.Fukuda, and H.Miki. 2009. A coated vesicle-associated kinase of 104 kDa (CVAK104) induces lysosomal degradation of frizzled 5 (Fzd5). *J.Biol.Chem.* 39:26716-26724.

227. Blitzer,J.T. and R.Nusse. 2006. A critical role for endocytosis in Wnt signaling. *BMC.Cell Biol.* 7:28.

228. Königshoff,M., N.Balsara, E.M.Pfaff, M.Kramer, I.Chrobak, W.Seeger, and O.Eickelberg. 2008. Functional Wnt signaling is increased in idiopathic pulmonary fibrosis. *PLoS.ONE.* 3:e2142.

229. Yoshikawa,Y., T.Fujimori, A.P.McMahon, and S.Takada. 1997. Evidence that absence of Wnt-3a signaling promotes neuralization instead of paraxial mesoderm development in the mouse. *Dev.Biol.* 183:234-242.

230. Lee,S.M., S.Tole, E.Grove, and A.P.McMahon. 2000. A local Wnt-3a signal is required for development of the mammalian hippocampus. *Development* 127:457-467.

231. Ikeya,M. and S.Takada. 2001. Wnt-3a is required for somite specification along the anteroposterior axis of the mouse embryo and for regulation of cdx-1 expression. *Mech.Dev.* 103:27-33.

232. Nakaya,M.A., K.Biris, T.Tsukiyama, S.Jaime, J.A.Rawls, and T.P.Yamaguchi. 2005. Wnt3a links left-right determination with segmentation and anteroposterior axis elongation. *Development* 132:5425-5436.

233. Shang,Y.C., S.H.Wang, F.Xiong, C.P.Zhao, F.N.Peng, S.W.Feng, M.S.Li, Y.Li, and C.Zhang. 2007. Wnt3a signaling promotes proliferation, myogenic differentiation, and migration of rat bone marrow mesenchymal stem cells. *Acta Pharmacol.Sin.* 28:1761-1774.

234. Jia,L., J.Zhou, S.Peng, J.Li, Y.Cao, and E.Duan. 2008. Effects of Wnt3a on proliferation and differentiation of human epidermal stem cells. *Biochem.Biophys.Res.Commun.* 368:483-488.

235. Davidson,K.C., P.Jamshidi, R.Daly, M.T.Hearn, M.F.Pera, and M.Dottori. 2007. Wnt3a regulates survival, expansion, and maintenance of neural progenitors derived from human embryonic stem cells. *Mol.Cell Neurosci.* 36:408-415.

236. Neth,P., M.Ciccarella, V.Egea, J.Hoelters, M.Jochum, and C.Ries. 2006. Wnt signaling regulates the invasion capacity of human mesenchymal stem cells. *Stem Cells* 24:1892-1903.

237. Spencer,G.J., J.C.Utting, S.L.Etheridge, T.R.Arnett, and P.G.Genever. 2006. Wnt signalling in osteoblasts regulates expression of the receptor activator of NFkappaB ligand and inhibits osteoclastogenesis in vitro. *J.Cell Sci.* 119:1283-1296.

238. Luis,T.C., F.Weerkamp, B.A.Naber, M.R.Baert, E.F.de Haas, T.Nikolic, S.Heuvelmans, R.R.De Krijger, J.J.van Dongen, and F.J.Staal. 2009. Wnt3a deficiency irreversibly impairs hematopoietic stem cell self-renewal and leads to defects in progenitor cell differentiation. *Blood* 113:546-554.

239. Malhotra,S. and P.W.Kincade. 2009. Canonical Wnt pathway signaling suppresses VCAM-1 expression by marrow stromal and hematopoietic cells. *Exp.Hematol.* 37:19-30.

240. Gattinoni,L., X.S.Zhong, D.C.Palmer, Y.Ji, C.S.Hinrichs, Z.Yu, C.Wrzesinski, A.Boni, L.Cassard, L.M.Garvin, C.M.Paulos, P.Muranski, and N.P.Restifo. 2009. Wnt signaling arrests effector T cell differentiation and generates CD8+ memory stem cells. *Nat.Med.* 15:808-813.

241. Al Aly,Z., J.S.Shao, C.F.Lai, E.Huang, J.Cai, A.Behrmann, S.L.Cheng, and D.A.Towler. 2007. Aortic Msx2-Wnt calcification cascade is regulated by TNF-alpha-dependent signals in diabetic Ldlr-/- mice. *Arterioscler.Thromb.Vasc.Biol.* 27:2589-2596.

242. Stout,R.D. and J.Suttles. 2004. Functional plasticity of macrophages: reversible adaptation to changing microenvironments. *J.Leukoc.Biol.* 76:509-513.

243. Hesse,M., M.Modolell, A.C.La Flamme, M.Schito, J.M.Fuentes, A.W.Cheever, E.J.Pearce, and T.A.Wynn. 2001. Differential regulation of nitric oxide synthase-2 and arginase-1 by type 1/type 2 cytokines in vivo: granulomatous pathology is shaped by the pattern of L-arginine metabolism. *J.Immunol.* 167:6533-6544.

244. Lamberti,C., K.M.Lin, Y.Yamamoto, U.Verma, I.M.Verma, S.Byers, and R.B.Gaynor. 2001. Regulation of beta-catenin function by the IkappaB kinases. *J.Biol.Chem.* 276:42276-42286.

245. Carayol,N. and C.Y.Wang. 2006. IKKalpha stabilizes cytosolic beta-catenin by inhibiting both canonical and non-canonical degradation pathways. *Cell Signal.* 18:1941-1946.

246. Deng,J., S.A.Miller, H.Y.Wang, W.Xia, Y.Wen, B.P.Zhou, Y.Li, S.Y.Lin, and M.C.Hung. 2002. beta-catenin interacts with and inhibits NF-kappa B in human colon and breast cancer. *Cancer Cell* 2:323-334.

247. Deng,J., W.Xia, S.A.Miller, Y.Wen, H.Y.Wang, and M.C.Hung. 2004. Crossregulation of NF-kappaB by the APC/GSK-3beta/beta-catenin pathway. *Mol.Carcinog.* 39:139-146.

248. Du,Q., X.Zhang, J.Cardinal, Z.Cao, Z.Guo, L.Shao, and D.A.Geller. 2009. Wnt/beta-catenin signaling regulates cytokine-induced human inducible nitric oxide synthase expression by inhibiting nuclear factor-kappaB activation in cancer cells. *Cancer Res.* 69:3764-3771.

249. Sun,J., M.E.Hobert, Y.Duan, A.S.Rao, T.C.He, E.B.Chang, and J.L.Madara. 2005. Crosstalk between NF-kappaB and beta-catenin pathways in bacterial-colonized intestinal epithelial cells. *Am.J.Physiol Gastrointest.Liver Physiol.* 289:129-137.

250. Duan,Y., A.P.Liao, S.Kuppireddi, Z.Ye, M.J.Ciancio, and J.Sun. 2007. beta-Catenin activity negatively regulates bacteria-induced inflammation. *Lab. Invest.* 87:613-624.

251. Königshoff,M. and O.Eickelberg. 2010. WNT Signaling in Lung Disease: A Failure or a Regeneration Signal? *Am.J.Respir.Cell Mol.Biol.* 42:21-23.

252. Yamamoto,H., S.K.Yoo, M.Nishita, A.Kikuchi, and Y.Minami. 2007. Wnt5a modulates glycogen synthase kinase 3 to induce phosphorylation of receptor tyrosine kinase Ror2. *Genes Cells* 12:1215-1223.

253. Kikuchi,A., S.Kishida, and H.Yamamoto. 2006. Regulation of Wnt signaling by protein-protein interaction and post-translational modifications. *Exp.Mol.Med.* 38:1-10.

254. Gagliardi,M., E.Piddini, and J.P.Vincent. 2008. Endocytosis: a positive or a negative influence on Wnt signalling? *Traffic.* 9:1-9.

255. Zilberberg,A., A.Yaniv, and A.Gazit. 2004. The low density lipoprotein receptor-1, LRP1, interacts with the human frizzled-1 (HFz1) and down-regulates the canonical Wnt signaling pathway. *J.Biol.Chem.* 279:17535-17542.

256. Howell,B.W. and J.Herz. 2001. The LDL receptor gene family: signaling functions during development. *Curr.Opin.Neurobiol.* 11:74-81.

257. Gliemann,J. 1998. Receptors of the low density lipoprotein (LDL) receptor family in man. Multiple functions of the large family members via interaction with complex ligands. *Biol.Chem.* 379:951-964.

258. Dubois,L., M.Lecourtois, C.Alexandre, E.Hirst, and J.P.Vincent. 2001. Regulated endocytic routing modulates wingless signaling in Drosophila embryos. *Cell* 105:613-624.

259. Piddini,E., F.Marshall, L.Dubois, E.Hirst, and J.P.Vincent. 2005. Arrow (LRP6) and Frizzled2 cooperate to degrade Wingless in Drosophila imaginal discs. *Development* 132:5479-5489.

260. Doyle,A.G., G.Herbein, L.J.Montaner, A.J.Minty, D.Caput, P.Ferrara, and S.Gordon. 1994. Interleukin-13 alters the activation state of murine macrophages in vitro: comparison with interleukin-4 and interferon-gamma. *Eur.J.Immunol.* 24:1441-1445.

261. Doherty,T.M., R.Kastelein, S.Menon, S.Andrade, and R.L.Coffman. 1993. Modulation of murine macrophage function by IL-13. *J.Immunol.* 151:7151-7160.

262. Mucenski,M.L., J.M.Nation, A.R.Thitoff, V.Besnard, Y.Xu, S.E.Wert, N.Harada, M.M.Taketo, M.T.Stahlman, and J.A.Whitsett. 2005. Beta-catenin regulates differentiation of respiratory epithelial cells in vivo. *Am.J.Physiol Lung Cell Mol.Physiol.* 289:L971-L979.

263. Morrisey,E.E. 2003. Wnt signaling and pulmonary fibrosis. *Am.J.Pathol.* 162:1393-1397.

264. Chilosi,M., V.Poletti, A.Zamo, M.Lestani, L.Montagna, P.Piccoli, S.Pedron, M.Bertaso, A.Scarpa, B.Murer, A.Cancellieri, R.Maestro, G.Semenzato, and C.Doglioni. 2003. Aberrant Wnt/beta-catenin pathway activation in idiopathic pulmonary fibrosis. *Am.J.Pathol.* 162:1495-1502.

265. Lama,V.N., L.Smith, L.Badri, A.Flint, A.C.Andrei, S.Murray, Z.Wang, H.Liao, G.B.Toews, P.H.Krebsbach, M.Peters-Golden, D.J.Pinsky, F.J.Martinez, and V.J.Thannickal. 2007. Evidence for tissue-resident mesenchymal stem cells in

human adult lung from studies of transplanted allografts.
J.Clin.Invest. 117:989-996.

266. Sabatini,F., L.Petecchia, M.Tavian, d.V.Jodon, V, G.A.Rossi, and D.Brouty-Boye. 2005. Human bronchial fibroblasts exhibit a mesenchymal stem cell phenotype and multilineage differentiating potentialities.
Lab. Invest. 85:962-971.

267. Warburton,D., L.Perin, R.Defilippo, S.Bellusci, W.Shi, and B.Driscoll. 2008. Stem/progenitor cells in lung development, injury repair, and regeneration.
Proc.Am.Thorac.Soc. 5:703-706.

268. Etheridge,S.L., G.J.Spencer, D.J.Heath, and P.G.Genever. 2004. Expression profiling and functional analysis of wnt signaling mechanisms in mesenchymal stem cells. *Stem Cells* 22:849-860.

269. Christman,M.A., D.J.Goetz, E.Dickerson, K.D.McCall, C.J.Lewis, F.Benencia, M.J.Silver, L.D.Kohn, and R.Malgor. 2008. Wnt5a is expressed in murine and human atherosclerotic lesions.
Am.J.Physiol Heart Circ.Physiol. 294:2864-2870.

270. van der Sar,A.M., H.P.Spaink, A.Zakrzewska, W.Bitter, and A.H.Meijer. 2009. Specificity of the zebrafish host transcriptome response to acute and chronic mycobacterial infection and the role of innate and adaptive immune components. *Mol.Immunol.* 46:2317-2332.

8. Appendix

8.1 List of figures and tables

Tables:

8.2 Abbreviations

Also see the Reagents section (2.1.3.1) for abbreviations of additives used in media and solutions.

AIDS	Acquired immune deficiency syndrome
AP1	Activator protein 1
APC	Adenomatous polyposis coli
approx.	Approximately
Arg1	Arginase 1
Asn	Asparagine
AT2	Alveolar type 2 epithelial cell
ATCC	American type culture collection
β-TrCP	β-trancducin repeat containing protein
BMDM	Bone marrow-derived macrophages
BMP2	Bone morphogenic protein 2
c-Jun	Jun oncogene
c-myc	Myelocytomatosis oncogene
Calcn	Calcineurin
CamKII	Calcium/calmodulin-dependent kinase II
CCR2/5	CC chemokine receptor
CD	Cluster of differentiation
cDNA	Complementary DNA
CFH	Cubic feet per hour
CFU	Colony forming units
CK1α	Casein kinase 1α
CL	Chemiluminescence
CM	Conditioned medium
CPM	Counts per minute
CRD	Here: Cysteine-rich domain (also: carbohydrate recognition domain)
Ctrl	Control
CXCl	CXC chemokine (ligand)

Cys	Cysteine
d	Day
DAG	Diacylglycerol
DC-SIGN	Dendritic cell-specific ICAM-3 grabbing non-integrin
Dfz	*Drosophila* frizzled homolog
DKK	Dickkopf
DNA	Deoxyribonucleic acid
dNTP	Deoxyribonucleotide
Dvl	Disheveled
EC	Extracellular
EGF	Epidermal growth factor
Egr1	Early growth response protein 1
ELISA	Enzyme-linked immunosorbent assay
ER	Endoplasmatic reticulum
ES cell	Embryonal stem cell
Evi	Evenness interrupted
FACS	Fluorescence-activated cell sorting
FGF	Fibroblast growth factor
FITC	Fluorescein isothiocyanate
FSC	Forward scatter
Fzd	Frizzled
g; x g	Gram; times gravity
GAPDH	Glyceraldehyde-3-phosphate dehydrogenase
GFP	Green fluorescent protein
Gln	Glutamine
GOPC	Golgi-associated PDZ and coiled-coil motif containing protein
GPCR	G protein-coupled receptor
GSK3β	Glycerin synthase kinase 3β
Hh	Hedgehog
His	Histidine
HIV	Human immune deficiency virus
Hox	Homeobox
HPRT	Hypoxanthine phosphoribosyltransferase
HRP	Horseradish peroxidase
HSC	Hematopoietic stem cell
IC	Intracellular
IFN-γ	Interferon-γ
IgG	Immunoglobulin G
IκB	Inhibitor of NF-κB
IKK	Inhibitor of NF-κB kinase
IL	Interleukin
IP_3	Inositol 1,4,5,-triphosphate
IPF	Ideopathic pulmonary fibrosis
IPSC	Inducible pluripotent stem cell
IRAK	Interleukin-1 receptor-associated kinase
IRF3	Interferon regulatory factor 3
IVC	Individually ventilated cage
JNK	c-Jun N-terminal kinase
K_d	Dissociation konstant
kDa	Kilo Dalton

LacZ	β-galactosidase
LAM	Lipoarabinomannan
LBP	LPS-binding protein
Lck	Leukocyte-specific protein tyrosine kinase
Lef	Lymphoid enhancer factor
LH	Luteinizing hormone
LNA	Locked nucleic acid
LPS	Lipopolysaccharide
LRG-47	47-kDa member of the guanosine triphosphatase family
LRP5/6	Low-density-lipoprotein receptor-related protein 5/6
LTA	Lipoteichoic acid
Lys	Lysozyme
Lys	Lysine
M. av	*Mycobacterium avium*
M. tb	*Mycobacterium tuberculosis*
Mab	Monoclonal antibody
MAL	MyD88 adapter-like protein
MAPK	Mitogen-activated protein kinase
MARCO	Macrophage receptor with collagenous structure
MCP-1	Monocyte chemoattractant protein 1
MD-2	Lymphocyte antigen 96 (gene name)
MHC	Major histocompatibility complex
MIP-1	Macrophage inflammatory protein 1
MMP	Matrix metalloproteinase
MMTV	Mouse mammary tumor virus
MNC	Mononuclear cell
MOI	Multiplicity of infection
MR	Mannose receptor
mRNA	Messenger RNA
MSC	Mesenchymal stem cell
MTBC	*Mycobacterium tuberculosis* complex
MyD88	Myeloid differentiation primary response gene 88
NALP	NACHT-LRR-pyrin domain-containing proteins
Nanog	Nanog homeobox gene
NF-AT	Nuclear factor of activated T cells
NF-kB	Nuclear factor kappa-light-chain-enhancer of activated B cells
NK cell	Natural killer cell
NLK	Nemo-like kinase
NLR	NOD-like receptors
NOD2	Nucleotide-binding oligodimerization domain 2
NOS2	Nitric oxide synthase 2
NTM	Nontuberculous mycobacteria
Oct4	Octamer-4
OD_{600}	Optical density 600 nm
PAGE	Polyacrylamide gel electrophoresis
Pam_3CSK_4	[(S)-[2,3-Bis(palmitoyloxy)-(2-RS)-propyl]-N-palmitoyl-(R)-Cys-(S)-Ser-(S)-Lys_4-OH]
PAMP	Pathogen-associated molecular pattern
PBMC	Peripheral blood mononuclear cell
PCP	Planar cell polarity
PCR	Polymerase chain reaction

PDG	Platelet-derived growth factor
PDZ	**P**ost synaptic density protein, *Drosophila* **d**isc large tumor suppressor, **z**onula occludens-1 protein
PE	Phycoerythrine
PEC	Peritoneal exudate cells
PG	Peptidoglycan
PIM	Phosphatidyl myo-inositol mannosides
PIP_2	Phosphatidylinositol 4,5-bisphosphate
PKC	Protein kinase C
PLC	Phospholipase C
Porc	Porcupine
Pro	Proline
PRR	Pattern recognition receptor
PTH	Parathyroid hormone
Rac	Rac GTPase
RANTES	Regulated on activation normal T cell expressed and secreted also known as chemokine CCL5
RhoA	Ras homolog gene family member A
RIP1	Receptor-interacting protein 1
RLR	Retinonic acid-inducible gene-like receptor
RNI	Reactive nitrogen intermediates
ROCK	Rho-associated kinase
ROI	Reactive oxygen intermediates
ROR2	Receptor tyrosine kinase-like orphan receptor 2
rTNF-α	Recombinant TNF-α
RTQ-PCR	Real-time quantitative PCR
Ryk	Related to receptor tyrosine kinase
Scgb	Secretoglobin or clara cell secretory protein (CCSP)
SEM	Standard error of the mean
Ser	Serine
sFRP	Secreted Frizzled-related protein
Sftpc	Surfectant-associated protein C
Shh	Sonic hedgehog
SMC	Smooth muscle cell
SOST	Sclerostin
Sox	Sex-determining region Y protein (SRY) box gene
SRA	Class A scavenger receptor
SSC	Side scatter
T cell	Thymus cell
TAB	TAK binding protein
TAK1	TGF-β-activated kinase 1
Taq	*Thermus aquaticus*
TB	Tuberculosis
Tcf	T cell factor
TGF-β	Transforming growth factor β
Th1	T helper cell type 1
TIR	Toll/Interleukin-1-receptor
TIRAP	TIR domain containing adapter protein
TLR	Toll-like receptor
TNF-α	Tumor necrosis factor α

TRAF	TNF receptor-associated factor
TRAM	TRIF-related adapter molecule
TRIF	TIR domain containing adapter inducing interferon-β
UPL	Universal probe library
V-CAM	Vascular cell adhesion molecule
v/v	Volume per volume
w/v	Weight per volume
Wg	Wingless
WHO	World health organization
WIF	Wnt inhibitory factor
Wls	Wntless
Wnt	Wingless-related MMTV integration site
WT	Wild type
XWnt	*Xenopus* Wnt homolog

Acknowledgements

I would like to thank everybody who has helped me along the way and thereby contributed to this work.

I would like to express my gratitude to PD Dr. Norbert Reiling for giving me the opportunity to work on this versatile topic, his doors that were always open and his excellent supervision of this study. Thank you Norbert for your advice, your constrictive criticism and that you never lost the personal factor out of sight. To make it short, thank you for creating ideal working conditions.

I am very grateful for Prof. Dr. Stefan Ehlers, his proposals to this work and the time that he took despite an all time busy schedule.

Thank you very much Svenja Kröger, Kerstin Kopp and Katrin Seeger for introducing me to many methods, for your expert technical assistance and support. You have always created a pleasant atmosphere in the lab.

Thank you Kolja Schaale, Christine Steinhäuser, Johanna Pott and Dagmar Schneider for your constructive discussions, your help, your good mood and for sharing moments of frustration and fun with me.

I would like to thank Prof. Dr. Christoph Hölscher's lab for helping me out with reagents and for the support with words and deeds. I thank Dr. Martin Ernst for his assistance at the luminometer, as well as PD Dr. Stefan Niemann and Tanja Ubben for their support with the genotyping of knockout mice. Thank you, Steffi Pfau, Prof. Dr. Brade and Prof. Dr. Wiesmüller (EMC Microcollections, Tübingen) for the supply of stocks of mycobacteria, LPS and lipopeptide.

I thank Dr. Jürgen Fritsch from the Christian-Albrechts-University of Kiel, for performing first 2D-gel electrophoresis analyses on Wnt3a and Fzd1.

Thank you Dietrich Lemke for helping me through the English orthography.

Further thanks goes to all my collegues at the Research Center Borstel for providing an open and cooperative working atmosphere, that makes out the "Borstel Spirit"; and thank you my carpool from and to Hamburg, for many comforting hours.

In the end I would like to speak out my appreciation and thankfulness to my parents who are a constant basis for me. I would not have reached my goals without them.

Words are not enough to express my deepest and most sincere gratitude to my beloved wife, who despite pregnancy and the birth of our son supported and encouraged me at all times. Dear Katrin, dear Justus, you have made me a happy person!

Presentations

Manuscript in preparation

Frizzled1 is a marker of inflammatory macrophages and is involved in Wnt3a-mediated reprogramming of *Mycobacterium tuberculosis*-infected macrophages
J. Neumann, K. Schaale, K. Farhat, T. Endermann, A. Ulmer, S. Ehlers and N. Reiling.

National and International Meetings

New insights into Wnt/Frizzled signaling during inflammation: The role of Wnt3a and Frizzled1 in *M.tuberculosis* infection.
J. Neumann, S. Ehlers and N. Reiling
2nd European Congress of Immunology, Sep. 13. – 16. 2009, Berlin (**Abstract**)

The role of Frizzled1 in *M.tuberculosis* infection: Modes of induction and first insights into function.
J. Neumann, T. Endermann, S. Ehlers and N. Reiling
13th Mini-Symposium „Infection and Immune Response, Mar. 12. – 14. 2009, Burg Rothenfels (**Oral Presentation**)

WNT/Frizzled signaling in *M.tuberculosis* infection: Deciphering the role of FZD1
J. Neumann, T. Endermann, S. Ehlers and N. Reiling
Keystone Symposium: „Tuberculosis: Biology, Pathology and Therapy“, Jan. 25. – 30. 2009, Keystone, Colorado, USA (**Poster presentation**)

Wnt/Frizzled signaling in infectious diseases: Deciphering the role of FZD1 in mycobacterial infections.
N. Reiling, T. Endermann, S. Ehlers and **J. Neumann**
Joint Annual Meeting of Immunology of the Austrian and German Societies (ÖGAI, DGfI), Sep. 3. – 6. 2008, Wien, Austria (**Abstract**)

Die Infektion mit Mykobakterien führt zu einer erhöhten Expression von Frizzled1 in murinen Makrophagen.
J. Neumann, T. Endermann, S. Ehlers and N. Reiling
Uni im Dialog, June 4. 2008, Lübeck (**Poster presentation**)

WNT/Frizzled signaling in infectious diseases: Mycobacteria and conserved bacterial structures lead to an enhanced expression of Frizzled1.
J. Neumann, T. Endermann, S. Ehlers and N. Reiling
12th Mini-Symposium “Infection and Immune Response”, Mar. 7. – 9. 2008, Burg Rothenfels (**Oral presentation**)

Frizzled1: Enhanced expression on murine macrophages in response to mycobacteria and conserved bacterial structures.
J. Neumann, T. Endermann, S. Ehlers and N. Reiling
30. Arbeitstagung der Norddeutschen Immunologen, Nov. 16. 2007, Borstel
(**Oral presentation**)

Enhanced expression of Frizzled1 in response to mycobacteria and conserved bacterial structures.
J. Neumann, T. Endermann, S. Ehlers and N. Reiling
11th Joint Meeting of the Signal Transduction Society, Nov. 1. – 3. 2007, Weimar
(**Poster presentation**)

Murine macrophages show an enhanced expression of Frizzled1 in response to mycobacteria and conserved bacterial structures.
J. Neumann, T. Endermann, S. Ehlers and N. Reiling
The 2nd Luminy Advanced Course in Immunology, Jan. 8. – 10. 2007, Marseille, France (**Abstract**)

Erklärung

Hiermit versichere ich, dass ich die vorliegende Arbeit selbständig angefertigt habe und keine weiteren als die angegebenen Quellen und Hilfsmittel verwendet wurden.

Diese Arbeit wurde in der jetzigen oder ähnlichen Form noch bei keiner anderen Hochschule eingereicht und hat darüber hinaus noch keinen Prüfungszwecken gedient.

Jan Neumann

Hamburg, 6. März 2010